NASA CONTRACTOR
REPORT

NASA CR-1

C. 1

PERFORMANCE OF CYLINDRICAL CONVERTERS
WITH PREFERRED-CRYSTAL-ORIENTATION
EMITTERS OF CHEMICALLY VAPOR
DEPOSITED TUNGSTEN

by G. I. Samstad, J. C. Danko, and J. M. Case

Prepared by
GENERAL ELECTRIC COMPANY
Pleasanton, Calif. 94566
for Lewis Research Center

NATIONAL AERONAUTICS AND SPACE ADMINISTRATION • WASHINGTON, D. C. • SEPTEMBER 1971

1. Report No. NASA CR-1898	2. Government Accession No.	3. Recipient's Catalog No.
4. Title and Subtitle PERFORMANCE OF CYLINDRICAL CONVERTERS WITH PREFERRED-CRYSTAL-ORIENTATION EMITTERS OF CHEMICALLY VAPOR DEPOSITED TUNGSTEN		5. Report Date September 1971
		6. Performing Organization Code
7. Author(s) G. I. Samstad, J. C. Danko, and J. M. Case		8. Performing Organization Report No. GESP-9018
		10. Work Unit No.
9. Performing Organization Name and Address General Electric Company P.O. Box 846 Pleasanton, California 94566		11. Contract or Grant No. NAS 3-8511
		13. Type of Report and Period Covered Contractor Report
12. Sponsoring Agency Name and Address National Aeronautics and Space Administration Washington, D.C. 20546		14. Sponsoring Agency Code

15. Supplementary Notes

16. Abstract

A cylindrical out-of-pile thermionic converter test vehicle was designed to determine the performance of tungsten emitters with a preferred crystal orientation. The design included provisions for the direct measurement of emitter temperature: three high temperature thermocouples and a black-body hole. Also included was the design provision for changing the electron bombardment heater without altering the converter proper. Each emitter was carefully characterized by chemistry, microstructural analyses, vacuum work functions, and X-ray diffraction analyses. Three converters were fabricated and tested. The emitters of these converters included two of chloride vapor-deposited tungsten with a preferred (110) crystal orientation and one with a fluoride vapor-deposited tungsten of nominal (100) crystal orientation which was deep electroetched to expose the (110) crystal facets. A niobium collector and a 0.010-inch interelectrode spacing was used on all converters. The test program included periodic thermionic performance mapping and steady-state operation for 5000 hours at an emitter temperature of 1700° C. The test results of these converters showed that there is comparable thermionic performance after 5000 hours of operation even though their emitters were produced by two distinctly different methods. The operating results together with the post-test examination of all three converters are presented and discussed.

17. Key Words (Suggested by Author(s)) Cylindrical thermionic converters Chemically vapor deposited tungsten Life tested	18. Distribution Statement Unclassified - unlimited	
19. Security Classif. (of this report) Unclassified	20. Security Classif. (of this page) Unclassified	21. No. of Pages 151	22. Price* $3.00

FOREWORD

The research described in this report was conducted by the General Electric Company under NASA contract NAS 3-8511. Mr. Dominic C. Di Ianni of the Lewis Research Center Nuclear Systems Division was the NASA Project Manager. The report was originally issued as General Electric report GESP-9018.

TABLE OF CONTENTS

CONTENTS (continued)

LIST OF FIGURES

SUMMARY

The development work described in this report is part of a continuing technology program on thermionic conversion initiated under NASA Contract NAS 3-2544. Follow-on development activity is supported under NASA Contract NAS 3-8511 in the form of two tasks. The first task was a basic investigation into the effects of electrode materials, surface treatments and spacing on thermionic performance. The results of this task served as an information and guidance source for the second task--testing and evaluation of high performance cylindrical thermionic converters. It is this latter task which is the subject of this report.

The course of activity of this latter task included a comprehensive program of test vehicle design and development, emitter electrode characterization and selection, thermionic performance mapping and extended steady-state testing, and post-test examination and analysis. Some of the more important features incorporated into the new test vehicle include:

(1)   Provision for the direct measurement of emitter temperature by both Hohlraum and high temperature thermocouples.

(2)   Simple geometry and reduced number of parts to both reduce cost and increase reliability.

(3)   Ease of fabrication and replacement of electron bombardment filament and emitter thermocouples to facilitate long-term life testing.

(4)   Direct potential leads on each electrode to facilitate data reduction and accuracy by eliminating need for calculating lead-loss corrections.

(5)   Capability of operation in a high vacuum environment.

The converter was designed to have a niobium (Nb) collector, a fixed interelectrode spacing of 0.010 inch and an effective emitting area of 11.0 cm^2.

Its design operating range included testing to emitter temperatures of 1700°C, collector temperatures as high as 1000°C, and cesium (Cs) reservoir temperatures between 300° and 400°C.

The emitter electrode was separated on the primary variable for test and evaluation, the range of exploration being further defined as tungsten (W) emitters of preferred (110) crystal orientation. In metals such as W which have a body-centered-cubic (bcc) crystal lattice, the (110) crystal plane is the desired emitting surface for enhanced thermionic performance because it has the highest atomic density and, therefore, exhibits the highest electron emission in the presence of Cs vapor.

The characterization of emitters included:

(1)   Chemical and microstructural analysis,

(2)   Vacuum work function measurements,

(3)   X-ray diffraction analysis to determine degree of preferred crystal orientation, and

(4)   Etch pit analysis to determine orientation of surface grains.

This information was used as the basis for selection of emitters for use in the test converters. The testing of each converter included performance mapping and steady-state life testing for 5000 hours at emitter temperatures of 1700°C. The post-test examination of the converters included:

(1)   Vacuum work function measurements,
(2)   Dimensional measurements,
(3)   Surface light microscopy and scanning electron microscopy,
(4)   X-ray diffraction analysis,
(5)   Surface etch pit analysis,
(6)   Bulk chemistry,

2

(7) spark spectrographic analysis, and

(8) Destructive metallography.

The following observations and conclusions resulted from this task. The three devices built and tested under this program had strikingly comparable thermionic performance after 5000 hours of operation. This is shown by the plot of their output power versus emitter temperature at a current density of 10 Amps/cm^2, shown in Figure 1. Their emitters, however, were produced by two distinctly different methods. The first two devices (No. 362 and 363) employed W emitter surfaces of preferred (110) crystal orientation produced by the hydrogen reduction of tungsten hexachloride (WCl_6). The latter converter (No. 364) employed an emitter produced from the hydrogen reduction of tungsten hexafluoride (WF_6) which was electroetched to expose the (110) crystal planes.

Perhaps equally important is the fact that, although the various techniques of emitter characterization (vacuum work function, x-ray diffraction, and etch pitting) tended to corroborate each other in ranking the emitters, the rather significant spread so indicated was not reflected in the thermionic performance. Further, it is noteworthy that the closely-grouped band of thermionic performance produced by these three devices fell well within the band established by other reported converters having (110) emitter surfaces: single crystal planar, polycrystalline planar, and polycrystalline cylindrical (Figure 2 and Table 1).

Converter 364 was an exceedingly stable performer, as indicated by both thermionic output and cesiated work function measurements taken over the 5000 hours of operation. However, performance changes did occur during the life testing of converters 362 and 363. These changes, while not completely understood, are thought to be due to inadequate outgassing of these earlier devices. Nevertheless, the effects of the resulting contamination are believed to have reduced and stabilized with time to the point where there was no appreciable impact on the thermionic performances at the end of steady state testing.

3
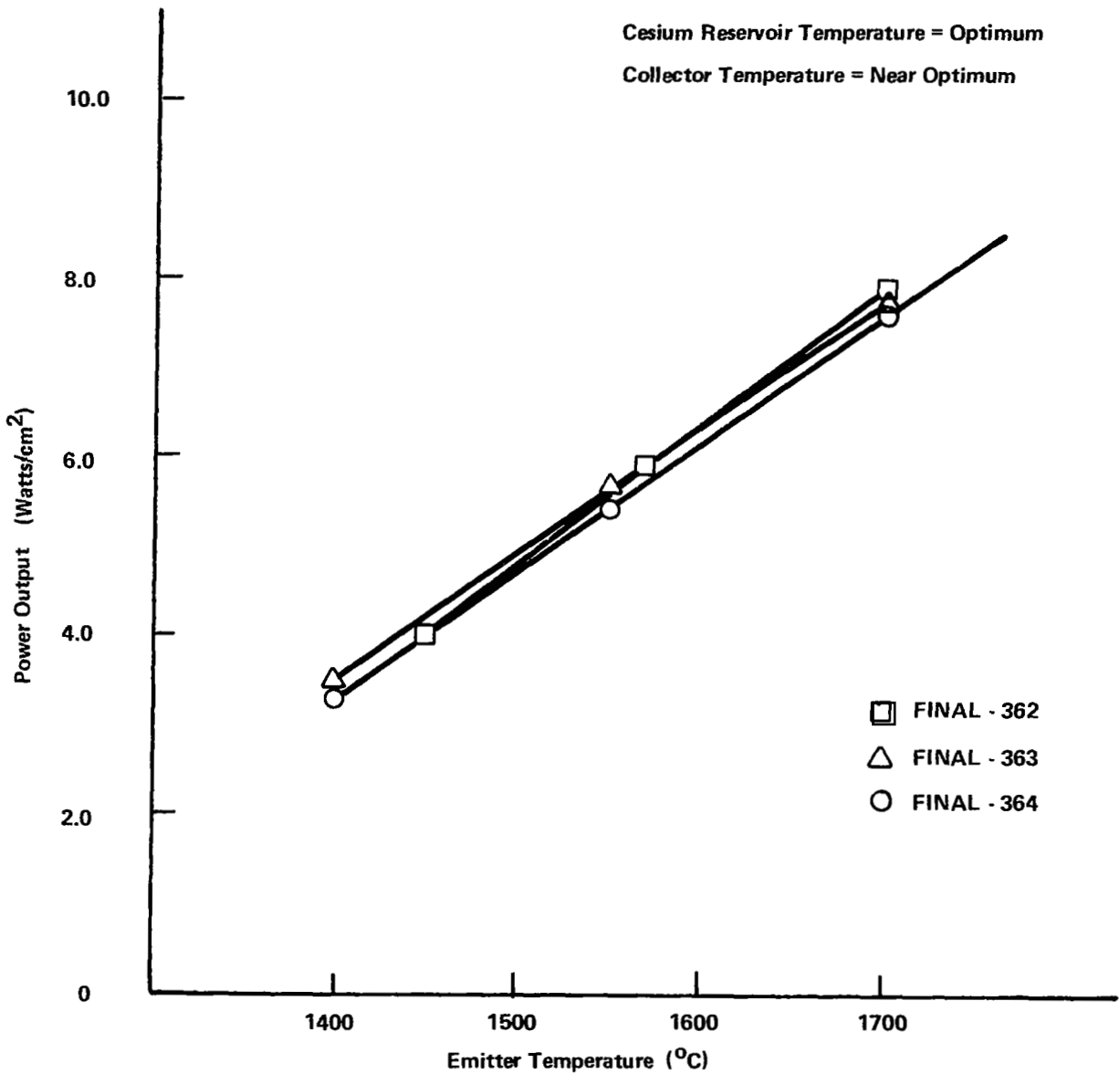
Figure 1. CONVERTER 362, 363 AND 364 PERFORMANCE
COMPARISON AT 10 AMPS/CM^2

4
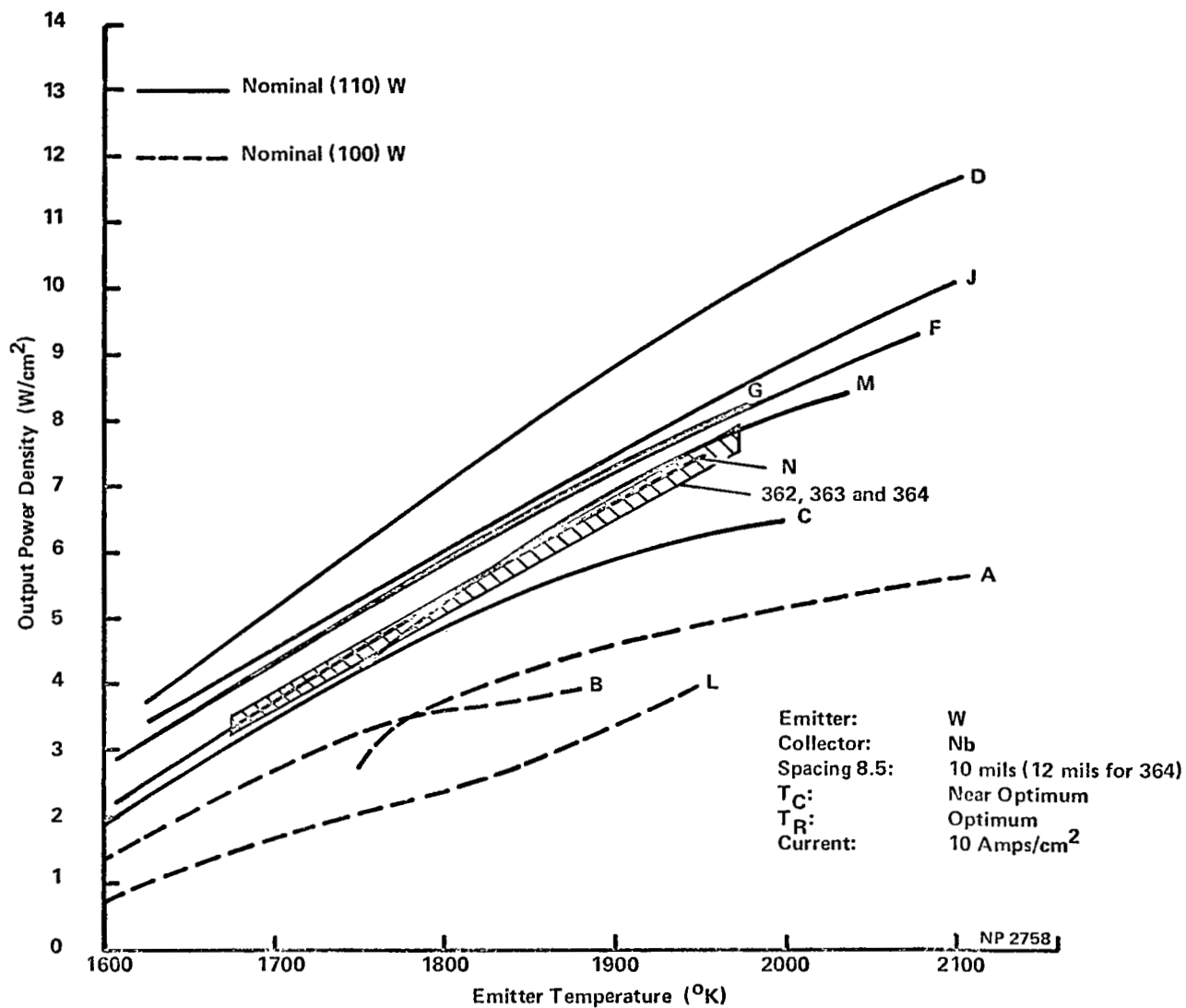
Figure 2. COMPARISON OF CONVERTER PERFORMANCE WITH
SELECTED RESEARCH DIODES (IDENTIFIED IN TABLE 1)

5

Table 1. ELECTRODE AND GEOMETRIC DATA FOR SELECTED RESEARCH DIODES

Symbol	Emitter	Preparation	Bare Work Function, Volts	Collector	Spacing Mils	Builder
D	F CVD W	Electropolished/ Electroetched	4.83	Nb	10	R&DC
F	Poly Powder Metallurgy W	Coldworked Resulting in Preferred (110) Orientation	4.58	Nb	10	R&DC
G	Cl CVD W	Electropolished	4.91	Nb	8.5	TECO
M	Cl CVD W	Electropolished	5.0	Nb	10	TECO
N	Cl CVD W	Electropolished	4.91	Nb	10	TECO
J	Cl CVD W	Preferred (110) Electropolished	4.95	Nb	10	R&DC
C	F CVD W	Electropolished/ Chemically Etched	4.77	Nb	8.5	TECO
A	F CVD W	Mechanical	--	Nb	8.5	TECO
B	F CVD W	Mechanical/ Electropolished	--	Nb	8.5	TECO
L	F CVD W	Mechanical	4.65	Nb	10	TECO

Upon post-test examination of all converters, no dimensional changes
or collector electrode changes were revealed which could have influenced
a change in thermionic performance. Some rounding of the etched crystal
facets on emitter 364 was observed after test. This occurrence, however,
did not display any influence on the converter's thermionic performance history.
Carbide contamination was discovered on the emitters of both 362 and 363 after
test. This discovery supports the contention that inadequate outgassing caused
the observed performance changes during the initial portions of their test
history.

Finally, this converter test series, with its extensive instrumentation,
provided the opportunity to evaluate and verify the Wilkins diagnostic
technique[1] for emitter temperature determination. Emitter temperatures of
converter 363, as determined by this diagnostic tool, high temperature
thermocouples and optical pyrometry, all cross checked well within a useful
range ($\pm 50^{\circ}C$).

INTRODUCTION

The importance of crystal orientation on the thermionic performance of W emitters was recognized and documented as early as 1962.[2] In metals such as W which have a body-centered-cubic (bcc) crystal lattice,[3] the (110) crystal plane is the preferred emitting surface for enhanced thermionic performance. It is that plane that has the highest atomic density and exhibits the highest electron emission in the presence of Cs vapor.

However, in order to take advantage of the performance offered by the (110) crystal plane, a suitable method of producing W emitters with single crystals of (110) orientation or polycrystalline W with a preferred (110) crystal orientation is required. In recent years, W planar and cylindrical emitters have been produced by a chemical vapor deposition (CVD) process. Investigations[4, 5] on CVD-W emitters revealed that W produced by the hydrogen reduction of WF_6 had a preferred (100) crystal orientation, whereas W produced from WCl_6 developed a (110) preferred orientation. The latter development made it possible to directly produce cylindrical W emitters with a (110) orientation and, thus, proceed with their thermionic performance evaluation. Another innovation which was investigated was the electroetching of fluoride CVD-W emitters to expose the preferred (110) crystal surface.

Under this contract, two tasks were identified for the performance evaluation of CVD-W emitters. The first task was a basic investigation into the effects of electrode materials, surface treatments and spacing on converter performance. This task was to provide information and guidance to the second task--the testing of high performance cylindrical converters. It is the second task which is the subject of this report.

PROGRAM OBJECTIVE

The objective of this program is summarized below, from its contract work statement.

8

A thermionic converter will be designed which will be unfueled, electrically heated, of cylindrical geometry and with a 10-mil interelectrode spacing. The converter design will include four emitter thermocouples for the measurement of emitter temperature and temperature gradients. Two collector thermocouples will be used to measure the collector temperature. Converter testing and post-test analysis will be performed to experimentally investigate the correlation between electrode work functions, degree of crystal orientation and thermionic performance.

The CVD-W emitters will be characterized to include:

(1)   Chemical and microstructural analysis of each emitter,

(2)   Vacuum work functions of each emitter, and

(3)   X-ray diffraction analysis to determine the degree of preferred crystal orientation.

This information is to be used in the selection of the emitters for use in the converters. The testing of each converter shall include performance mapping and steady-state life testing. The life testing will be conducted for 5000 hours at emitter temperatures of $1700^{\circ}C$. Post-test analysis will be performed on each converter.

TEST SERIES

CONVERTER DESIGN

The thermionic converters described in this report were tested to determine the long-term stability of cylindrical W emitters which were especially prepared to yield a preferred (110) crystal orientation. The test vehicle described herein was specifically designed to accomplish this task. Testing considerations included provision for wide performance mapping and extensive steady-state testing. Some of the more important features incorporated into the design include:

(1) Provision for the direct measurement of emitter temperature by both Hohlraum and high temperature thermocouples.

(2) Simple geometry and reduced number of parts to both reduce cost and increase reliability.

(3) Ease of fabrication and replacement of electron bombardment filament and emitter thermocouples to facilitate long-term life testing.

(4) Direct potential leads on each electrode to facilitate data reduction and accuracy by eliminating need for calculating lead-loss corrections.

(5) Capability of operation in high vacuum environment.

In addition to the W emitter with an effective emitting area of 11.0 cm^2, the converter was designed to have a Nb collector and an interelectrode spacing of 0.010 inch. The converter design allowed testing to emitter temperatures of $1700^{o}C$, collector temperatures as high as $1000^{o}C$ and Cs reservoir temperatures in the 300 to $400^{o}C$ range. The converter cross section, as shown in Figure 3, contains several basic subassemblies. Their detailed description follows.
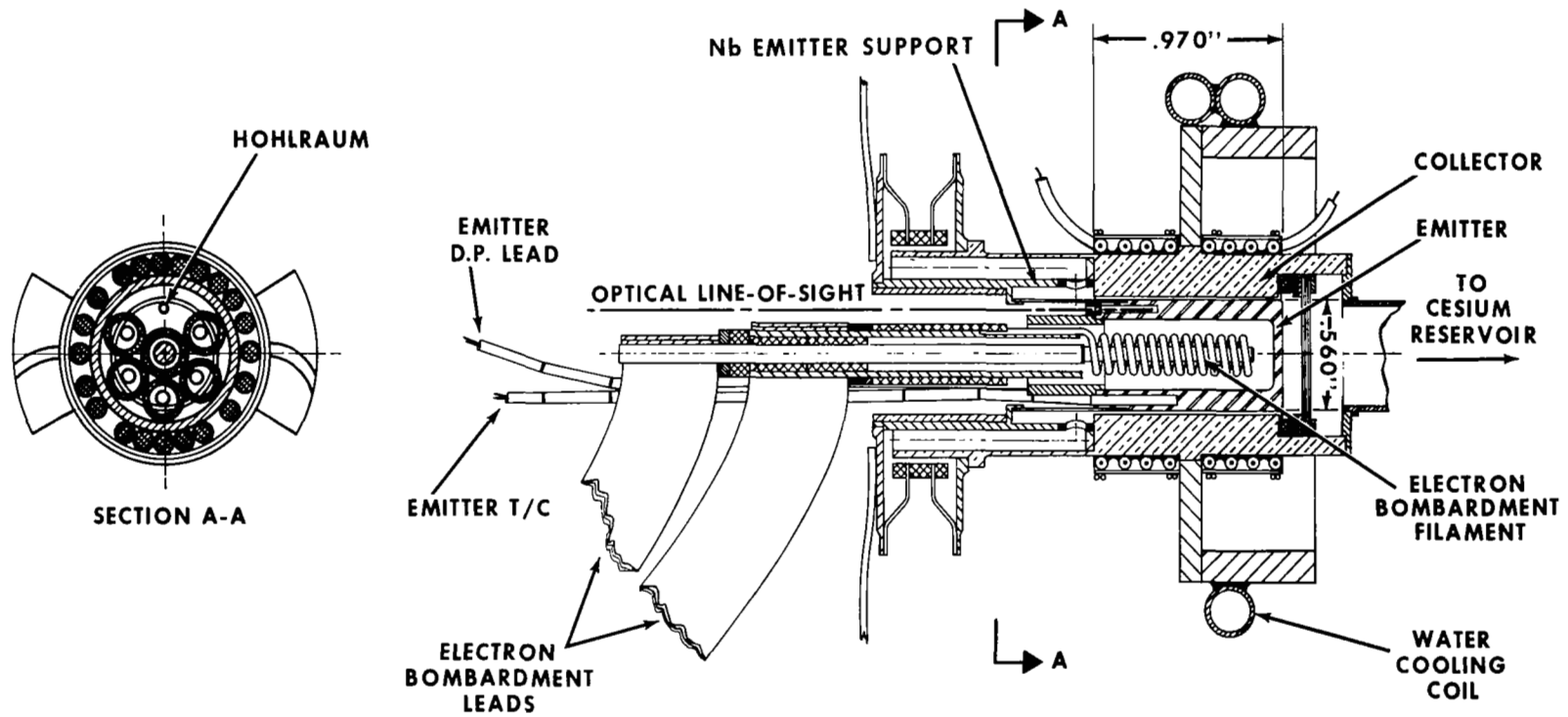
Figure 3. CROSS SECTIONAL VIEW OF CONVERTER TEST VEHICLE

1.   Emitter Subassembly

The W emitter has an O. D. of 0.560 inch and active length of 0.970 inch.
It was machined from a CVD-W crucible. Two vapor deposition processes
were used: one by the hydrogen reduction of WCl_6 and a second by the reduc-
tion of WF_6. The special surface preparations used for emitters fabricated
by each of these processes are described elsewhere in this report.

The wall thickness of each emitter was designed to be large (0.100
inch) in order to aid in obtaining uniform emitter temperatures and to allow
for axial holes along the emitter wall for the measurement of emitter temp-
eratures. Four holes were used for high temperature thermocouples (one at
a depth of 0.200 inch, two at 0.400 inch, and one at 0.800 inch). One hole,
0.200-inch deep was used as a Hohlraum with an aspect ratio of greater than
12:1 (0.15-inch diameter opening). Provision was also made for attaching a
direct potential lead to a small hole in the top of the emitter.

Component thermal tests were conducted as an evaluation of emitter
integrity. These component tests consisted of temperature cycling between
approximately 300° and $1800^{\circ}C$ 100 times and isothermal testing in vacuum at
$1850^{\circ}C$ for over 500 hours. The results of all tests indicated vacuum,
mechanical and metallurgical integrity.

The top of the emitter was attached to a thin-walled tungsten-22 weight
percent rhenium (W-22w/o Re) tube. The tube, formed by chemical vapor
deposition, served two functions. First, it provided the vertical support for
the emitter; and second, it formed the optimum heat choke and electrical
lead from the emitter. Tests were initially made on two methods for
attaching the emitter to the W-Re sleeve--EB welding and EB welding plus
molybdenum-rhenium (Mo-Re) brazing. While both methods appeared
feasible, the EB welding only approach was selected so that the emitter would
not have to be raised to the $2550^{\circ}C$ brazing temperature (which could have
altered the characteristics of the emitter prepared surface). Metallographic

studies of the welded only joints and the welds plus Mo-Re braze joints after the thermal cycle tests revealed good joint microstructure.

The upper end of the W-Re sleeve was attached to a Nb emitter support structure. Since this joint operates well below 1000°C, a vanadium (V) braze was used. Test samples of this V braze joint were thermal cycled quickly from 1100 to 700°C 25 times to simulate a power failure. The samples remained vacuum tight after the cycling and results of metallography showed a good braze joint after the testing.

The final assembly steps for the emitter subassembly consisted of copper (Cu) brazing the upper emitter structure to a Kovar flange which was, in turn, welded to a ceramic-to-metal insulator seal. The insulator seal was fabricated from Kovar and high purity alumina (Al_2O_3) using a Cs resistant metallizing material. While sufficient history had been accumulated to give high confidence on this type of seal, an acceptance test was performed for a seal with this particular type of geometry. One seal which was thermal cycled 25 times from room temperature to 600°C in a hydrogen furnace remained leak tight. Next, it was isothermally tested at 600°C in an environment of 7 torr Cs pressure for 775 hours. Examination of the seal after testing showed mechanical and vacuum integrity with no evidence of Cs attack.

2.   Collector Subassembly

The collector was fabricated from EB melted Nb. The collector surface was as-machined and no further special preparation was attempted. The I. D. was 0.580 inch with an O. D. of 1.000 inch, giving a thick collector wall which allowed for brazing thermocouples in the collector for accurate temperature measurement.

Below the collector cavity was a set of Al_2O_3 ceramic disks into which were positioned four Mo spacer pins to maintain a positive radial spacing between the collector and the bottom of the emitter when the converter was

assembled. Immediately below the spacer ceramics was a series of 4 dimpled W heat shields. These shields prevented a direct line-of-sight from emitter to Cs reservoir and, consequently, assisted in decoupling the two temperatures.

Surrounding the collector was a brazed coaxial heater to provide trim control of the collector temperature. Radially outward from the collector were Mo fins which were used to conduct reject heat to a water cooling coil. A Kovar flange Cu brazed to a heat choke section near the top of the collector body, which was used to ·ttach to the ceramic-to-metal seal, completes the collector subassembly.

3.   Cesium Reservoir Subassembly

The Cs reservoir was fabricated from an oxygen-free high conductivity (OFHC) Cu cylinder. Above the Cs reservoir is an 0.020-inch wall Nb tube, 2-1/2-inch long, which served as a thermal choke to isolate the Cs reservoir temperature from the collector temperature. The tube, which was Cu-Mn brazed to the Cs reservoir, was EB welded to a Nb flange at the top which joined to the collector subassembly.

Surrounding the Cs reservoir was a coaxial heater to provide trim control for the Cs reservoir temperature. A Cu strap brazed to the bottom of the reservoir was used to conduct the reject heat to a water cooling coil. Thermocouples were brazed into holes in the Cs reservoir Cu block to provide a means for direct measurement of Cs reservoir temperature.

The pump-out and Cs distillation tubulation complete the Cs reservoir subassembly. This tubulation of OFHC Cu was pinched off close to the Cs reservoir after the assembled converter was processed and Cs distilled.

4.   Electron Bombardment Gun Subassembly

The electron bombardment gun which was used to supply heat to the emitter was designed to be inexpensive to fabricate and easy to replace within

the emitter. The geometry consisted chiefly of rods and tubes. The filament dimensions were designed to be optimum with respect to the emitter dimensions to be heated.

5.   Other Design Considerations

Three additional design considerations deserve special description.

(1)   Spacing methods,
(2)   Instrumentation, and
(3)   Heat transfer and temperature distributions.

The radial spacing mechanism for the bottom of the emitter has already been described as consisting of spacer pins imbedded in Al_2O_3 ceramic disks. The method used for spacing the top of the emitter from the collector made use of very accurately ground ceramic pins located in the annular space between the Nb emitter support structure and the Nb extension above the collector (Figure 3). This method selection was based primarily on the ease with which insulators having a highly accurately ground O.D. can be obtained. Filament-to-emitter alignment was maintained by the use of 5 hollow insulator tubes arranged in a similar fashion to the upper emitter arrangement. This technique allowed simple replacement of the bombardment filament. The use of hollow insulator rods permitted ready access to the emitter thermocouple holes, Hohlraum, and direct potential lead.

As mentioned earlier, the emitter temperature was monitored by a Hohlraum and 4 W-5 w/o Re versus W-25 w/o Re thermocouples located at three different depths in the emitter wall. Collector and Cs reservoir temperatures were measured by chromel/alumel thermocouples imbedded in holes in each location. Other instrumentation included emitter and collector direct potential leads attached directly to each electrode.

Three major heat input mechanisms and two prime heat rejection paths were employed in the design of these converters. The emitter was heated and

15

its temperature controlled by the electron bombardment filament, while the collector and Cs reservoir temperatures were controlled by separate surrounding coaxial heaters. The primary heat rejection paths were metallic straps connecting the collector and Cs reservoirs to water cooling coils. In the thermal design of the converter, several important objectives were considered.

(1) Ability to reach the desired temperature ranges of:
    (a) Emitter - 1450 to 1700°C,
    (b) Collector - 650 to 1000°C, and
    (c) Cs Reservoir - 280 to 400°C.

(2) Thermal isolation of the Cs reservoir so that changes in emitter and collector temperatures did not effect the Cs reservoir temperature.

(3) Prevention of possible secondary Cs reservoirs forming--i.e., for all operating conditions in the ranges stated above, there were to be no areas in the converter envelope colder than the temperature of the Cs reservoir.

(4) Limitation of the ceramic-to-metal seal temperature to a maximum of 600°C under all operating conditions.

To insure that these design objectives were achieved, the thermal heat transfer paths were mocked up both analytically and experimentally. The analytical mockup consisted of a computer code (THERMAL) which was developed especially for this application. The heat transfer model divided the converter structure into 23 constant temperature nodes which were connected by the appropriate heat transfer equations. The solution was obtained by an iterative procedure in which the temperature of all the nodes were first estimated and then, in sequence, the temperature of each node was adjusted to satisfy the heat balance relation for that node. The correct temperature distribution was converged upon by sequentially iterating through the node temperature adjustment procedure until no significant change in any of the node temperatures were necessary to satisfy all of the node heat balance relations.

The code was used to make several decisions during design of the converter geometry. For example, the Cs reservoir conduction cooling strap geometry, the thermal choke size between collector and Cs reservoir, and the shielding for the emitter/collector insulator ceramic were investigated and designed using the THERMAL code.

To further verify the adequacy of the design, an experimental mockup of the converter envelope was made. In this mockup (Figure 4), all components were represented except the Cs vapor which would be in an operating converter. This experiment was used to insure that the thermal design objectives (such as no secondary Cs reservoir) were met. The mockup was also used to insure that the THERMAL computer code was operating satisfactorily. Good agreement was obtained for the envelope temperature distributions between analysis and experiment as shown in Table 2. The discrepancy in the collector flange temperature was determined to be due to the collector heater being positioned too far up the collector choke.

Table 2.

	Filament Input Power (Watts)		Temperature (^{O}C)			
	Radiation	Bombardment	Cesium Reservoir	Cesium Choke	Col. Flange	Collector
Calculated	100	227	136	299	367	378
Measured	97	210	134	293	458	380

Several major observations were made as a result of this thermal mockup test.

(1)   The temperature distributions in the converter were independent of Cs reservoir temperature.

(2)   The insulator seal temperature should remain in the 500 to 600°C temperature range for all operating conditions.

(3)   Thermal conditions that give rise to a secondary Cs reservoir were not evident.
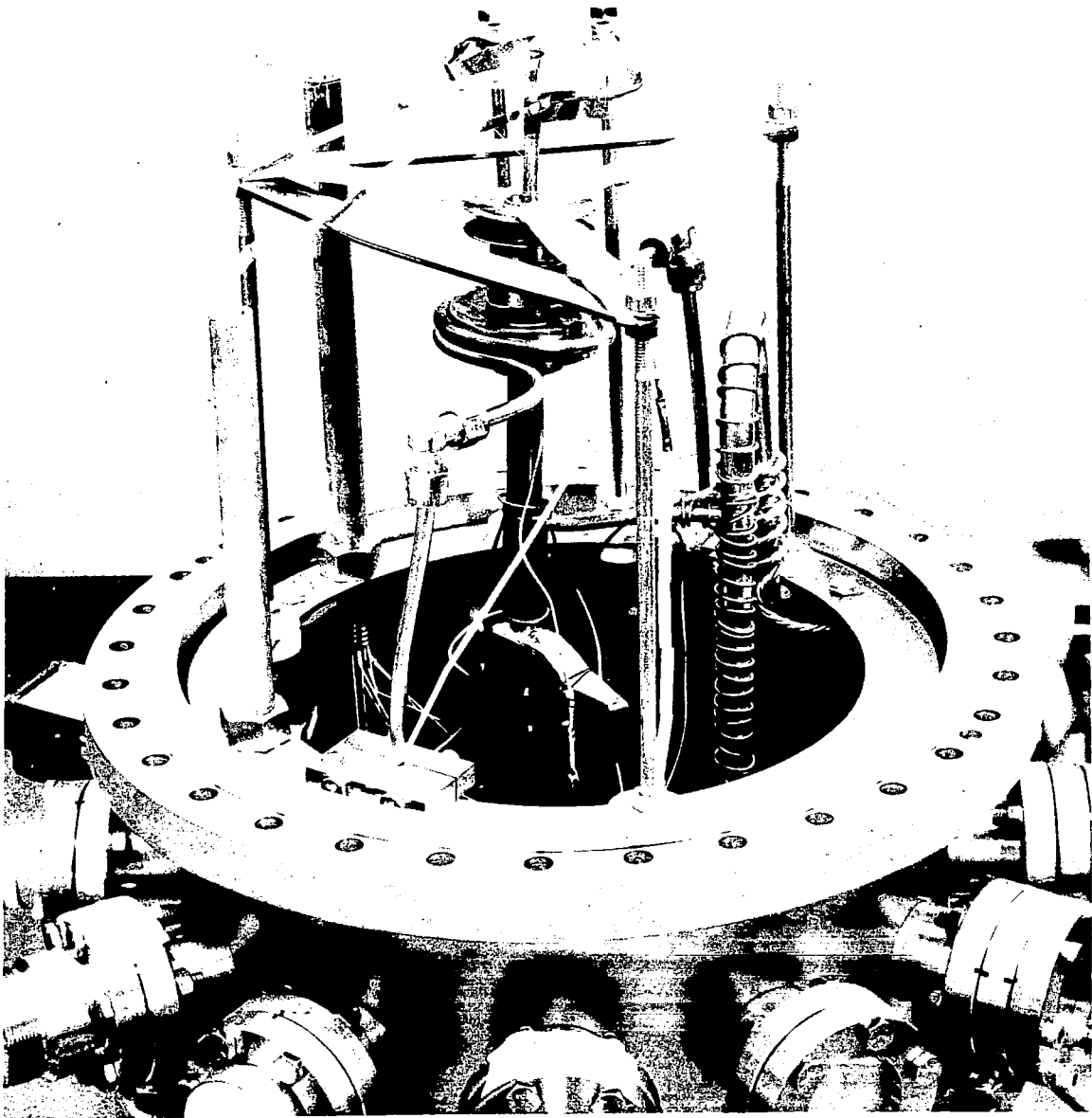
Figure 4.   THERMAL MOCKUP TEST INSTALLED IN VACUUM TEST
            STAND

(4) Ease of testing station and vacuum system operation was demonstrated.

(5) Filament structure was easily removed and replaced on four separate occasions.

TEST SERIES MATERIALS CHARACTERIZATION

CHEMICAL VAPOR DEPOSITED EMITTERS

The emitters prepared by the hydrogen reduction of WCl_6 and WF_6 were subjected to detailed characterization which included:

(1)   Chemical and spectrographic analysis,

(2)   Microstructural analysis,

(3)   High temperature grain growth and dimensional stability tests,

(4)   Vacuum work function measurements,

(5)   Crystal orientation by x-ray diffraction, and

(6)   Scanning electron microscopy of emitters with etched surfaces.

The sequence of emitter characterization was to first consider items 1, 2 and 3; those as-received emitter blanks that satisfied these requirements were selected for further characterization.

The emitter blanks were then machined to size, electropolished, vacuum fired and then placed into a vacuum work function apparatus for measurements. Emitter bodies that satisfied the requirements of acceptable work function values--i.e., values that indicate preferred crystal orientation, were used for x-ray diffraction analysis for determining the degree of preferred crystal orientation. For emitter bodies that were electroetched, scanning electron microscope examination was performed to determine the surface topography. On the basis of the various emitter characterization data, emitters were selected for use in the various converters.

A more detailed description of some of the emitter characterization technique is given below.

1.   Emitter Acceptance Criteria

Thirteen chloride and 4 fluoride CVD-W emitters were procured from San Fernando Laboratories-Fansteel, Inc. on a best-effort basis. The W was deposited on a stainless steel mandrel in a cup or crucible emitter configuration. A photograph of an as-deposited CVD-Cl W emitter is illustrated in Figure 5. The crucible emitters were produced by deposition from either WCl_6 or WF_6. No CVD-W duplex structures were used in this program.

A piece of the W emitter was removed from the open end for chemical and spectrographic analysis, microstructural analysis and high temperature dimensional stability tests. Typical spectrographic and chemical analysis for the Cl and F vapor deposited W emitters are presented in Table 3. Microstructures of the CVD-W were examined in the as-received condition and typical microstructures are shown in Figure 6 and 7 (chloride and fluoride, respectively). Both the chloride and fluoride microstructures were clean single phase with typical columnar grains. However, the chloride W (Figure 6) had larger and more uniform columnar grains than the fluoride material (Figure 7).

Samples of the CVD-W were vacuum heat treated at two different conditions:

(1)   Two hours at $2000^{\circ}C$ for information on the grain growth characteristics, and

(2)   One hour at $2500^{\circ}C$--an accelerated test to determine the high temperature dimensional stability of the material. These tests were performed only on the fluoride W emitter bodies. The reason for this was twofold: (a) the chloride emitter bodies were procured early in the program and the material was in its initial stages of technology, and (b) the technology of the fluoride material was more advanced and data were available on this material that established qualitatively grain growth, dimensional stability and fluorine content. The extent of grain growth resulting from a vacuum heat treatment at $2000^{\circ}C$ for 2 hours for a fluoride W sample (Figure 8) is

21

Table 3. SPECTROGRAPHIC AND CHEMICAL ANALYSIS

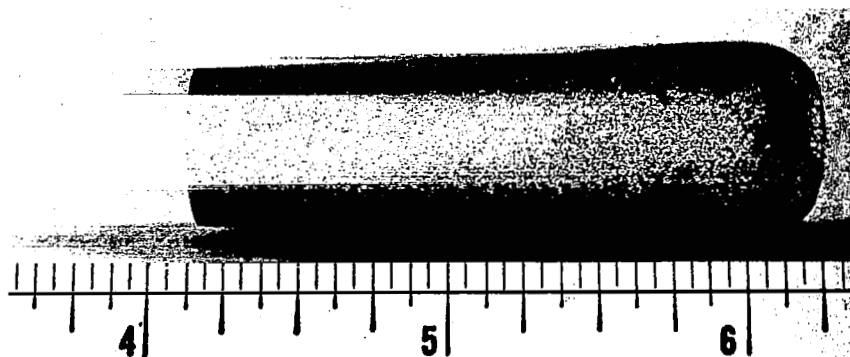| Identification	CVD-Chloride Tungsten Sample No.		CVD-Fluoride Tungsten Sample No.	
	2	8	14	15
Spectrographic Analysis:	Values reported as parts per million			
Aluminum	< 10	< 10	< 5	< 5
Cobalt	< 5	< 5	< 5	< 5
Chromium	< 5	< 5	< 5	< 5
Copper	< 2	< 2	< 2	< 2
Iron	≤10	< 10	< 10	<10
Magnesium	< 2	< 2	< 2	< 2
Manganese	< 1	< 1	< 1	< 1
Nickel	< 1	< 1	< 1	< 1
Lead	< 5	< 5	< 5	< 5
Silicon	< 20	< 20	< 20	< 20
Titanium	40	25	20	30
Vanadium	< 5	< 5	< 5	< 5
Molybdenum	< 20	< 20	< 10	< 10
Tin	20	15	30	30
Zirconium	< 100	< 100	< 100	< 100
Calcium	70	150	< 40	< 40
Chemical Analysis:				
Carbon	20	20	30	40
Hydrogen	< 1	< 1	< 1	< 1
Oxygen	< 20	< 20	< 20	< 20
Nitrogen	< 10	< 10	< 10	< 10
Chlorine	< 200	< 200	--	--
Fluorine	---	---	< 5	< 5

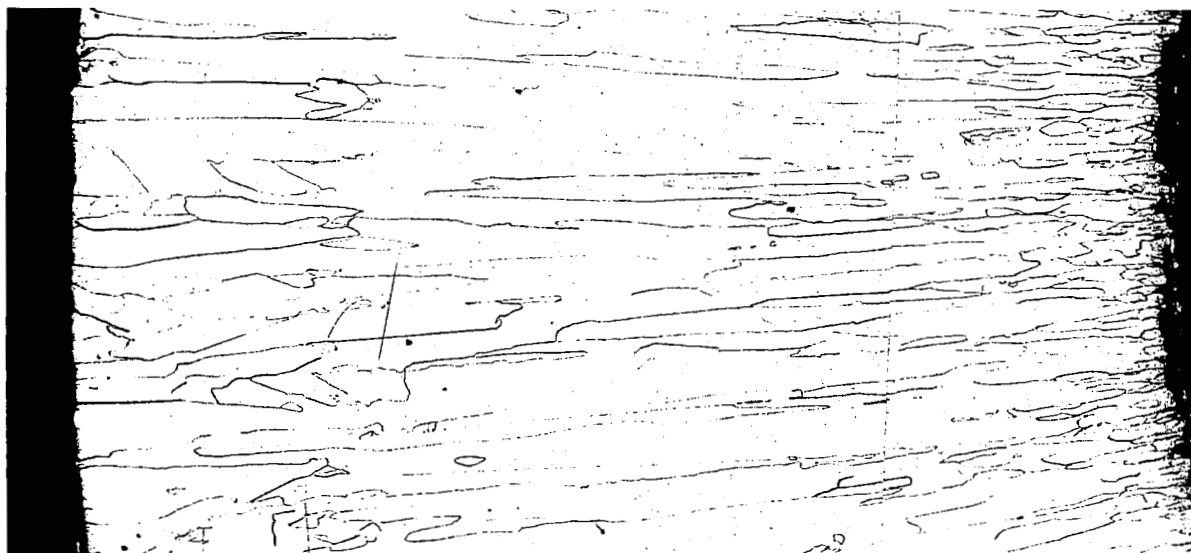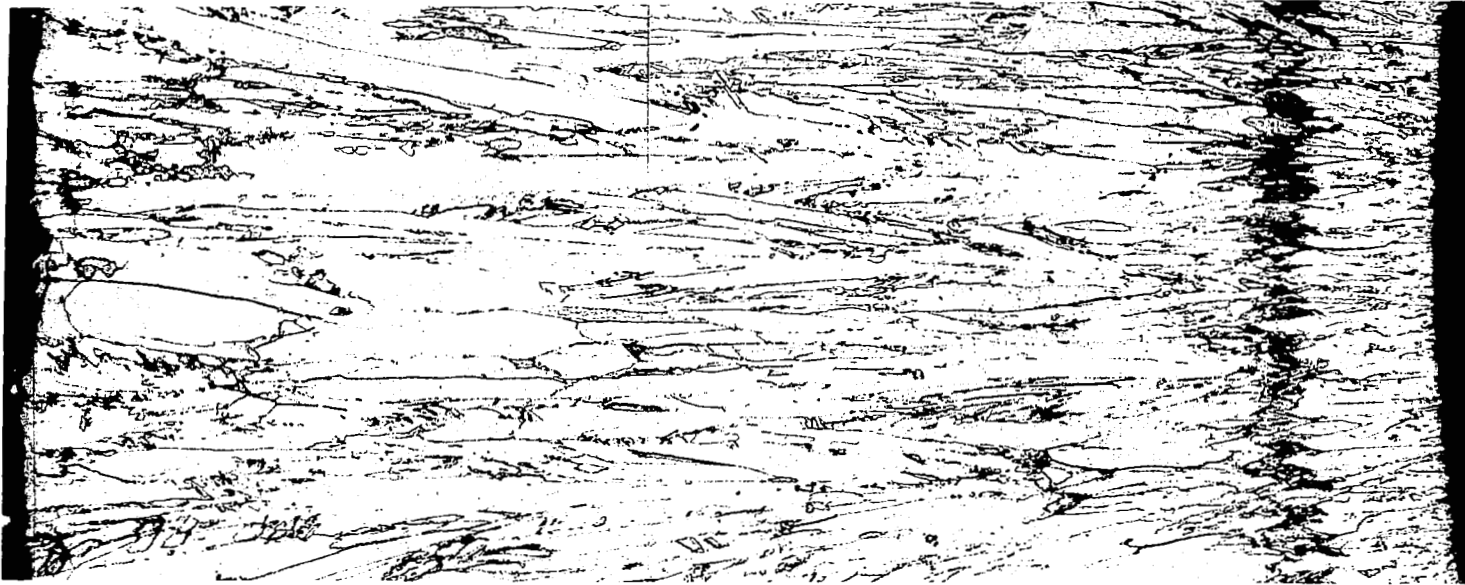Figure 5.   AS-DEPOSITED CVD-CHLORIDE TUNGSTEN
            EMITTER

Etched   50X

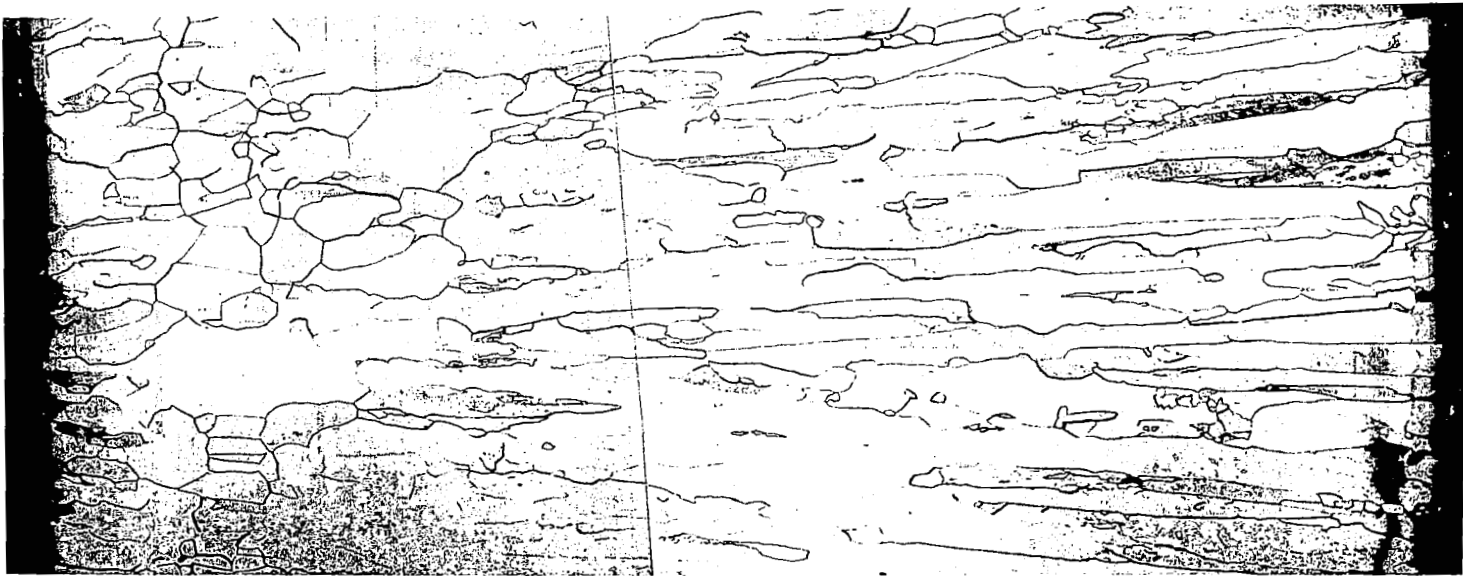Figure 6.   MICROSTRUCTURE OF AS-DEPOSITED CVD-
            CHLORIDE TUNGSTEN, SAMPLE No. 2.

23

Etched   50X

Figure 7. MICROSTRUCTURE OF AS-DEPOSITED CVD-FLUORIDE TUNGSTEN,
           SAMPLE No. 15

Etched   50X

Figure 8. MICROSTRUCTURE OF CVD-FLUORIDE TUNGSTEN AFTER
2 HOURS AT 2000°C, SAMPLE No. 15

illustrated by comparing this microstructure with that of Figure 7. After 1 hour at 2500°C, the fluoride material experienced still further grain growth (Figure 9); however, there was no evidence of void formation or dimensional changes. In general, for fluoride W with fluorine contents of approximately 25 to 30 ppm, [6] the material shows grain boundary porosity and dimensional changes. The extent of dimensional change usually is cause for reject of the material. On the basis of the results of the chemical and spectrographic analysis, microstructure and heat treatments, the emitter bodies were selected for further characterization.

2.   Vacuum Work Function Measurements

Measurements of vacuum work functions were made on emitter bodies that were machined, chemically cleaned and electropolished. The emitter was then placed in a work function apparatus.

The effective work function was obtained by placing the emitter in a thermally isolated environment and heating the emitter to high temperature using electron bombardment. The current was collected on a $10 \ cm^2$ Mo collector. Guard rings were used to adequately define the collector area.

Data were taken after the emitter reached a stable temperature and then recording:

(1)   Black-body hole temperature,
(2)   Emitter surface temperature.
(3)   Thermocouple emf,
(4)   Vacuum system pressure,
(5)   Filament voltage and current,
(6)   Bomber voltage and current, and
(7)   Two-color pyrometer reading.

An a.c. sine wave of about 17 volts peak-to-peak was applied between emitter and collector, the oscilloscope calibrated, and a picture taken of the oscilloscope trace of the voltage-current characteristic for the emitter at the

26

Etched   50X
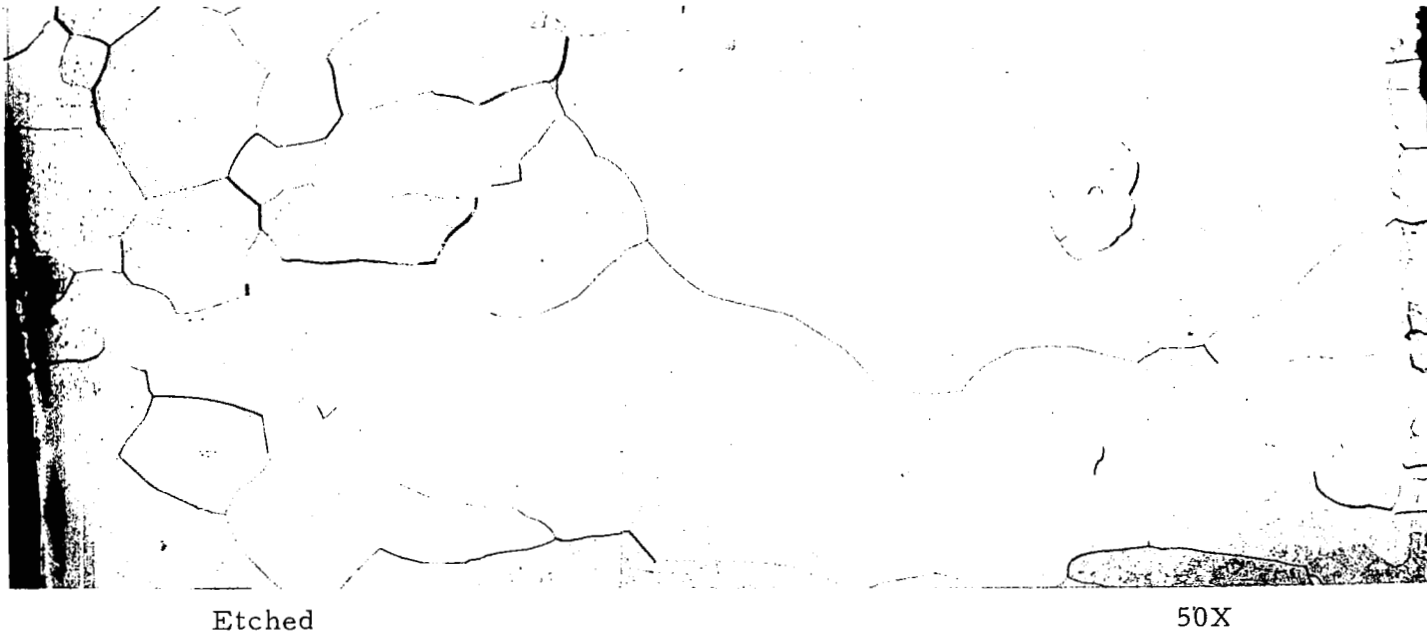
Figure 9. MICROSTRUCTURE OF CVD-FLUORIDE TUNGSTEN AFTER
           1 HOUR AT 2500°C, SAMPLE No. 15

stable temperature. To provide a more accurate trace of the characteristic, the sweep voltage between emitter and collector was changed to the d.c. mode and a manually adjustable voltage from -10 to -30 volts replaced the a.c. sweep. An X-Y plotter was adjusted to get the complete trace on an 8-inch by 10-inch plot. A sweep was taken from -10 to greater than +25 volts by slowly increasing the d.c. supply voltage. The pen was then lifted, the supply voltage reduced to -10 volts and a recording of emitter-collector voltage and current taken with a digital voltmeter. The d.c. voltage was increased in steps, with data system recording at each step providing a calibration of the complete manual d.c. sweep taken previously.

The work function for each curve was found by extrapolating the saturation current line for the positive sweep voltage back to 0 volts, calculating the saturation current density from this current value and then using the Richardson-Dushman curves for A = 120 with the known saturation current density and the temperature of the black-body hole.

The emitter surface temperature and black-body hole temperature used a disappearing filament pyrometer, calibrated against a National Bureau of Standards calibrated strip filament lamp. The thermocouple was read out as a d.c. millivolt signal by the data system with a correction being added to the reading for the 25°C reference junction temperature compensation.

Work functions were initially determined over a range of temperatures from 1400 to 1800°C in 100°C steps. The data obtained at temperatures below 1800°C always showed large scatter, while data taken at 1800°C was always reproducible within $\pm$ 0.02 volts. The scatter at the lowest temperature was due to oxygen pickup on the surface of the emitter. This effect decreases with temperature increase. When a lower temperature data point was repeated after being at high temperature, the effective work function was usually close to the higher temperature effective work function. With the passage of time, the work function increased by 3 to 5%. When data was

obtained on the temperature "up-swing"--i.e., room-ambient to 1400°C, the work function was always on the high side. Emitters were thus compared by comparing the effective work function at 1800°C.

The first three emitters had the following work functions.

(1)   C1W emitter number 2 - 4.92 ± 0.03 volts at 1800°C.
(2)   C1W emitter number 8 - 4.70 ± 0.03 volts at 1800°C.
(3)   C1W emitter number 11 - 4.76 ± 0.03 volts at 1800°C.

3.   Crystal Orientation by X-ray Diffraction

The determination of crystal orientation of the cylindrical emitter bodies required a modification to the x-ray apparatus. A special specimen holder was fabricated to receive the cylindrical W emitter. The x-ray diffraction unit consisted of a modified siemens Texture Diffractometer. The experimental geometry for the crystal orientation measurements is shown in Figure 10.

Orientation determinations were made by aiming a circular x-ray beam of approximately 1.5-cm diameter at the emitter so the beam center was on the edge of the emitter. The determination of relative intensities of the various (hkl) reflections at α = 0° used a rectangulary x-ray beam approximately 1.5-cm high by 0.2-cm wide. Nickel filtered Cu Kα radiation was used in all cases. The emitter was rotated about its longitudinal axis at about 50 to 60 rpm to get 8 to 10 complete sample revolutions per data point; thus, the beam covered the entire circumference of the emitter for a longitudinal distance of 1.5 cm. The radiation detector was set at the Bragg refraction double angle for the crystal face of interest. The emitter was then rotated (tilt) about the center of the beam and the relative intensity of the refracted x-rays detected on a counting system.

Data processing was done by programs within for the GE-235 computer. No inquiry into the effects of β rotation rate, variation of background intensity,
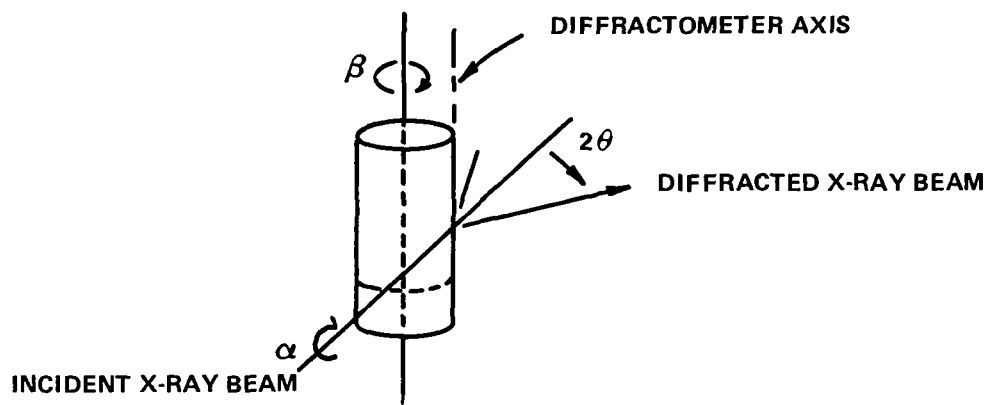
Figure 10.   EXPERIMENTAL ARRANGEMENT OF EMITTER FOR
X-RAY DIFFRACTION

or geometric factors on the observed intensity was made. The results were normalized and plotted as the fraction of the emitter sample area having <110> or <100> axes lying within the angle θ. Such a plot for several chloride W emitters with <110> axes normal to the sample surface is presented in Figure 11. Also shown on this plot are the values of the respective emitter vacuum work function.

4. Scanning Electron Microscopy of Emitter Surfaces

For those emitter bodies that were etched to yield the desired (110) crystal orientation, scanning electron microscope examination was performed. A fluoride W emitter with a preferred (100) crystal orientation was deep etched to yield (110) crystal facets. A scanning electron microscope photograph of a typical surface structure is illustrated in Figure 12.

OTHER MATERIALS

The collector material, Nb, was produced by a vacuum electron beam melting process. Spectrographic and chemical analysis, hardness and micro-structural examination were performed to assure that the Nb satisfied our materials specifications.

Alumina ceramic parts were fabricated from high purity material. The Al_2O_3 used in the ceramic-to-metal seal had to satisfy the requirement of Cs vapor compatibility. Therefore, an Al_2O_3 with low silica content was specified.

The W-Re stem material was produced by chemical vapor deposition to our specifications. The material received chemical and spectrographic analysis, microstructural examination and high temperature heat treatments. The results of these tests were used to determine acceptance or rejection of the material.
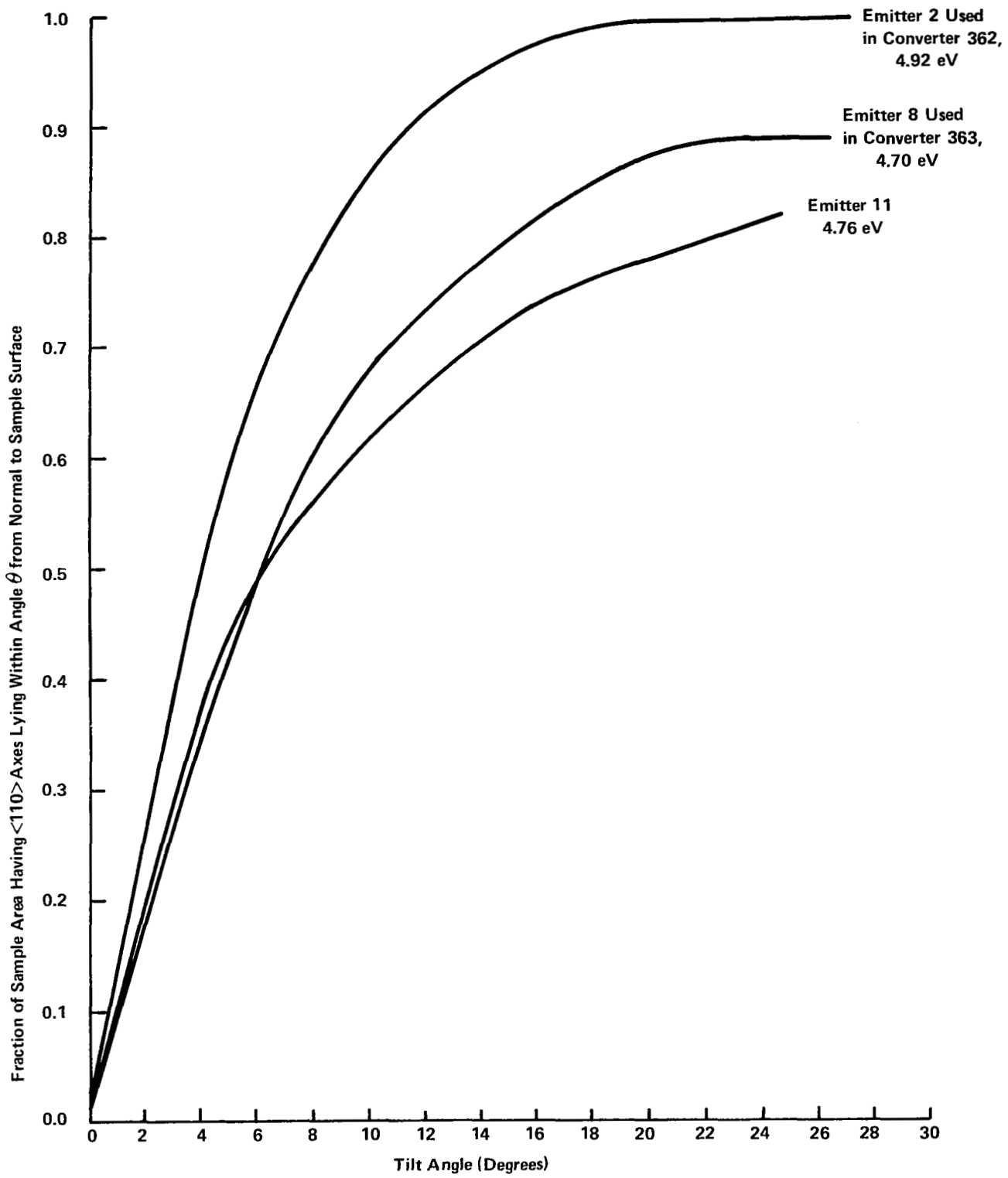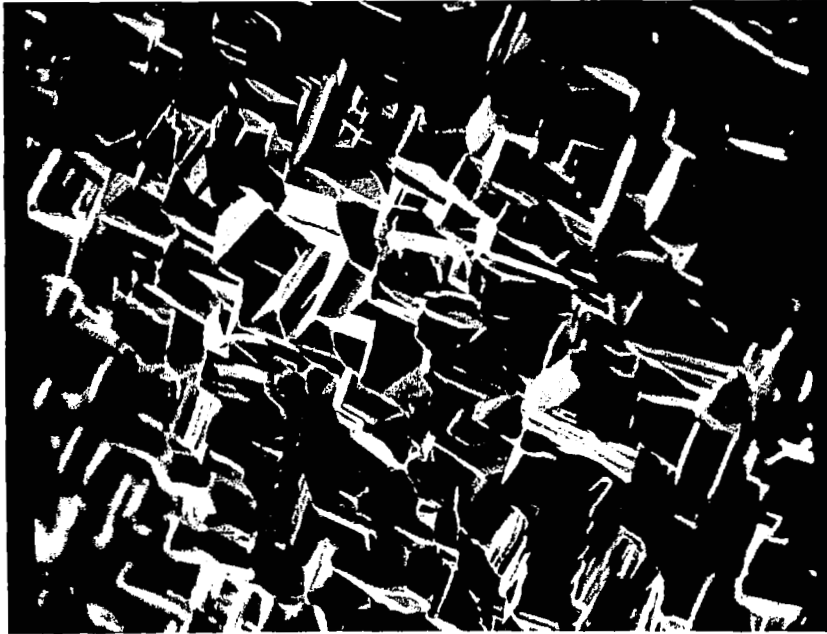
Figure 11. PLOTS OF <110> AXES OF CHLORIDE TUNGSTEN
EMITTERS AS FUNCTION OF TILT ANGLE

Etched   300X

Figure 12. SCANNING ELECTRON MICROSCOPE OF SURFACE
            MICROSTRUCTURE OF FLUORIDE TUNGSTEN
            SAMPLE No. 15 AFTER DEEP ETCH

TEST SERIES PERFORMANCE RESULTS

Three cylindrical thermionic converters were built and tested. The first two (362 and 363) contained emitters vapor deposited by the hydrogen reduction of WCl_6. After machining they were electropolished to expose the preferred (110) crystal orientation obtained by the deposition process. The third converter contained an emitter fabricated by the WF_6 deposition process which normally yields the (100) surface crystal orientation. However, after machining, this emitter was heavily electroetched to expose (110) crystal facets on the emitter surface (described elsewhere in this report). While the detailed descriptions of each of these converters are described in the next sections, several general comments can be made regarding the thermal, mechanical and thermionic behavior of these devices.

THERMAL CHARACTERISTICS

The thermal design of the converters proved to be adequate to meet the desired objectives as outlined earlier. That is, no problems with secondary Cs reservoirs were encountered during operation of the three devices. Excellent decoupling of the emitter and collector temperatures from the Cs reservoir temperature was achieved, allowing data taking at various Cs pressures without readjusting other temperatures. The ceramic-to-metal seal operated in the desired temperature range. One thermal problem did exist on the first converter (362)--insufficient control over the collector heat balance. When the collector heat rejection path was made small enough so that adequate outgassing temperatures could be achieved during processing, the collector temperature ran too hot during full power operation at high current densities (when the reject heat is much higher). This constraint limited the maximum current density at which the converter could be operated. The problem was resolved on converters 363 and 364 by changing to a much higher power capacity Ta coaxial heater surrounding the collector and by making the heat rejection capability larger.

Emitter temperature measurements using the high temperature W versus W-Re thermocouples also proved difficult to achieve. Cs resistant ceramic-to-metal seals for thermocouple feedthroughs were eliminated by relocating the holes in the emitter wall on the vacuum side of the converter envelope (near the electron bombardment filament). This decision, in turn, caused difficulty due to the tendency for the filament to electron bombard the thermocouple leads. This tendency, together with the general difficulties associated with high temperature thermocouples, prevented amassing numerous data points to compare emitter temperatures and temperature distributions. However, using a Ta sleeve to shield the thermocouples from the bombardment filament aided greatly in alleviating this problem in converter 363.

Figure 13 shows a comparison plot of emitter temperatures determined by various methods on converter 363 and also shows a negligible effect due to varying the Cs temperature on these measurements. Compared are:

1. Thermocouple measurements 0.8-inch deep
2. Thermocouple measurements
3. The optical pyrometer reading
4. Temperature inferred by the Wilkins diagnostic technique[1] using both the knee and ignition currents.

The data show an approximately $60^{\circ}C$ temperature gradient along the emitter with the coolest end being near the emitter lead as would be expected. The optical pyrometer measured a temperature somewhat in between these two thermocouple measurements but favoring the top end. The temperature determinations by the Wilkins' diagnostic technique were in very good agreement with the averages of the thermocouple readings using both the ignition and knee currents. Pyrometer measurements were chosen for controlling emitter temperatures for the three converters during performance and life testing. These pyrometer measurements were chosen for control because of repeatability and they were in good agreement with both thermocouple readings and Wilkins' diagnostic techniques (within $20^{\circ}C$).
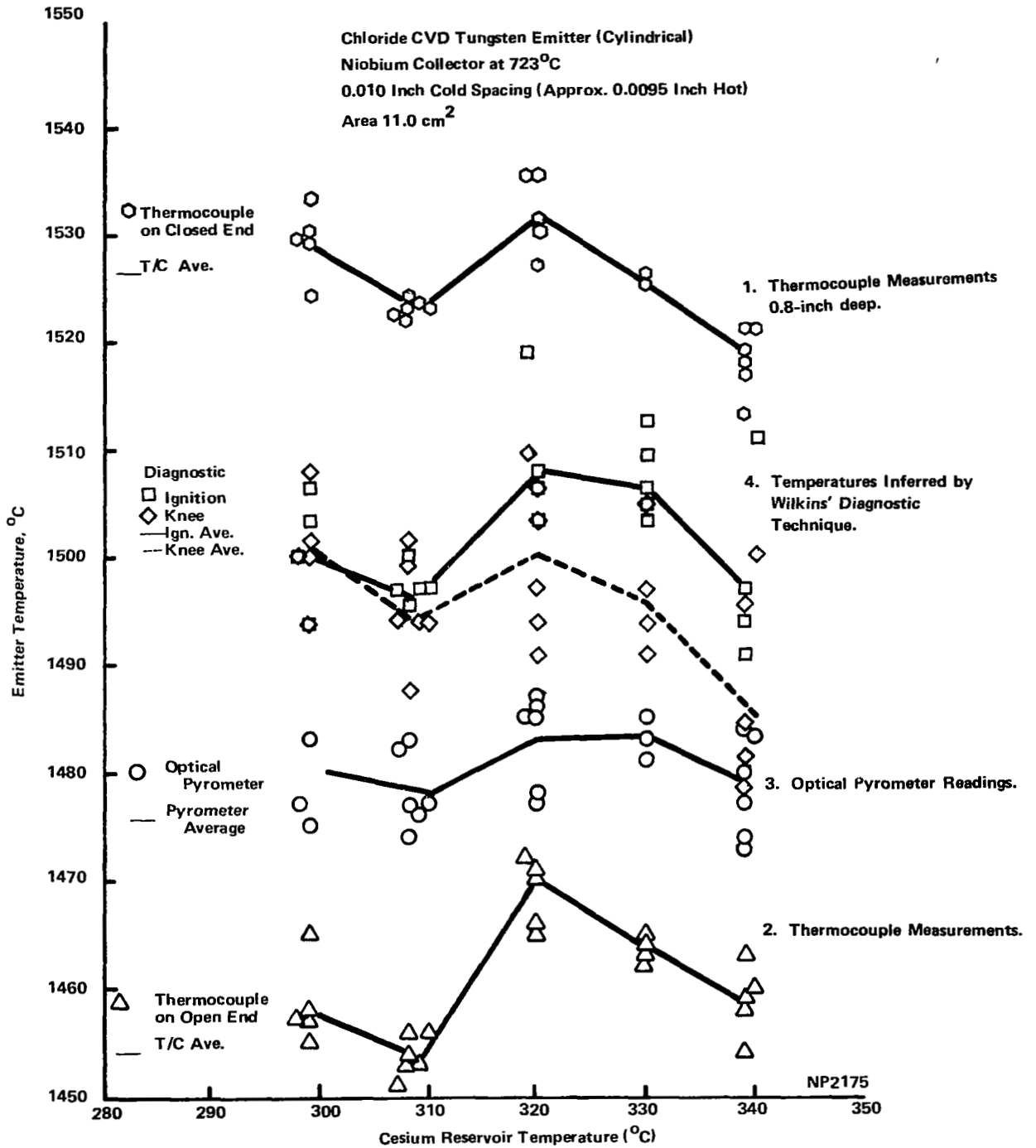
Figure 13. COMPARISON OF DIAGNOSTIC AND THERMOCOUPLE
MEASURING ON OUT-OF-PILE CYLINDRICAL CONVERTER
363

MECHANICAL BEHAVIOR

Mechanically, the three converters behaved as expected, with two exceptions. Early in the testing sequence, a problem occurred due to emitter-collector shorts. These shorts were found to be related to two possible causes. First, a heat shield above the top of the emitter could have been misplaced. Second, the possibility of the spacer pins becoming dislodged from the ceramics at the bottom of the emitter existed. Both of these possible causes were corrected. The second mechanical problem developed late in the operation of converter 364 when a very small leak developed between the Cs and vacuum environments. This leak in no way hindered the converter performance as the amount of Cs (1 gram) which had been loaded into the converter was sufficient to complete the life testing. However, the leak did shorten the filament life by about a factor of three, due to the resulting positive ion bombardment of the filament. Filament changes were made by letting the bell jar down to dry nitrogen to prevent any air from entering the converter and oxidizing the Cs. This nitrogen was complete exhausted from the converter again before testing was resumed. The location of this leak, while not positively identified, is thought to be in the electron beam welded region between the emitter and the W-Re emitter support tube. When the emitter was etched to produce a preferred surface, this weld area was inadvertently etched, possibly resulting in a weaker joint.

With these two exceptions, the mechanical design proved to be quite satisfactory. Each of the weld and braze joints maintained their integrity, including the ceramic-to-metal seals, for the desired converter lifetime. The filament design proved easy to fabricate and replace in the converter. Some filament changes were completed within a 4-hour period.

THERMIONIC TESTING

Each of the three converters were subjected to an initial performance map, a steady-state test period of 5000 hours, and a final performance map. The performance maps consisted of taking current-voltage plots at emitter

temperatures of 1400, 1550, and 1700°C; collector temperatures in the range of 600, 800, and 1000°C; with at least four Cs pressures for each combination of the above conditions.

The steady-state testing occurred at an emitter temperature of 1700°C, with collector and Cs reservoir temperatures at or near optimum conditions. During the steady-state testing period, cesiated emitter and collector work functions were measured at 1000, 3000 and 5000 hours. Each converter was operated at a different current density--converter 362 at 7.8 Amps/cm^2, converter 363 at 13.7 Amps/cm^2, and converter 364 at 10 Amps/cm^2. The current density for converter 362 was limited due to the heat rejection limitation mentioned earlier; converter 363 was operated at a current density representing its maximum power point; and converter 364 was operated at the current density which is most representative of presently envisioned thermionic reactor systems. The power output at the 10 Amps/cm^2 point either remained steady (converter 364) or increased (converters 362 and 363) during the 5000 hours of life test operation. The detailed operation of these devices is discussed in the next section, followed by a section comparing the performance of the three devices.

CONVERTER 362

1.   Emitter Characterization

The emitter for this converter was produced by the hydrogen reduction of WCl$_6$ at 1000°C. The chemical and spectrographic analyses are reported in Table 3, sample No. 2. An as-deposited microstructure, illustrated in Figure 6, was single phase with typical columnar grains. The x-ray diffraction data, plotted in Figure 11, show a high degree of preferred (110) crystal orientation. The vacuum work function, 4.92 eV, was high relative to the value of approximately 4.5 eV for (100) oriented W. The surface of the emitter after electropolishing is illustrated in Figure 14. After vacuum heat treatment for 200 hours at 1675°C, there was evidence of grain growth, thermal grooving of the grain boundaries and the surface topological changes (Figure 15).
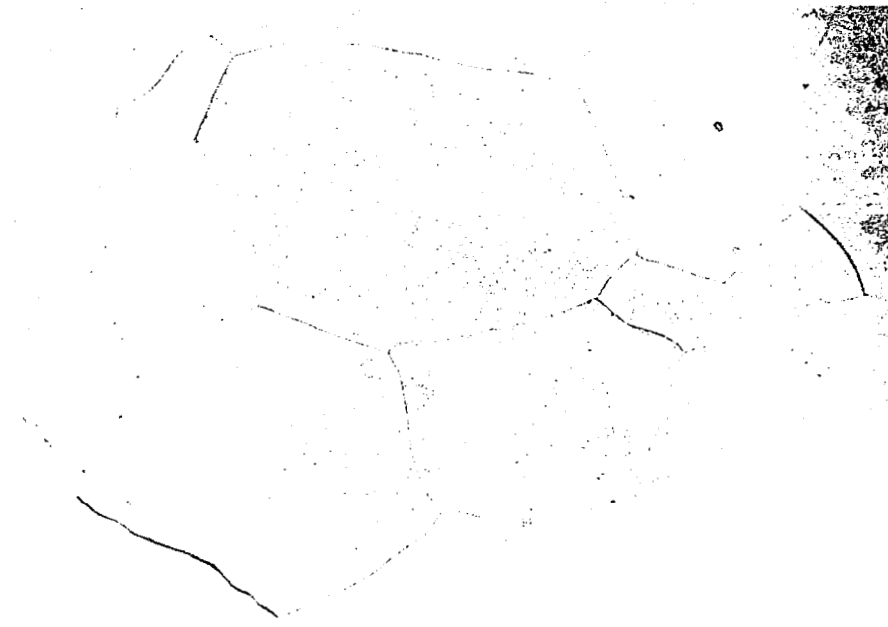
Electropolished   100X

Figure 14.   SURFACE MICROSTRUCTURE OF SAMPLE No. 2
             EMITTER AFTER ELECTROPOLISHING
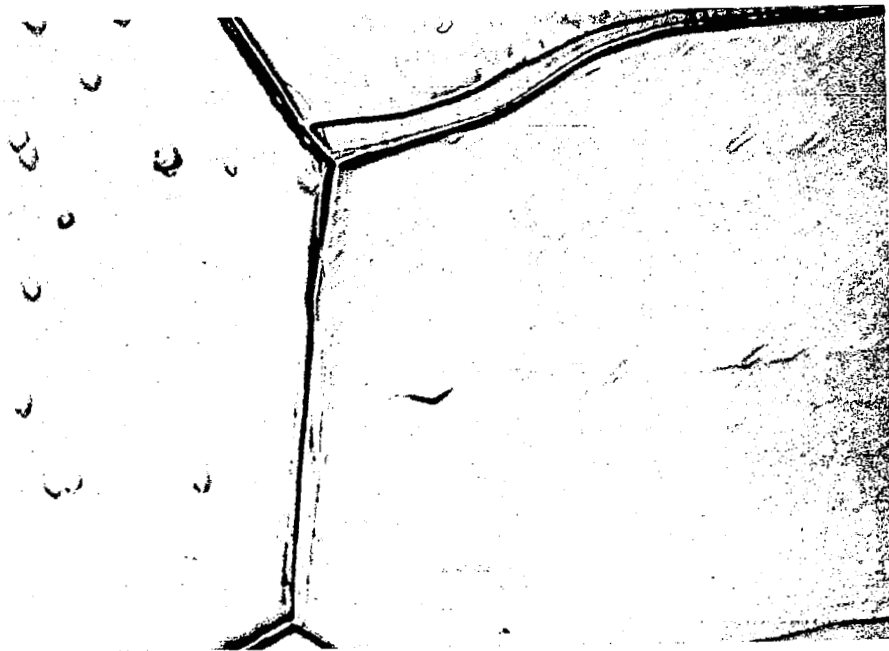
Electropolished   250X

Figure 15.   SURFACE MICROSTRUCTURE OF EMITTER
             SAMPLE No. 2 AFTER 200 HOURS AT 1675°C

This emitter was selected for use in the first prototype converter. However, during the initial operation of this device, an internal electrical short circuit occurred between the emitter and collector potentials. The device was disassembled and the cause of the short circuit investigated. The emitter was examined visually and metallographically and dimensional measurements were performed. No changes were detected and, therefore, the emitter was recommitted to thermionic testing in converter 362.

2.   Thermionic Performance

Following emitter characterization and first prototype converter fabrication, the assembly was processed and the vacuum work function of the emitter measured in situ prior to introduction of Cs. A value of 4.68 eV was measured--significantly lower than that determined during the emitter characterization. Cesium was then introduced into the device and initial testing started. At this time, an emitter-to-collector short occurred. The converter was then disassembled and the short was corrected.

The converter was then reassembled and processed for 115 hours at an emitter temperature of 1700°C and a collector temperature of 820°C. The final pressure obtained was 2×10^{-8} torr with the converter hot. The emitter work function was then remeasured and found to be 4.45 eV (these variations are discussed later). Following this measurement, Cs was distilled into the converter and the device was readied for testing.

Prior to initial testing, the converter was subjected to a stabilizing run of approximately 200 hours at an emitter temperature of 1700°C, a collector temperature of 600°C, and a Cs reservoir temperature of 350°C. Following this period, an initial performance map was taken at various combinations of emitter, collector, and Cs reservoir temperatures. Figure 16 shows the I-V characteristics for an emitter temperature of 1700°C, a collector temperature of 700°C and several Cs reservoir temperatures.
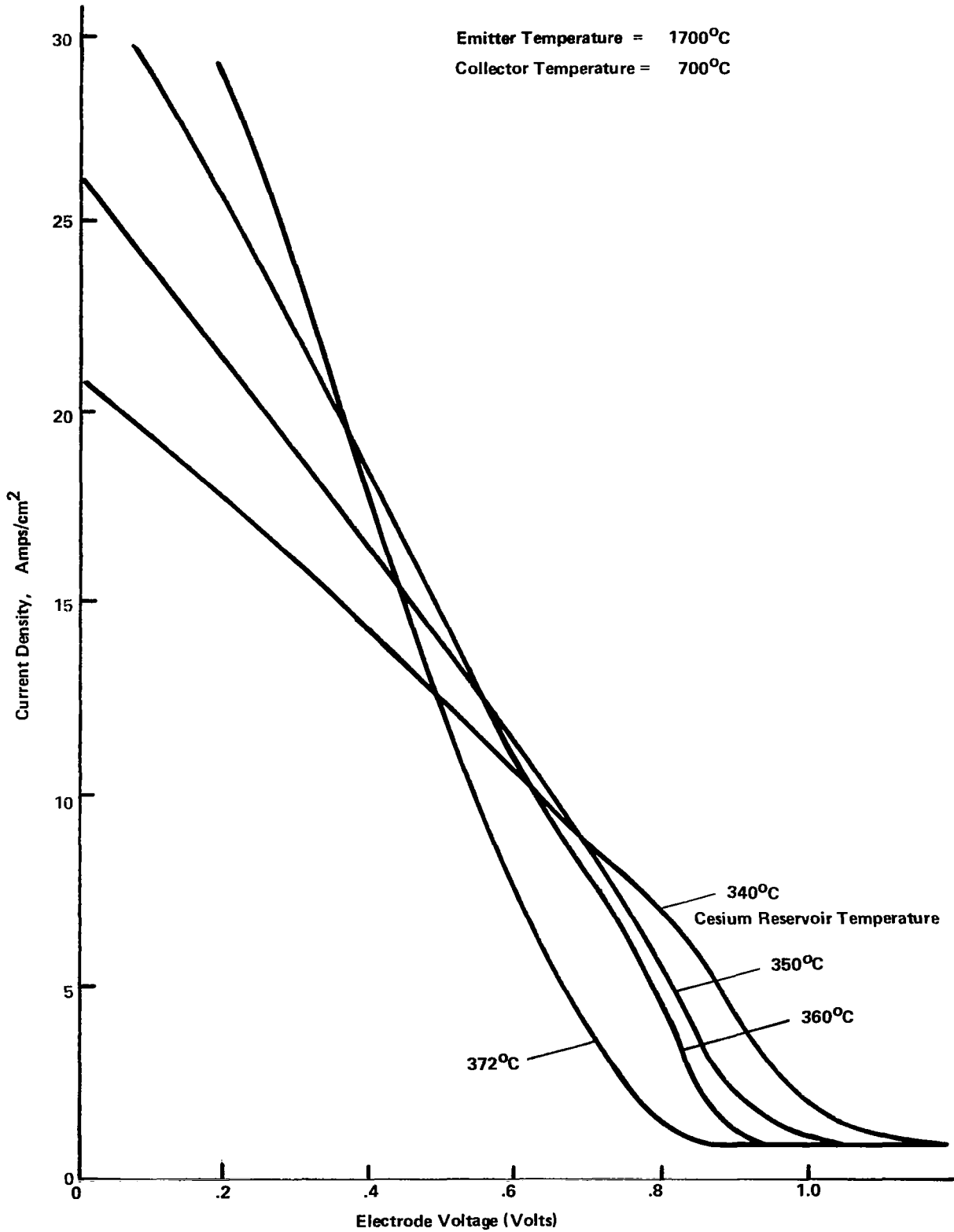
Figure 16. CONVERTER 362 VOLT-AMPERE CHARACTERISTICS--
INITIAL TESTING

41

The converter was next placed on life test at the conditions shown in Table 4.

Table 4.

Input Power Density	52.8 W/cm^2
Output Power Density	5.4 W/cm^2
Output Current Density	7.75 Amps/cm^2
Output Voltage	0.70 Volts
Emitter Temperature	1710°C
Collector Temperature (Optimum)	700°C
Cesium Reservoir Temperature	360°C

Direct current operation at a higher current density was precluded due to a limitation in the collector heat rejection system as described earlier. The Cs reservoir temperature was set, however, at the value which would give maximum power output if the converter were run at the higher current density (approximately 15.5 Amps/cm^2 as indicated in the initial performance maps).

The significant parameters maintained during the 5000-hour life test are plotted in Appendix A-1. The power input and power output track each other and are within about 5% of the initial life test point throughout the 5000 hours. The optimum Cs temperature at the maximum power point also remained very stable through this period (approximately 5°C maximum variation).

Following the 5000-hour life test, a performance map was again taken for the various emitter, collector and Cs reservoir temperatures. Figure 17 shows the I-V characteristics for an emitter temperature of 1700°C and a collector temperature of 710°C. Performance characteristics improved after 5000 hours of life testing (comparing Figure 16 with Figure 17).

Periodic checks of the higher current regimes were made during the life testing using an a.c. sweep. Figure 18 shows the maximum power point as a function of time using these measurements. From this figure, it can be seen that the maximum power point increased markedly during the first 1000

Figure 17. CONVERTER 362 VOLT-AMPERE CHARACTERISTICS --
FINAL TESTING (5011 HOURS)

43
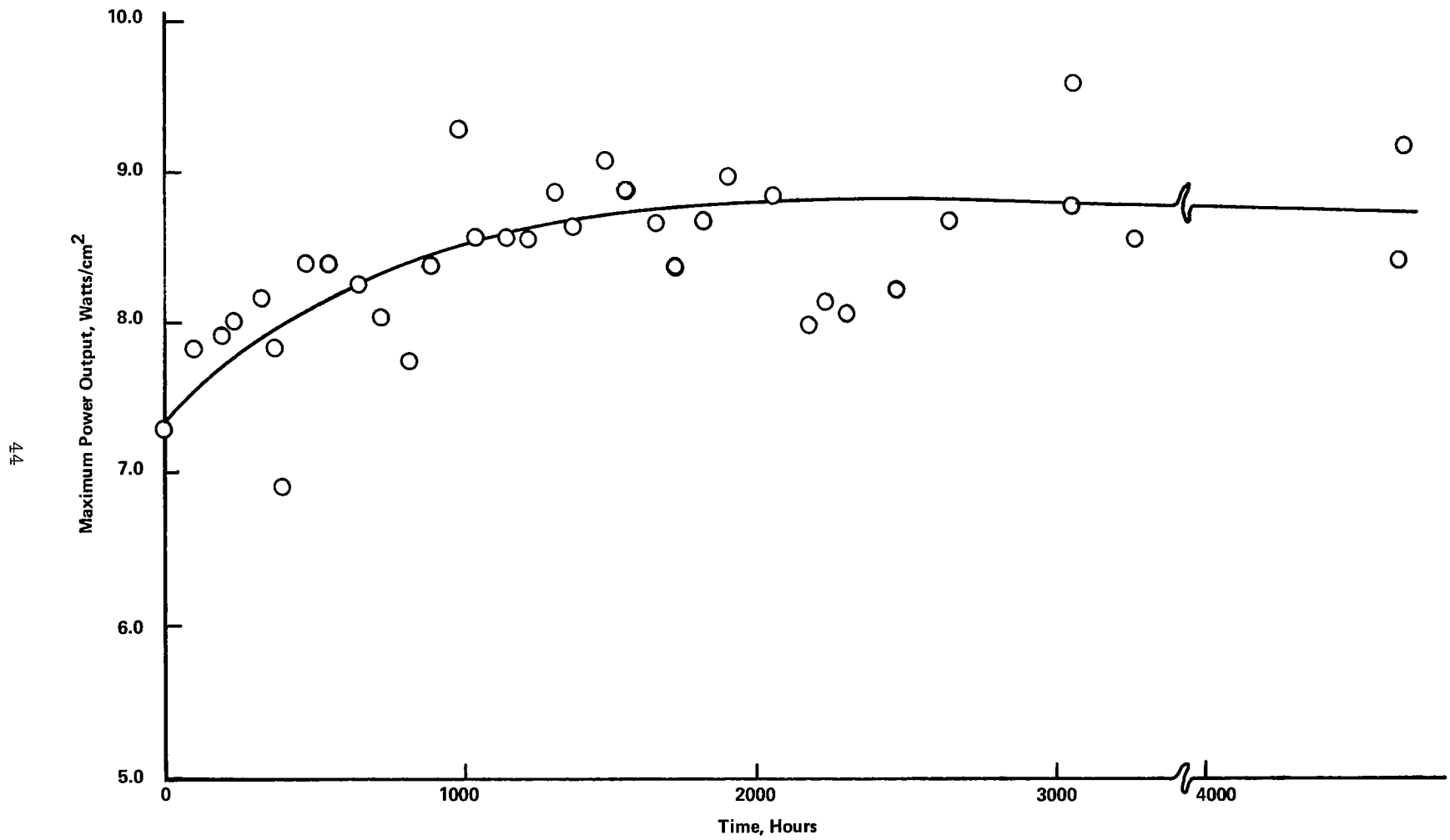
Figure 18. CONVERTER 362 MAXIMUM OUTPUT POWER DENSITY AS A FUNCTION OF TIME

hours, but was relatively steady thereafter. The same effect can be seen by comparing the initial and final performance at 10 Amps/cm^2 versus emitter temperature as shown in Figure 19.

This increased performance is believed to be due to changes in emitter work function. Some indications of cesiated emitter work function change are apparent from the T/T_R plots for the emitter as shown in Figure 20, although there is significant scatter in the data.

A better measurement of the emitter electrode change is shown by the vacuum work function measurement which was taken in situ following the 5000-hour test (and confirmed later during the post-test analysis described later). Following the life test, the Cs reservoir was removed and the converter replaced in the vacuum test stand. At 1700°C, a vacuum work function of 4.71 eV was measured and this value remained stable over a test time of 200 hours. Comparison of this work function with other historical measurements of the emitter is shown in Table 5.

Table 5. EMITTER VACUUM WORK FUNCTION MEASUREMENTS ON CONVERTER 362

	Condition	Work Function (Volts)
(1)	Initial, before assembly into converter	4.92
(2)	After assembly into converter, prior to introducing Cs	4.68
(3)	Removed due to internal short and reassembled into converter, before introducing Cs	4.45
(4)	After 5000-hour test at 1700°C in situ, Cs removed	4.71
(5)	In vacuum work function apparatus after 5000 hours, emitter removed from the converter	4.68
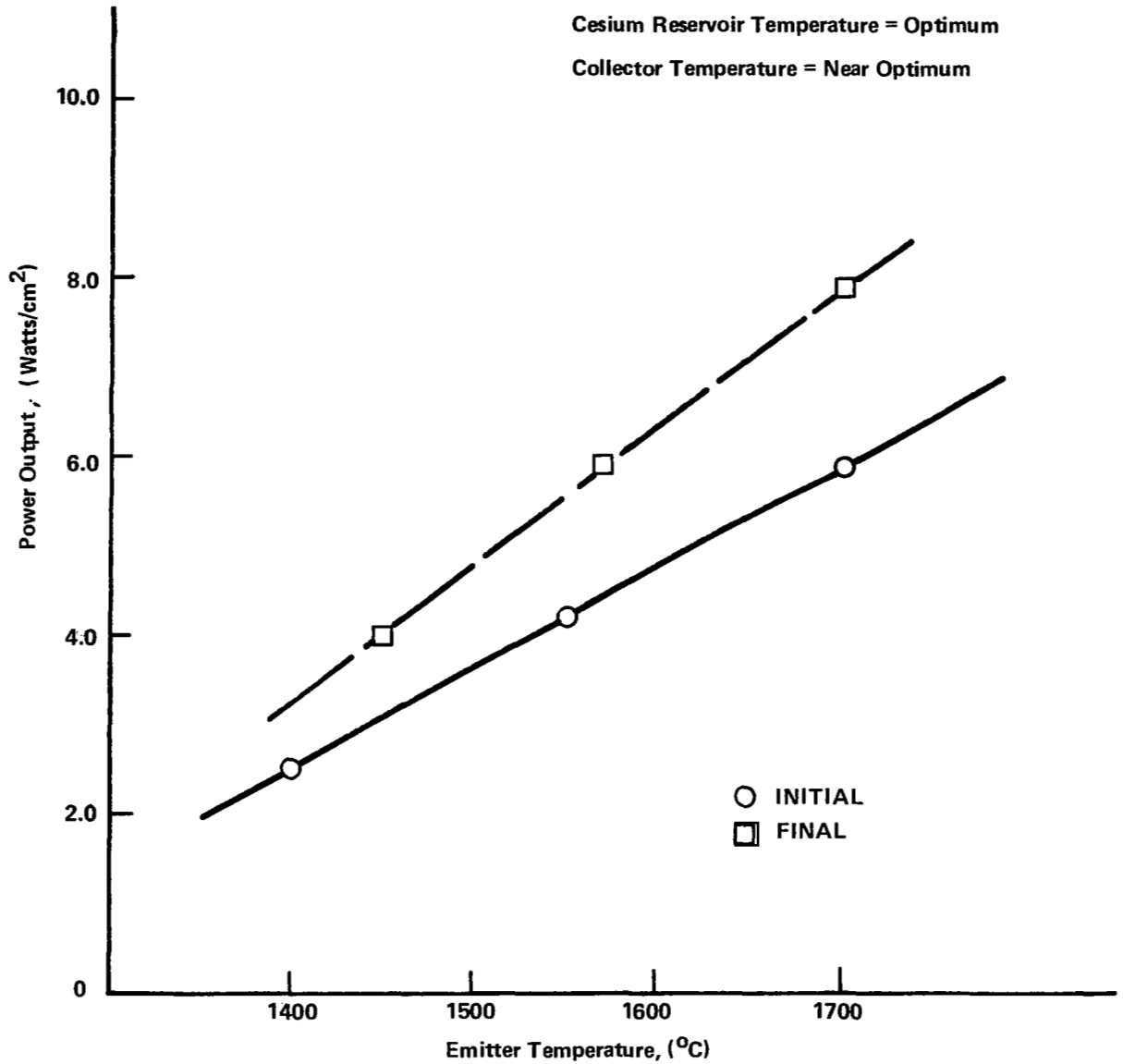
Figure 19. CONVERTER 362 OUTPUT POWER DENSITY AT A CURRENT DENSITY OF 10 Amps/cm^2
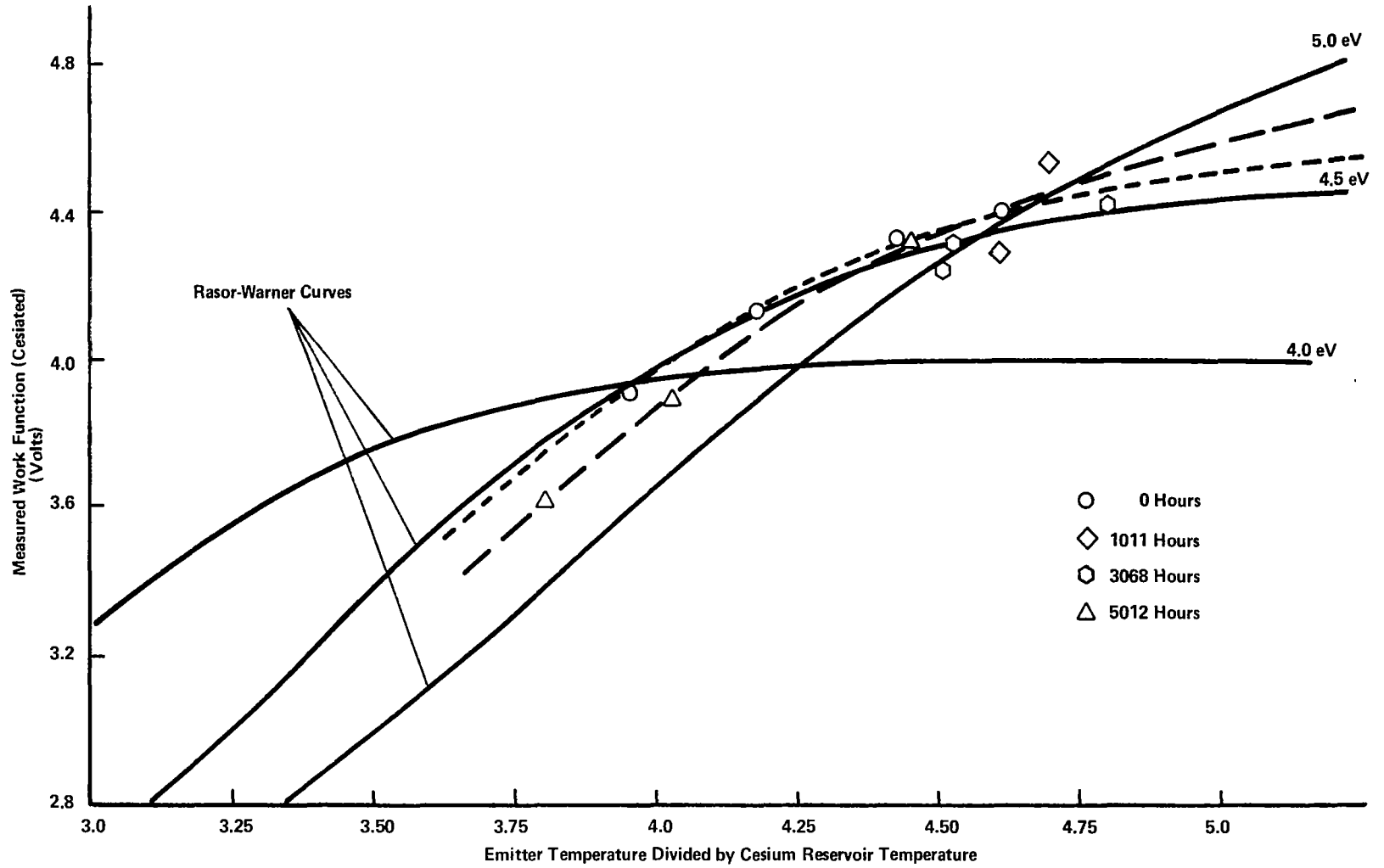
Figure 20. CONVERTER 362 CESIATED EMITTER WORK FUNCTION
MEASUREMENTS

These data indicate a significant change in work function between steps (1) and (2) and another between (2) and (3). The reason for these changes has not been definitely determined. However, the change from step (3) to step (4) could explain the increase in converter performance with increasing time during the first 1000 hours. A possible cause of these work function changes is discussed in the post-test examination portion of the report which follows.

3.   Post-test Examination

    a.   Emitter Examination

        After the 5000-hour life test, the Cs was removed from the converter by a low temperature heating cycle while maintaining the Cs reservoir at room temperature. Following this operation, the Cs reservoir was removed, the converter placed in the vacuum test stand and vacuum work functions were performed on the emitter. These results have been reported in a previous section.

        In the process of disassembly, dimensional measurements were performed on the emitter and no dimensional changes were observed. The emitter surface was very clean as shown in Figure 21. Surface examination of the emitter revealed thermal etched grain boundaries and very large grains (Figure 22). This surface microstructure is typical of other surfaces of CVD-W that have operated for prolonged periods at temperatures of 1600 to 1800°C.

        In order to determine if the preferred crystal orientation of the emitter had changed during the 5000-hour test, x-ray diffraction of the emitter surface was repeated. The before and after test data are plotted as the fraction of sample area having <110> axes lying within angle θ from the normal to the surface versus tilt angle in Figure 23. Although the data show a small change in the (110) poles, there were very large fluctuations in intensity as the sample was rotated which is an indication of very large grains

Figure 21. 362 EMITTER AFTER 5000-HOUR TEST
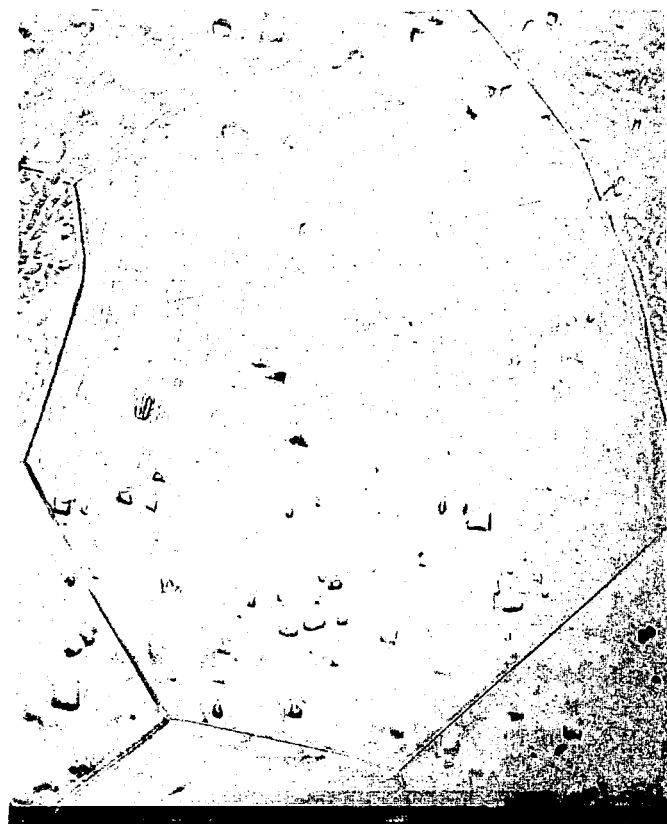
100X

Figure 22. EMITTER SURFACE AFTER TEST
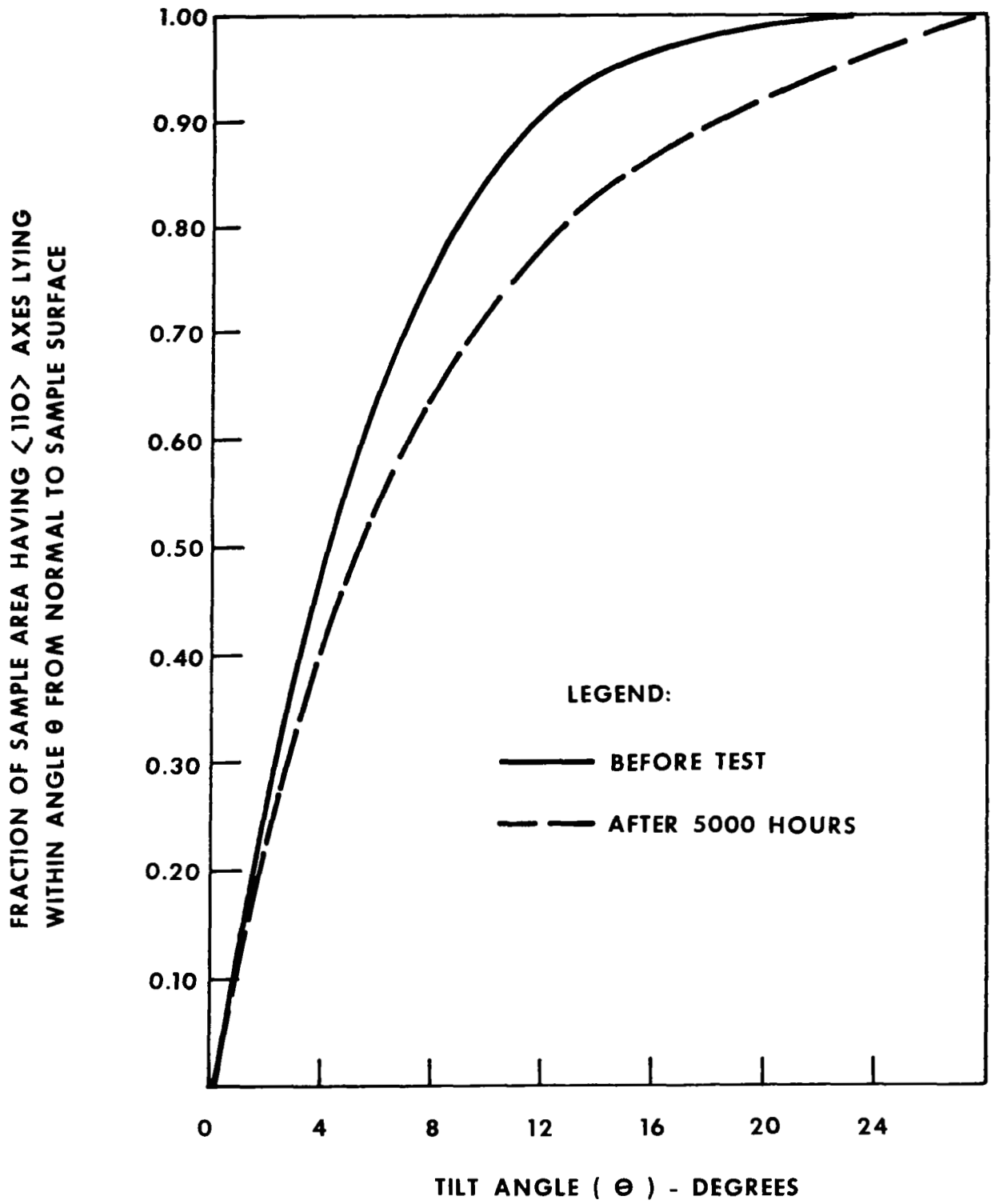
Figure 23. X-RAY ANALYSIS OF 362 EMITTER SURFACE

in the specimen. This effect leads to poor counting statistics and may account for the difference between the two curves shown in Figure 23. The (211) and (200) reflections were measured for $\alpha = 0^{\circ}$ and no significant intensity over background was observed for either of these planes.

After the x-ray diffraction analysis, the emitter was electro-etched to determine the surface orientation by this technique.[7, 8] Upon etching the surface, very large grains became very discernible. The etch pit geometry corresponded to crystal orientations predominantly of (110) orientation. However, there were a few grains of (114) and other orientations such as (112) and (111)--see Figure 24.

After the etch pits were introduced and during the course of surface examination, a second phase, Widmanstatten or acicular in nature, was observed (Figure 25). This phase was present in sufficient quantities to permit identification by x-ray diffraction. A weak x-ray diffraction was obtained, the lattice was indexed and the second phase was tentatively identified as tungsten carbide (WC). Two possible sources of carbon have been identified: the vacuum firing system which uses an oil diffusion pump and electric discharge machining operation which were used to make the emitter thermocouple holes.

Scanning electron microscope examination of the surface was performed prior to destructive metallography. The surface appeared smooth except for the appearance of a few scattered acicular or needle protrusions (Figure 26). These observations corroborate the findings of the conventional metallographic examination.

A transverse section of the emitter which included a thermo-couple hole, was prepared for metallographic examinations. Observations of this section were made both before and after etching. The microstructure of the Cl CVD-W had very large grains (Figure 27). In the region of the thermocouple hole (Figure 28) no second phase or contamination associated
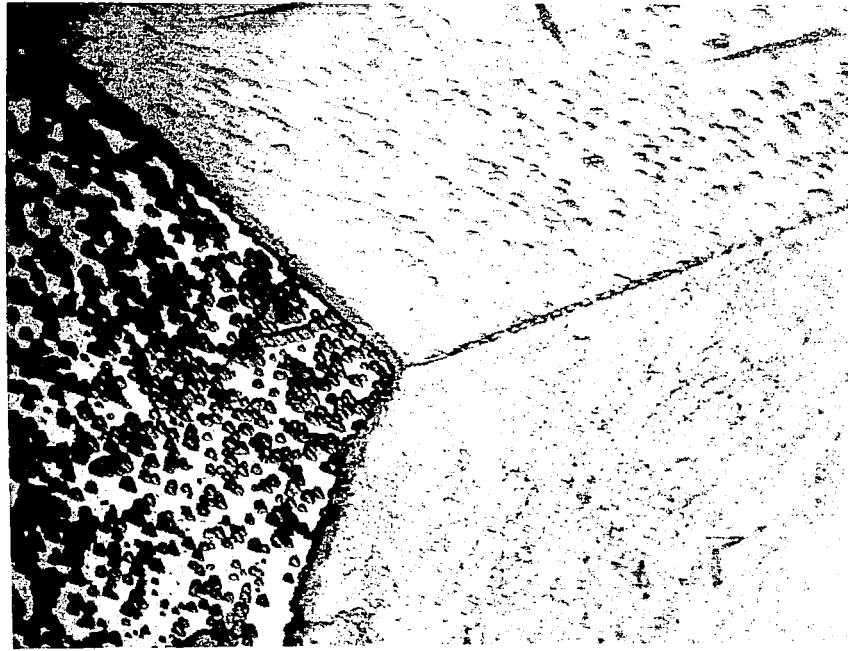
500X

Figure 24. SURFACE ETCH PITS ON 362 EMITTER

500X

Figure 25. ACICULAR STRUCTURE ON 362 EMITTER
SURFACE AFTER ETCHING

3000X

Figure 26. SCANNING ELECTRON MICROSCOPE
PHOTOGRAPH OF 362 EMITTER SURFACE

53
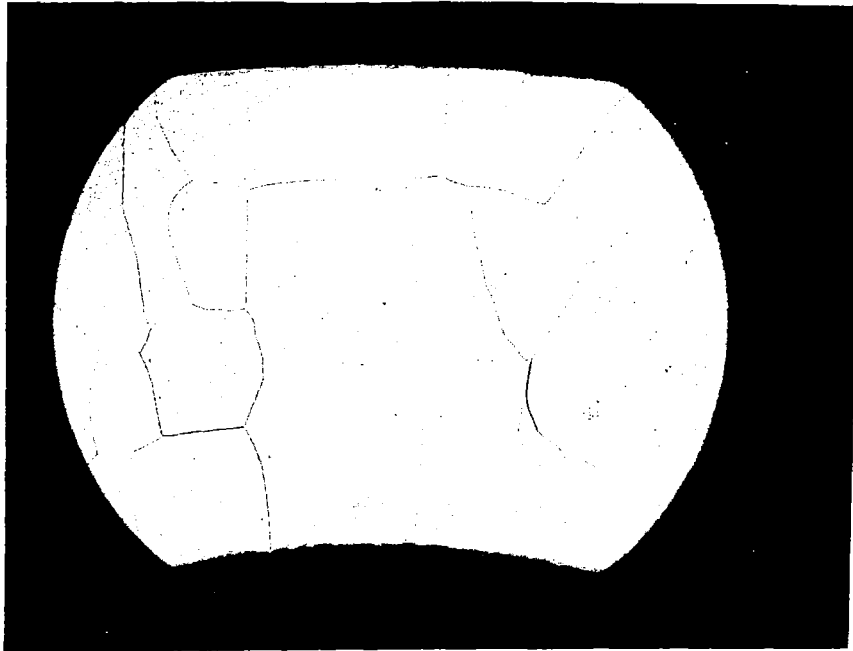
Etched   25X

Figure 27. LARGE GRAINS IN TRANSVERSE SECTION OF
            EMITTER 362
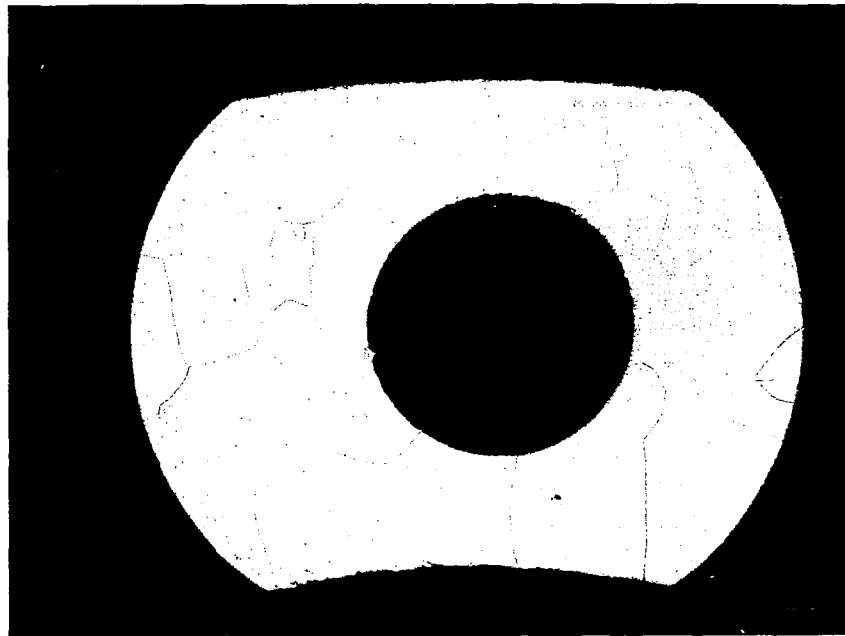
Etched   25X

Figure 28. THERMOCOUPLE HOLE IN TRANSVERSE
            SECTION OF EMITTER 362

with EDM was observed. At higher magnification, the grain boundaries in this region were clean--i.e., no second phases. However, observations at the surface revealed the presence of a second phase which penetrated at the grain boundaries of the W. The concentration of this phase was greater at the surface and rapidly diminished in progressing from the surface. These results indicate that the surface contamination is not associated with the EDM process but may be related to the vacuum firing in the oil diffusion system.

The contamination of the surface with carbon would alter the vacuum work function and, hence, performance of the converter. It is hypothesized that the presence of carbon on the emitter is responsible for both the variations in work function measurements and the measured changes in the converter maximum power point. It is important to note that the small amount of carbon present would not influence the x-ray results of crystal orientation.

b.   Collector Examination

A comparison of the pre- and post-dimensional measurements of the Nb collector revealed no change. Visual examination of the surface revealed a clean surface with very large grains as illustrated in Figure 29, a photograph of a longitudinal section of the collector. The surface was also examined under a scanning electron microscope and other than evidence of the machining marks no unusual surface features were discerned. A typical scanning electron microstructure of surface is shown in Figure 30.

The collector surface was subject to x-ray fluorescence and spark emission analysis spectrography. There was no evidence of W or other minor impurities on the Nb collector surface. On the basis of these data, it would appear that the observed changes in converter performance are associated with the changes in the thermionic characteristics of the emitter.

After these examinations, a transverse section of the collector was prepared for metallographic examination. The microstructure of the Nb revealed very large grains and a clean single phase microstructure (Figure 31).

Figure 29. LONGITUDINAL SECTION OF NIOBIUM COLLECTOR
OF CONVERTER 362
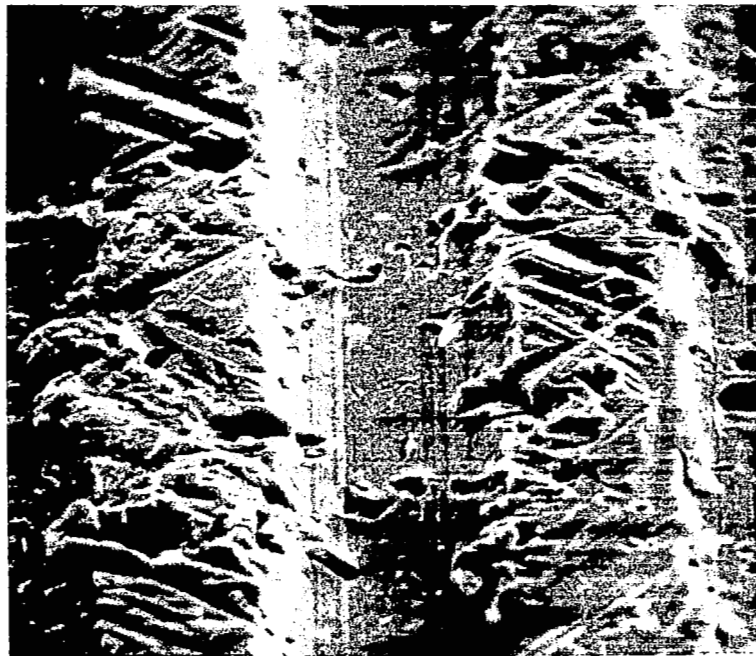
1000X

Figure 30. SCANNING ELECTRON MICROSCOPE VIEW OF THE
COLLECTOR SURFACE

56
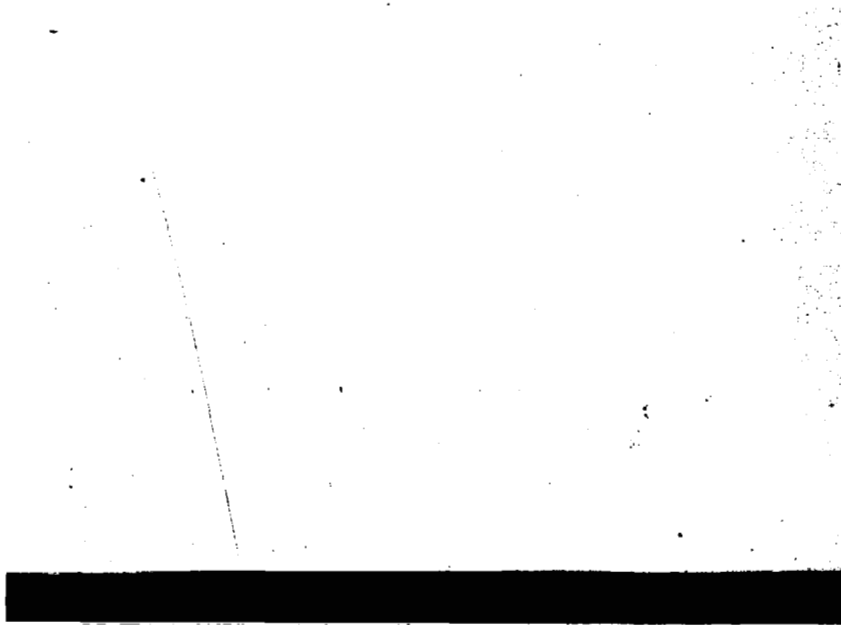
Etched   100X

Figure 31. MICROSTRUCTURE OF TRANSVERSE SECTION
            OF NIOBIUM COLLECTOR OF CONVERTER 362
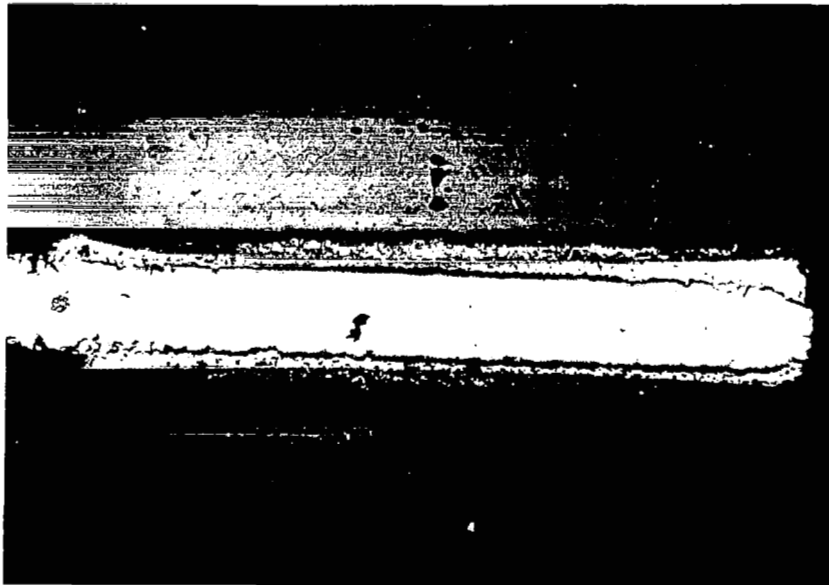
                                                50X

Figure 32. MICROSTRUCTURE OF TRANSVERSE SECTION
            OF ALUMINA-KOVAR SEAL JOINT OF
            CONVERTER 362

Examination of the collector surface at high magnifications (up to 1000 magnifications) revealed no unusual features or surface layers.

c. Examination of Other Converter Components

The post-test analysis also included examination of the ceramic-to-metal seal, the V braze of the Nb to W-Re emitter sleeve, and the electron beam weld of the W-Re sleeve to the emitter.

(1) Ceramic-to-Metal Seal

A microstructure of the transverse section of the alumina-to-Kovar seal joint using a Cu braze is shown in Figure 32. This seal joint remained leak tight for the 5000 hours of testing. The Kovar seal member was joined to a Nb upper emitter sleeve structure with a Cu braze. The microstructure of the joint in the unetched and etched condition is shown in Figures 33a and b, respectively.

(2) Niobium to W-Re Joint

The upper emitter sleeve structure consisted of a Nb sleeve joined to a W-22 w/o Re lower emitter sleeve with a V braze. This joint operated successfully throughout the life test of the converter. The excellent V braze penetration and microstructure are shown in Figures 34a and b. The microstructure appeared metallurgically sound--i.e., no porosity or intermediate phase formation.

(3) W-Re to Emitter Joint

The lower emitter structure was formed by electron beam welding the W-22 w/o Re sleeve to the CVD-W. A typical microstructure of this joint is illustrated in Figure 35. An excellent weld penetration and coarse grained structure is evident in this figure.
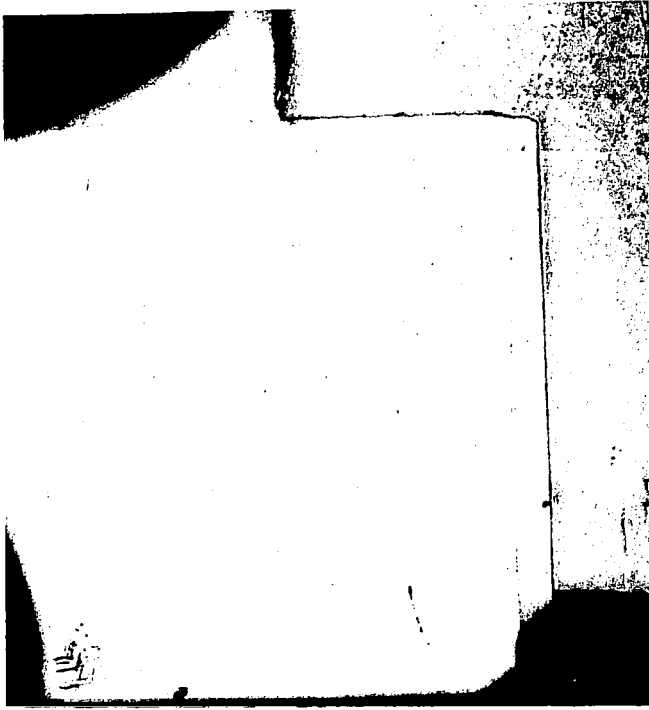
Unetched   50X

a.

Etched   50X

b.

Figure 33. MICROSTRUCTURE OF KOVAR-TO-NIOBIUM JOINT
OF SEAL AREA OF CONVERTER 362
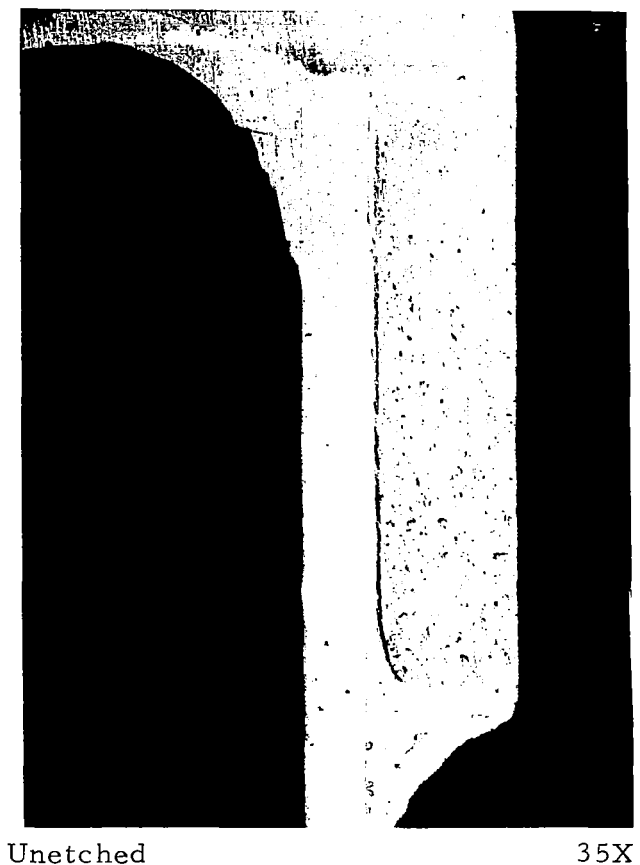
Unetched   35X
                   a.
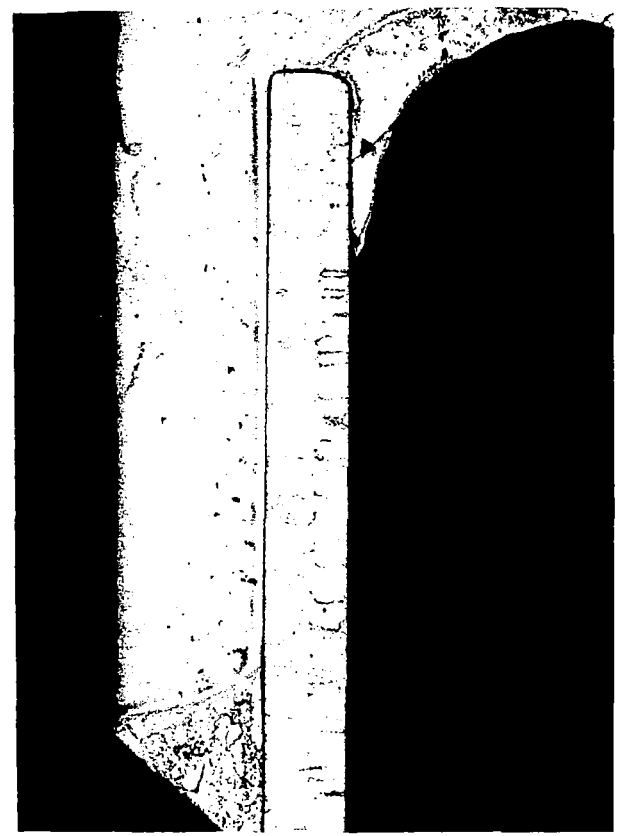
Etched   35X
                              b.

Figure 34.   MICROSTRUCTURE OF NIOBIUM TO W-Re JOINT IN
             UPPER EMITTER STRUCTURE OF CONVERTER 362
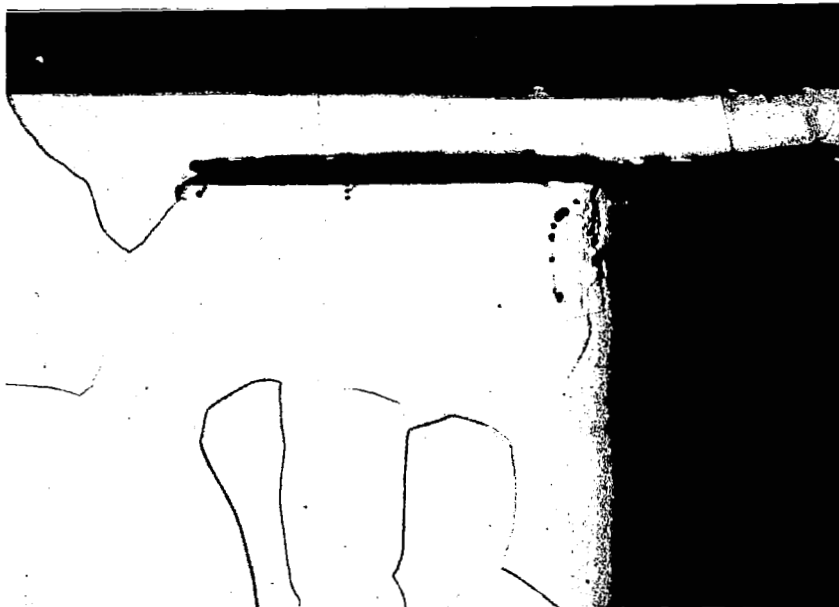
Etched   50X

Figure 35.   MICROSTRUCTURE OF ELECTRON BEAM
             WELD OF W-22 w/o Re EMITTER SLEEVE
             TO 362 W EMITTER

All of the key joints in the converter performed satisfactorily for the 5000-hour test life. Based upon these examinations, there is no reason to believe that life well beyond the 5000 hours could not be achieved.

CONVERTER 363

1. Emitter Characterization

The emitter used for this converter was produced from WCl_6. The chemical composition is reported in Table 3 and was identical to the Cl-CVD-W used in the emitter of converter 362. A microstructure consisting of fine columnar grains and clean single phase W was evident in the as-received material (Figure 36). This microstructure is not unlike that observed in the Cl-CVD-W emitter used in converter 362 (Figure 6).

The emitter specimen was machined and electropolished prior to vacuum work function measurements and x-ray diffraction analyses. Surface examination of the electropolished emitter revealed a clean surface with sharply defined grain boundaries. The vacuum heat treatment time for converter 362 extended to 200 hours to assure a stable vacuum work function. This heat treatment time was reduced to 50 hours for converter 363. Such a reduction was possible because there was no change in the measured vacuum work function during the 200 hour heat treatment period. After 50 hours at $1700^{\circ}C$ in vacuum work function apparatus, the surface microstructure showed evidence of some grain growth (Figure 37). The vacuum work function of this emitter was measured to be 4.70 ± 0.02 eV. This compares to a value of 4.92 ± 0.02 eV for the emitter of converter 362. X-ray diffraction analysis of the converter 363 emitter revealed a high degree of preferred (110) crystal orientation but was less than measured for emitter 362 (emitter No. 2, Figure 11).

2. Thermionic Performance

This converter was identical to converter 362 except for using: an emitter with a lower initial bare work function (4.72 eV instead of 4.92 eV),

50X

Figure 36. MICROSTRUCTURE OF AS-DEPOSITED Cl-CVD-W, SAMPLE
No. 8 (EMITTER 363)
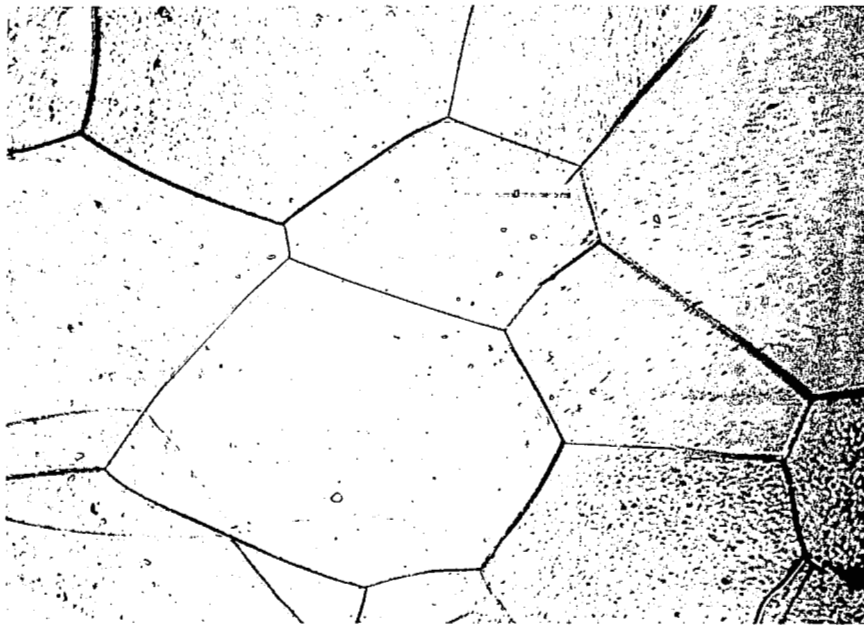
100X

Figure 37. SURFACE MICROSTRUCTURE OF EMITTER 363 (SAMPLE
No. 8) AFTER 50 HOURS AT 1700°C

a higher power capacity heater, and brazed-in collector thermocouples. Processing times varied for each converter since the criteria was that a pressure of less than 5×10^{-6} torr be attained. Although converter 362 was processed for 200 hours, this converter 363 was processed only 20 hours when a pressure of 2.7×10^{-6} torr was attained with the emitter at 1750°C and the collector at 865°C. Thereafter, the emitter work function was measured in situ and found to be 4.26 eV. Next, Cs was distilled in the converter and the device operated for a stabilizing run of 100 hours at an emitter temperature of 1700°C, a collector temperature of 800°C, and a Cs reservoir temperature of 355°C. Following this, initial testing was begun.

Performance maps were taken for emitter temperatures of 1400, 1550, and 1700°C, with collector temperatures from 600 to 960°C. Figure 38 shows a map of the I-V data taken at 1700°C with a collector temperature of 800°C. Maps taken at other conditions are shown in Appendix B-1. Following this testing, data points at emitter temperatures of 1550 and 1700°C and a collector temperature of 800°C were repeated. These maps showed a significant decrease in performance, as shown in Figure 39 for tne 1700°C emitter temperature case. The reason for this decrease has not been definitely determined but could possibly be due to insufficient outgassing of the converter. The converter was next placed in operation at conditions similar to the life test point of converter 362--i. e. , $T_E = 1700^{\circ}$C, $T_C = 730^{\circ}$C, $T_{Cs} = 340^{\circ}$C, and $I_o = 80$ Amps), while a decision was reached regarding the desired life test operating conditions. The converter operated steadily except for one interruption to conduct a special test. This test consisted of operating the converter at constant emitter, collector and Cs reservoir temperatures, while I-V pictures were obtained at various current densities ranging from 7. 5 Amps/cm^2 to 16 Amps/cm^2, to confirm that the d. c. and a. c. load lines were the same. The results did provide this confirmation; current density was found to have no effect upon the load lines obtained.

After 700 hours of initial testing and operation, the converter was placed on life test at the operating conditions shown in Table 6.

Figure 38. CONVERTER 363 VOLT-AMPERE CHARACTERISTICS --
INITIAL TESTING

65
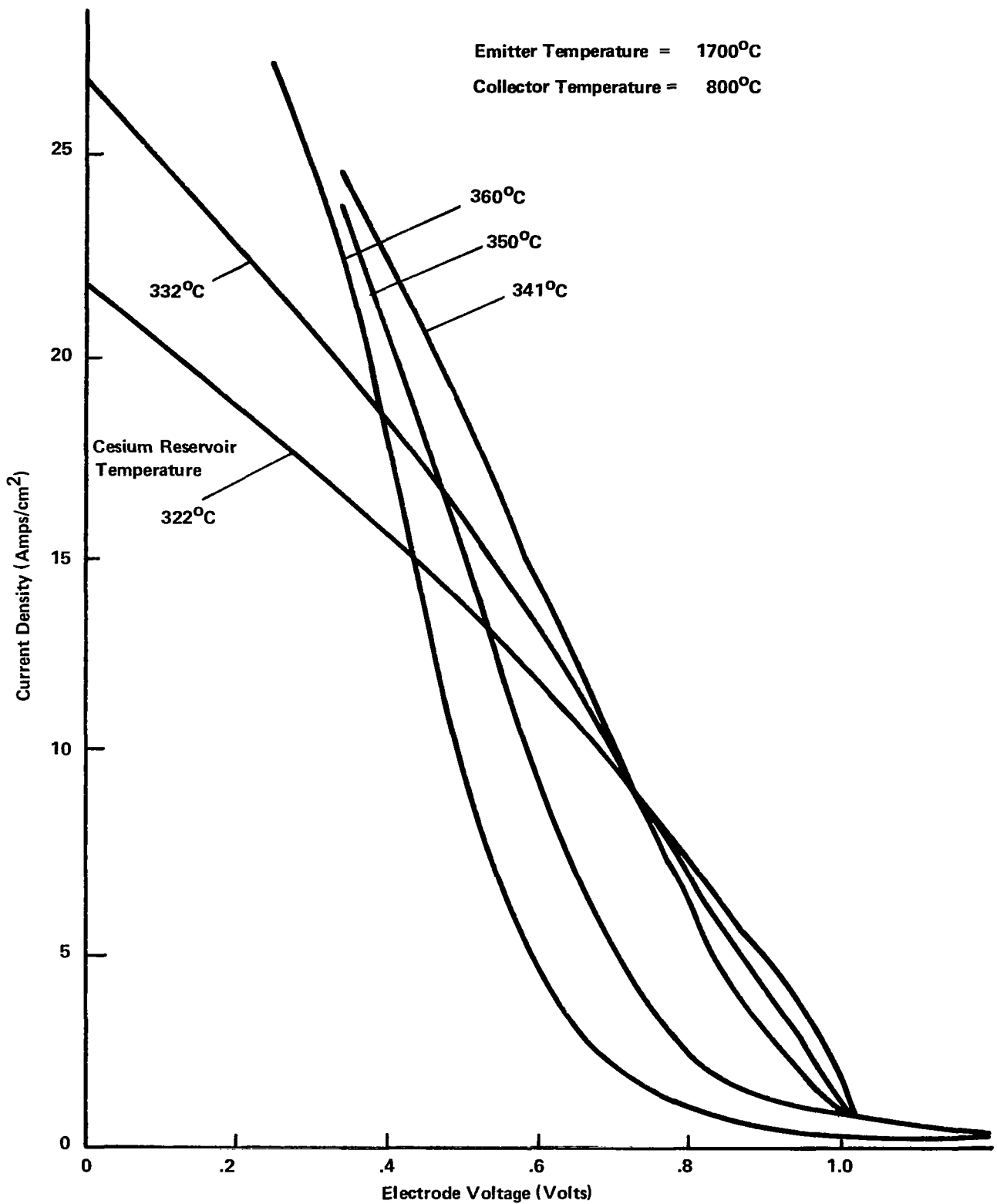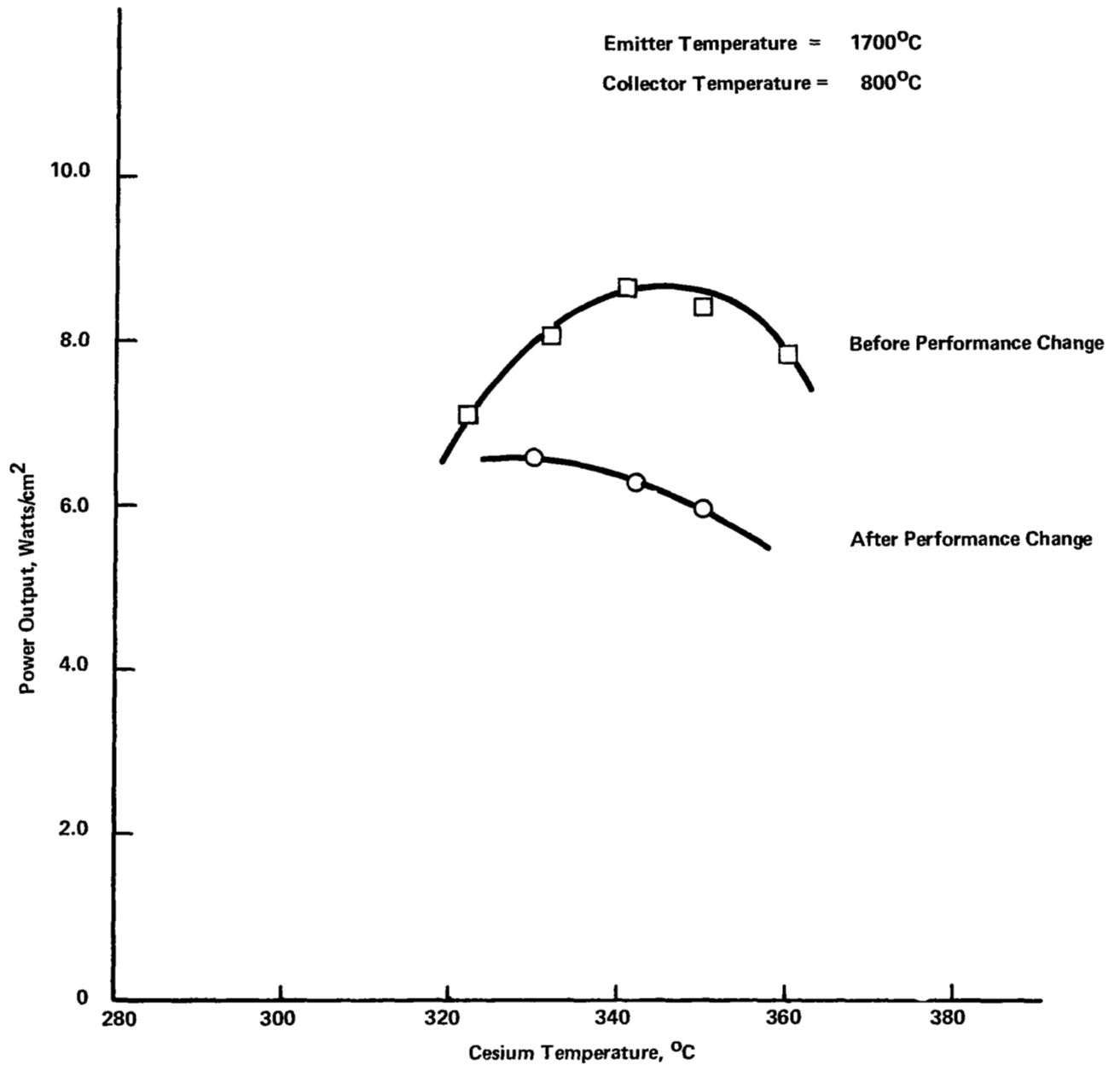
Figure 39. POWER OUTPUT VERSUS CESIUM TEMPERATURE
SHOWING PERFORMANCE CHANGE FOR CONVERTER 363

Figure 38. CONVERTER 363 VOLT-AMPERE CHARACTERISTICS --
INITIAL TESTING

67
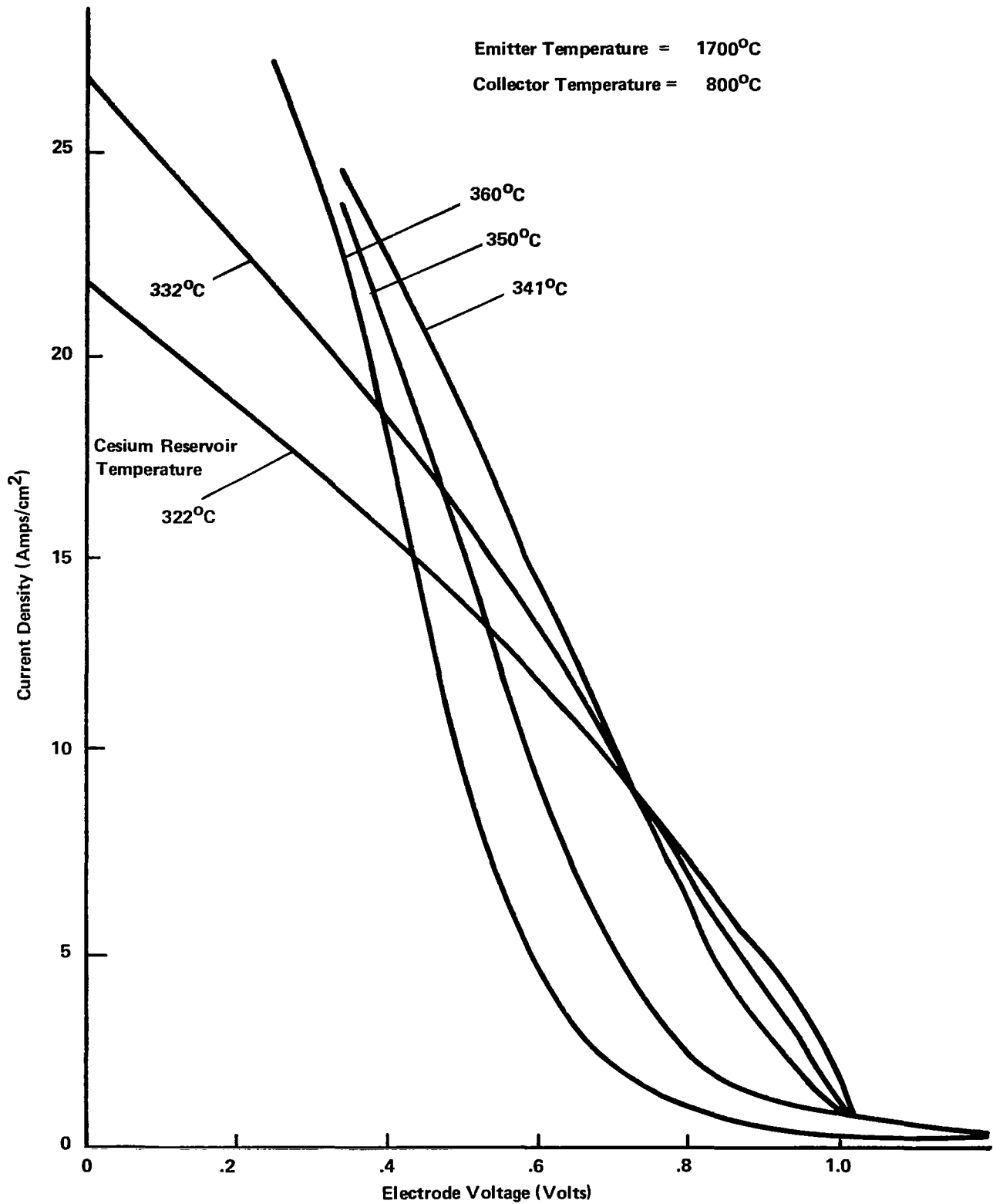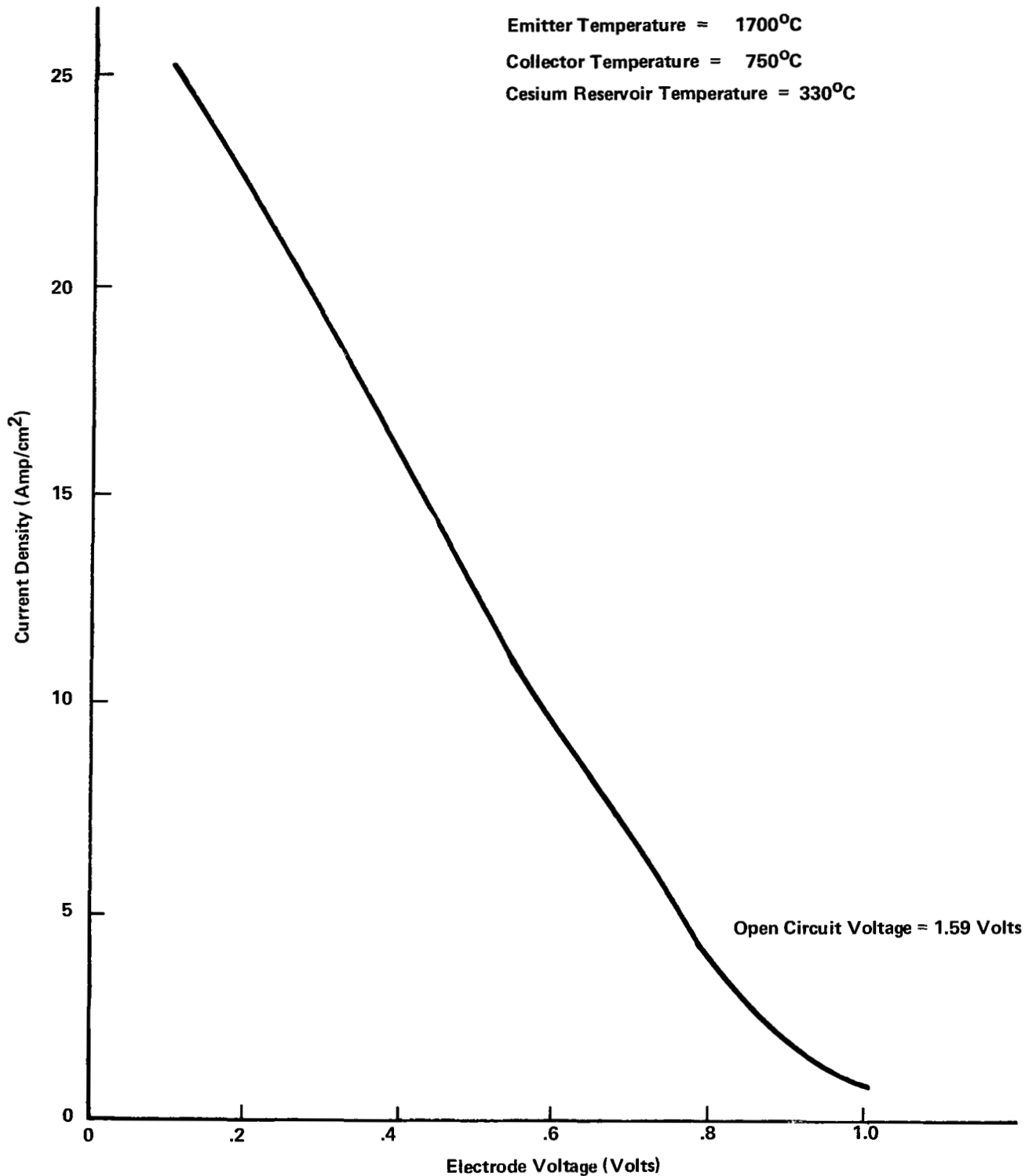
Figure 40. CONVERTER 363 VOLT-AMPERE CHARACTERISTIC -- LIFE TEST PERFORMANCE
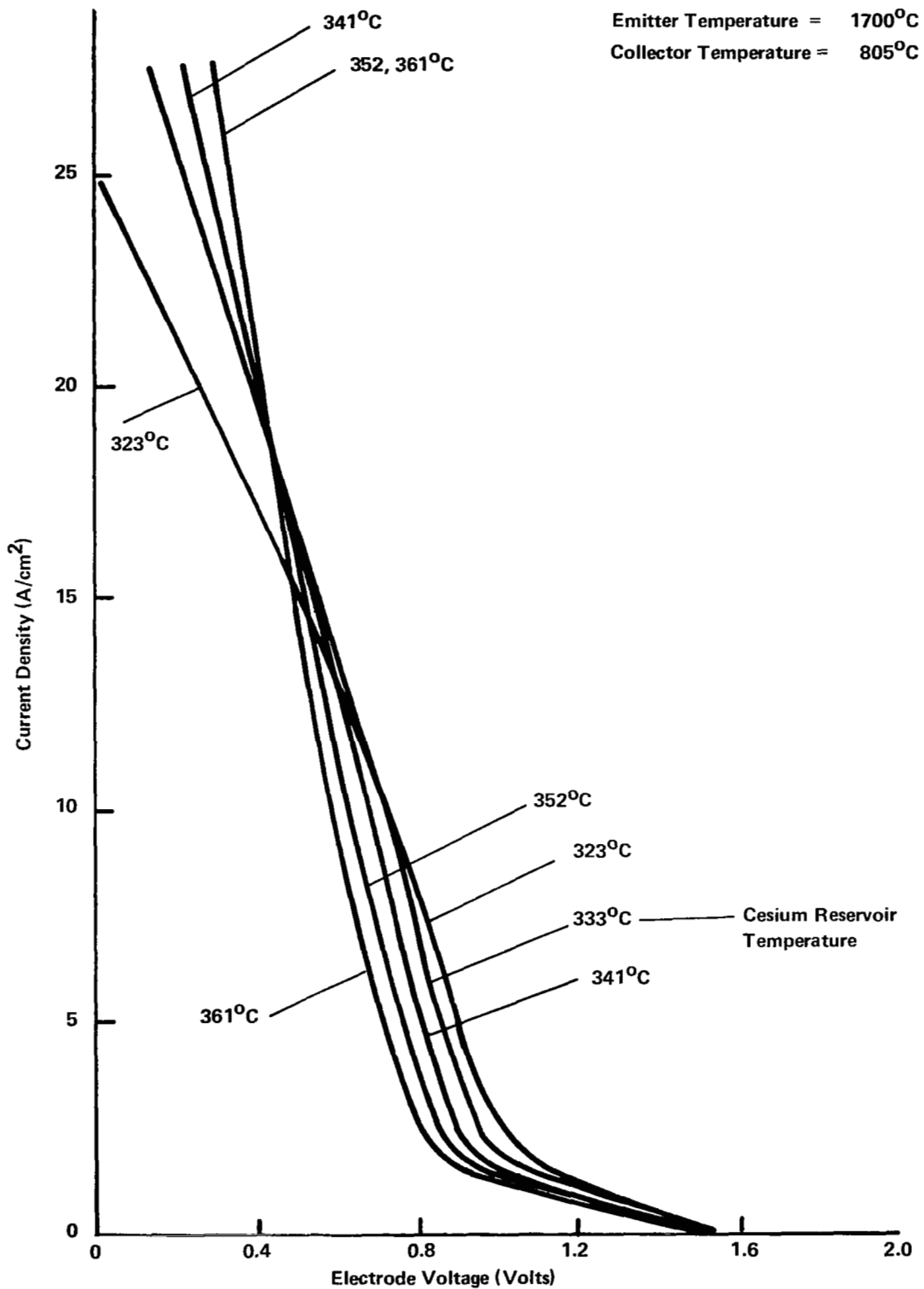
Figure 41. CONVERTER 363 VOLT-AMPERE CHARACTERISTICS
(T_E = 1700°C, T_C = 805°C) -- FINAL TEST
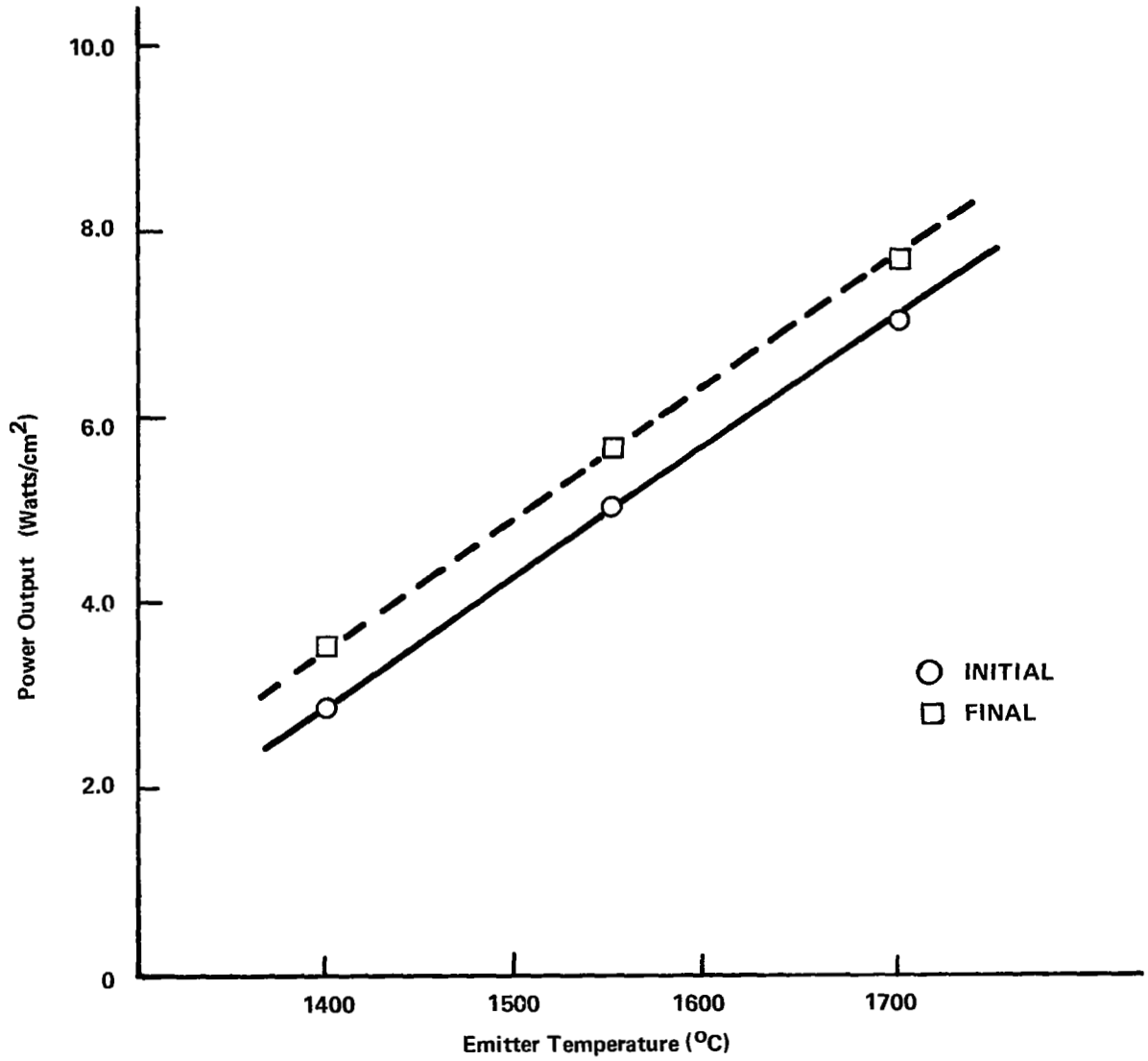
Figure 42. CONVERTER 363 OUTPUT POWER DENSITY AT A CURRENT DENSITY OF 10 Amps/cm^2
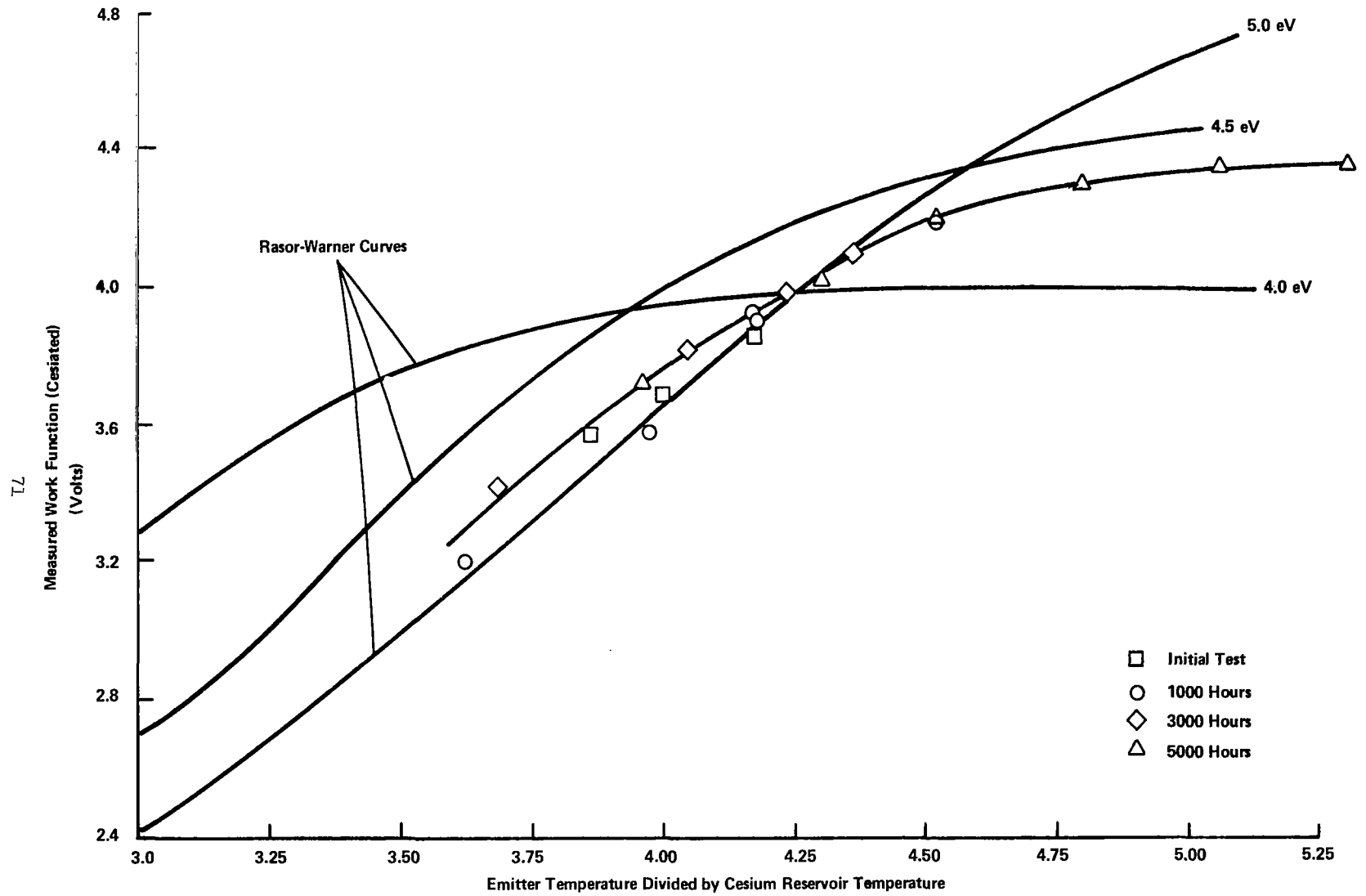
Figure 43. CONVERTER 363 CESIATED EMITTER WORK FUNCTION MEASUREMENTS

3.   Post-test Examination

A cursory examination was performed on the components of this converter. Emphasis, however, was placed on the examination of the emitter.

a.   Emitter Examination

No dimensional changes occurred in the emitter during the 5000 hours of testing at $1700^{\circ}C$, observations of the emitter surface revealed a clean microstructure with evidence of grain growth (Figure 44). Since x-ray diffraction analysis of crystal orientation was not included in the post-test examination, the emitter surface was electroetch pitted in order to obtain information on the crystal orientation of the emitter surface. After the electroetching procedure, the grain structure of the surface became very evident as shown in Figure 45. Very large grains are clearly discernible in this figure.

The electroetched emitter was scanned over most of the surface and the observations revealed no evidence of grains with (100) or near (100) orientation etch pits--i. e., (106) and (103). However, a number of grains did etch with etch pit geometries that define a (114) and (118) crystal orientation. A grain with (114) etch pits is illustrated in Figure 46. In general, it appeared that the surface of the emitter from converter 363 had a greater percentage of grains with (114) and (118) etch pits than did the emitter from converter 362.

During the examination of the etched surface of emitter 363, a second phase was observed. This phase was present in small amounts over the entire emitter and was of an acicular morphology (Figure 47). The structure was not as sharply defined and with the prounounced acicular or Widmanstatten morphology as that observed on the surface of the emitter of converter 362 (Figure 25).

100X

Figure 44. SURFACE MICROSTRUCTURE OF EMITTER 363
AFTER 5226 HOURS AT 1700°C

Figure 45. EMITTER FROM CONVERTER 363 AFTER
ELECTROETCHING OF SURFACE

73

Electroetched   500X

Figure 46.   ETCH PITS OF (114) ORIENTATION ON EMITTER
363 SURFACE

Electroetched   1000X

Figure 47.   SECOND PHASE PRESENT ON SURFACE OF
CONVERTER 363 EMITTER

Although the phase was present in small amounts, it was possible to perform an x-ray diffraction analysis in an attempt to identify this phase. A direct x-ray diffractometer method was used; this method could not detect the presence of the second phase. Therefore, a back-reflection pin hole technique was used with limited success. Weak and broad diffraction lines other than those caused by the W matrix were detected. The diffraction lines agreed fairly well with the ASTM data for α-W_2C. The phase WC was not checked because "d" values were not available from the back-reflection lines of this pattern. However, the possibility of this phase being present could not be ruled out. The presence of compounds of carbon on the surface is consistent with the results of the post-test examination of 362 emitter. The differences in the morphology of the second phase observed on the surfaces of 362 and 363 may, in part, explain the tentative identification of WC and α-W_2C, respectively, on the emitters.

b.   Collector Examination

Examination of the collector was limited to dimensional measurements and visual observation of the surface. No dimensional changes were observed. In order to examine the collector surface, the collector sub-assembly was sectioned in the longitudinal plane. A photograph of the longitudinal section is shown in Figure 48. The collector surface was clean with no evidence of any deposits or contamination. This was corroborated by scanning electron microscope examination of the surface. A view of the surface at 300X (Figure 49) shows the original machining marks and otherwise clean surface.

On the basis of the results of the limited post-test examination of converter 363, the change in converter performance was, in part, associated with the presence of carbon on the surface of the Cl-CVD-W emitter. Since the collector surface was clean, it would appear that the collector exerted little, if any, influence on the early changes in the performance of the converter.

Figure 48.   LONGITUDINAL SECTION OF NIOBIUM
COLLECTOR FROM CONVERTER 363
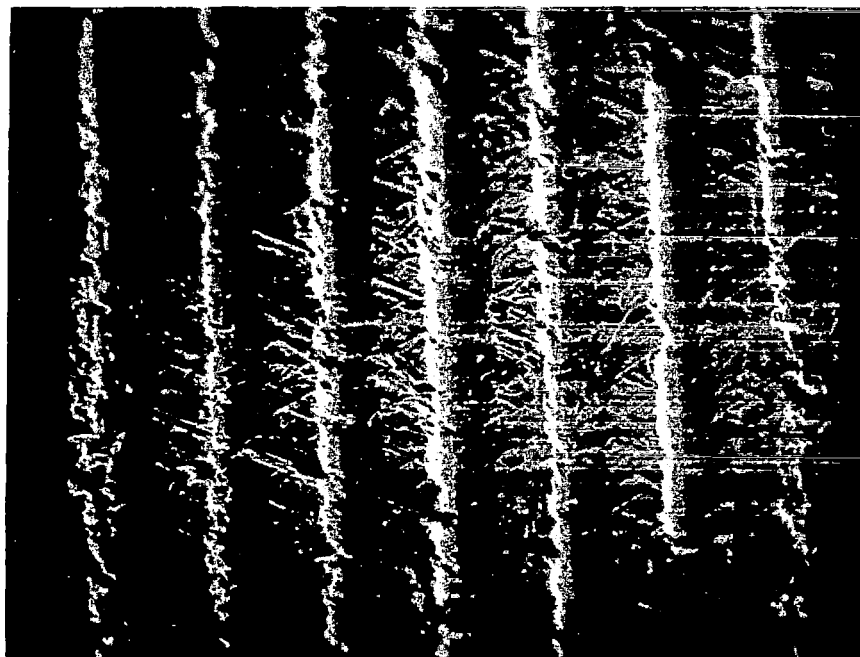
Figure 49.   SCANNING ELECTRON MICROSCOPE VIEW
OF 363 COLLECTOR SURFACE

76

CONVERTER 364

1. Emitter Characterization

The emitter for use in this converter was prepared by the hydrogen reduction of WF_6. Tungsten produced by this deposition method generally yields a preferred (100) crystal orientation on the emitter surface.

The chemical composition of the CVD-W emitter is presented in Table 3, sample 15. A typical microstructure of the as-received material is shown in Figure 7. The microstructural results of the grain growth test for 2 hours at 2000°C and the swell test of 1 hour at 2500°C are presented in Figures 8 and 9, respectively. Metallographic examination of this material revealed typical columnar grain structure with a clean single phase structure.

The cylindrical emitter was prepared for vacuum work function measurements and x-ray diffraction analysis to determine the degree of preferred (100) crystal orientation. Vacuum work function measurements on this emitter yielded a value of 4.72 $\pm$ 0.02 eV; a value slightly higher than that reported by other investigators. [5, 9] X-ray diffraction analysis to determine the degree of (100) preferred orientation was accomplished by measuring the x-ray intensity as the sample was rotated about the cylindrical axis to give an average over the circumference of the emitter. The spatial distribution of (100) axes as a function of tilt angle is shown in Figure 50. This plot shows a high degree of preferred crystal orientation.

After these characterization studies were made, the emitter was lightly etch pitted[5, 9] to corroborate the surface orientation. The surface etch pits revealed a high degree of preferred (100) crystal orientation in addition to a small amount of (110), (114), and (103) oriented grains. These data are consistent with the x-ray diffraction results. A typical surface microstructure of the etch pitted W is illustrated in Figure 51. Those grains that differ from the (100) orientation appear as the deeply etched grains in the figure. In Figure 51b, the attack on the grain boundaries is very evident.
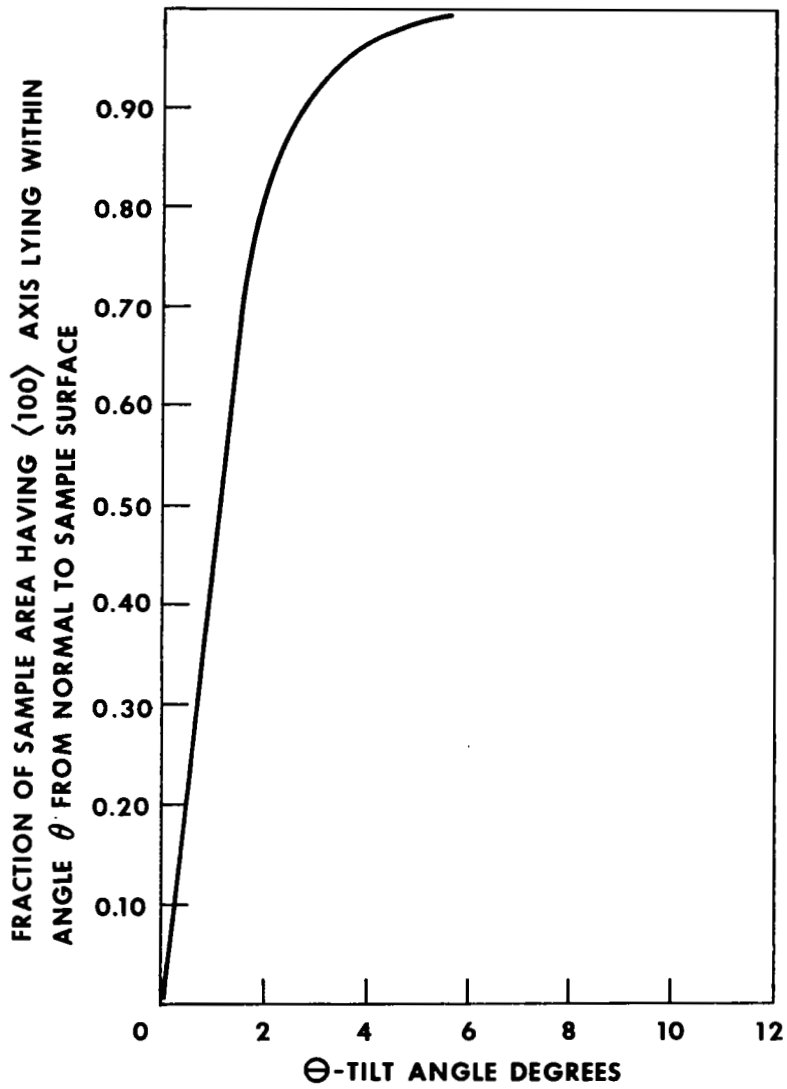
Figure 50. SPATIAL DISTRIBUTION OF <100> AXIS
AS FUNCTION OF TILT ANGLE FOR
EMITTER 364

78
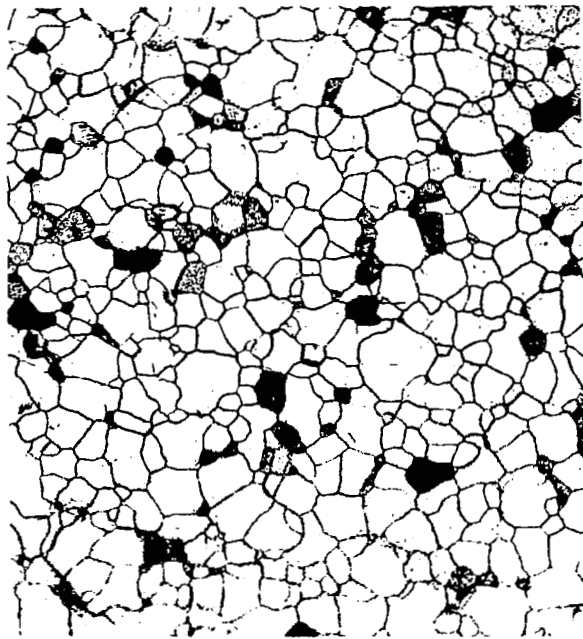
Electroetched   100X   Electroetched   500X
                 a.   b.

Figure 51.   MICROSTRUCTURES OF ELECTROETCHED SURFACE OF
             EMITTER 364
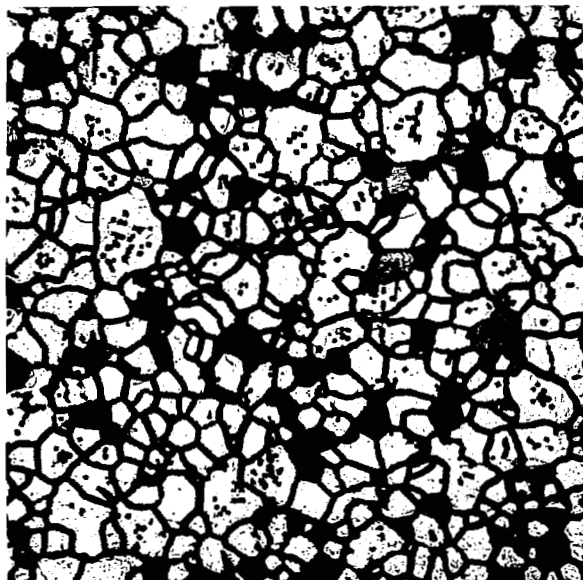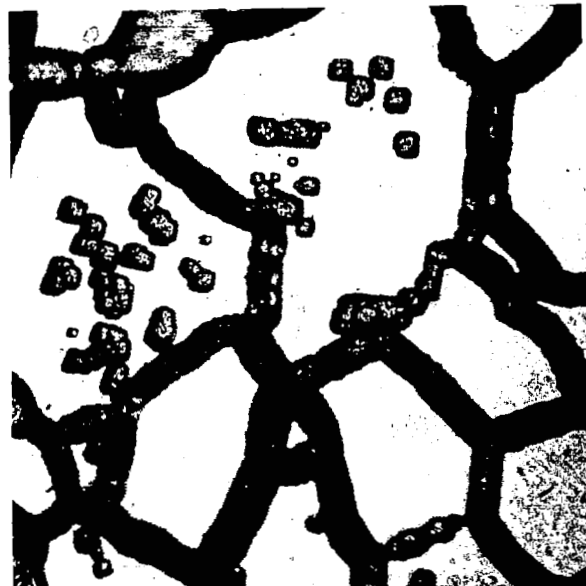
Electroetched   100X   Electroetched   500X
                 a.   b.

Figure 52.   MICROSTRUCTURES OF SURFACE OF EMITTER 364
             AFTER 40 SECONDS OF ELECTROETCHING

After 40 seconds of electroetching, there was greater penetration along the grain boundaries and more etch pits were produced as shown in Figure 52. The etch pits (Figure 52b) define the cube or (100) crystal orientation.

Following the surface etch pit analysis, the W emitter was electroetched to selectively expose the (110) crystal facets. These crystal facets exhibit the highest work function in metals with a body-centered-cubic crystal structure. A 3% sodium hydroxide (NaOH) etching solution was used with the voltage maintained at 1 volt. The current density under these conditions was 10.70 Amperes/cm^2.

After 2 hours of etching, some of the surface showed flat or unetched areas. However, after 6 hours, the entire surface was etched and the process was continued to 18 hours. Surface microstructures of the emitter after the 18-hour etch is shown in Figure 53. Because the surface was deeply etched, approximately 1 to 3 mils, the surface could not be focused upon with the limited depth of focus of the conventional microscope. Therefore, a scanning electron microscope examination of the etched surface was performed. With the improved depth of focus of this instrument, better surface details were observed; this is illustrated in Figure 54. A photograph of the final etched emitter is shown in Figure 55. The appearance of the surface is quite similar to that observed in the as-deposited condition.

The vacuum work function measurements of the etched emitter showed a value of 4.88 $\pm$ 0.02 eV and remained stable at this value for a 200-hour test at 1700°C. After this treatment, scanning electron microscope observations of the emitter surface revealed a small amount of rounding of the sharp edges (Figure 56). Based upon the promising indications of emitter surface stability, a decision was made to commit it to converter 364 and determine the following information.

    (1)   The long-term stability of the deep electroetched surface, and
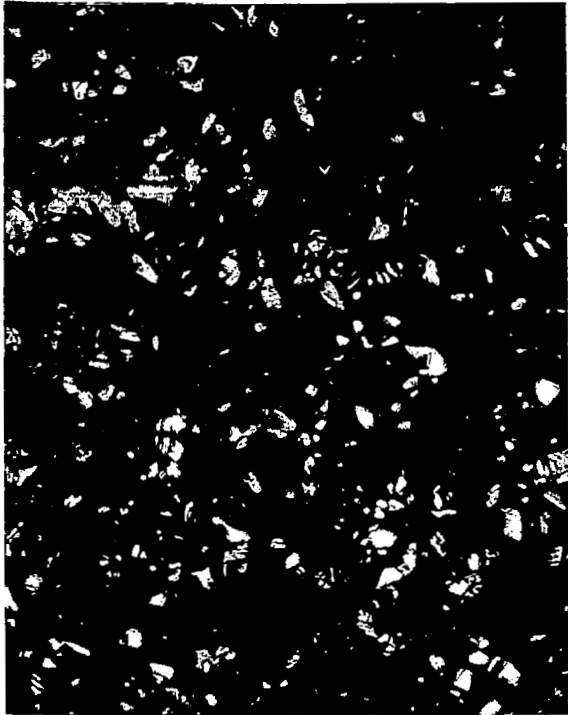
Electroetched 100X

a.

Electroetched 500X

b.

Figure 53.   MICROSTRUCTURE OF 364 EMITTER SURFACE
AFTER 18 HOURS OF ELECTROETCHING
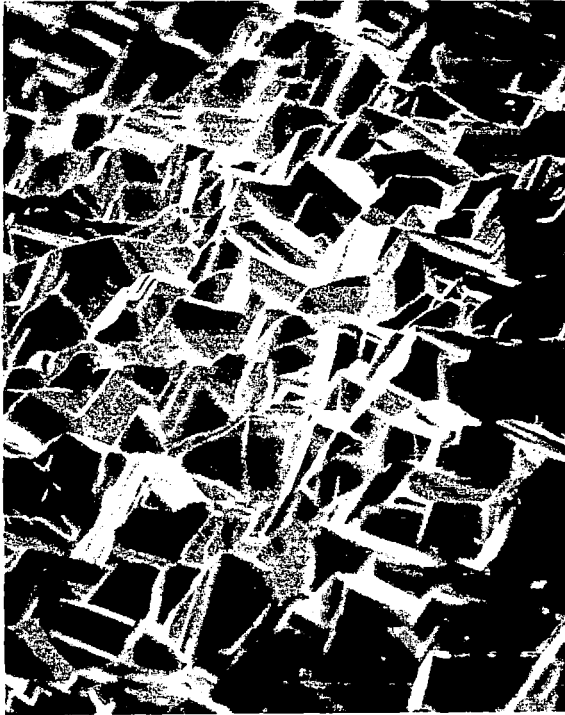
Electroetched   300X   Electroetched   1000X

            a.   b.

Figure 54.   SCANNING ELECTRON MICROSCOPE VIEWS OF
             364 EMITTER
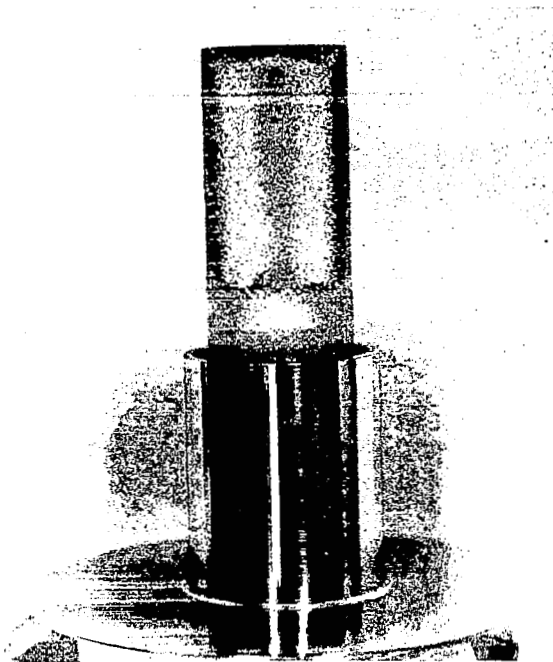
Figure 55.   ELECTROETCHED F-CVD-W
             EMITTER FOR CONVERTER
             364

1000X

Figure 56.   SCANNING ELECTRON MICRO-
             SCOPE VIEWS OF CVD-W EMITTER
             SURFACE ELECTROETCHED 18
             HOURS AND THEN HELD AT 1700°C
             FOR 200 HOURS IN VACUUM

83

(2)   The performance of this surface and a comparison of the results with (110) chloride W emitters (362 and 363).

2.   Thermionic Performance

This converter was similar to converter 362 and 363 with the exception of the emitter. As described earlier, this emitter was deposited using WF_6 and the surface deeply etched to expose (110) crystal facets. This etching reduced the emitter diameter by 0.004 inch, resulting in a converter with 0.012 inch interelectrode spacing; whereas the other two converters had a spacing of 0.010 inch. Following the emitter etching and characterization, and converter fabrication, the assembly was processed at an emitter temperature of 1760°C and a collector temperature of 960°C until a pressure of 5×10^{-8} torr was reached. Next, the emitter vacuum work function was measured in situ prior to the introduction of Cs. A value of 4.76 eV was measured, slightly lower than the value of 4.88 eV which had been measured during the initial emitter characterization. Comparisons of this work function with other historical measurements of the emitter is shown in Table 7.

Following introduction of Cs, initial performance mapping was conducted of the various families of emitter, collector, and Cs reservoir temperatures. A typical set of curves taken at 1700°C (emitter), 750°C (collector) and several Cs reservoir temperatures is shown in Figure 57. Curves taken at other conditions are included in Appendix C-1. The converter was next placed on 5000 hours life test at the operating conditions shown in Table 8. During this time, the converter performance remained very steady, as can be seen from the life test plots of the significant converter parameters (in Appendix C-2). This behavior can also be seen from the curves showing initial and final output power densities versus emitter temperature for current densities of 10 Amps/cm² shown in Figure 58. The final performance maps (Figure 59 and Appendix C-3) also show a close correspondence with initial data.

Table 7. EMITTER VACUUM WORK FUNCTION MEASUREMENTS ON CONVERTER 364

Condition	Work Function, eV
1. Initial, before assembly into converter	4.88
2. After assembly into converter, prior to introducing cesium	4.76
3. After 5000-hour test at $1700^{\circ}C$ in situ, cesium removed	4.62

Table 8. LIFE TEST OPERATING CONDITIONS FOR CONVERTER 364

Input Power Density	$57.7 \ W/cm^2$
Output Power Density	$7.41 \ W/cm^2$
Output Current Density	$10 \ Amp/cm^2$
Output Voltage	0.743 Volts
Emitter Temperature	$1700^{\circ}C$
Collector Temperature (Optimum)	$750^{\circ}C$
Cesium Reservoir Temperature (Optimum)	$345^{\circ}C$
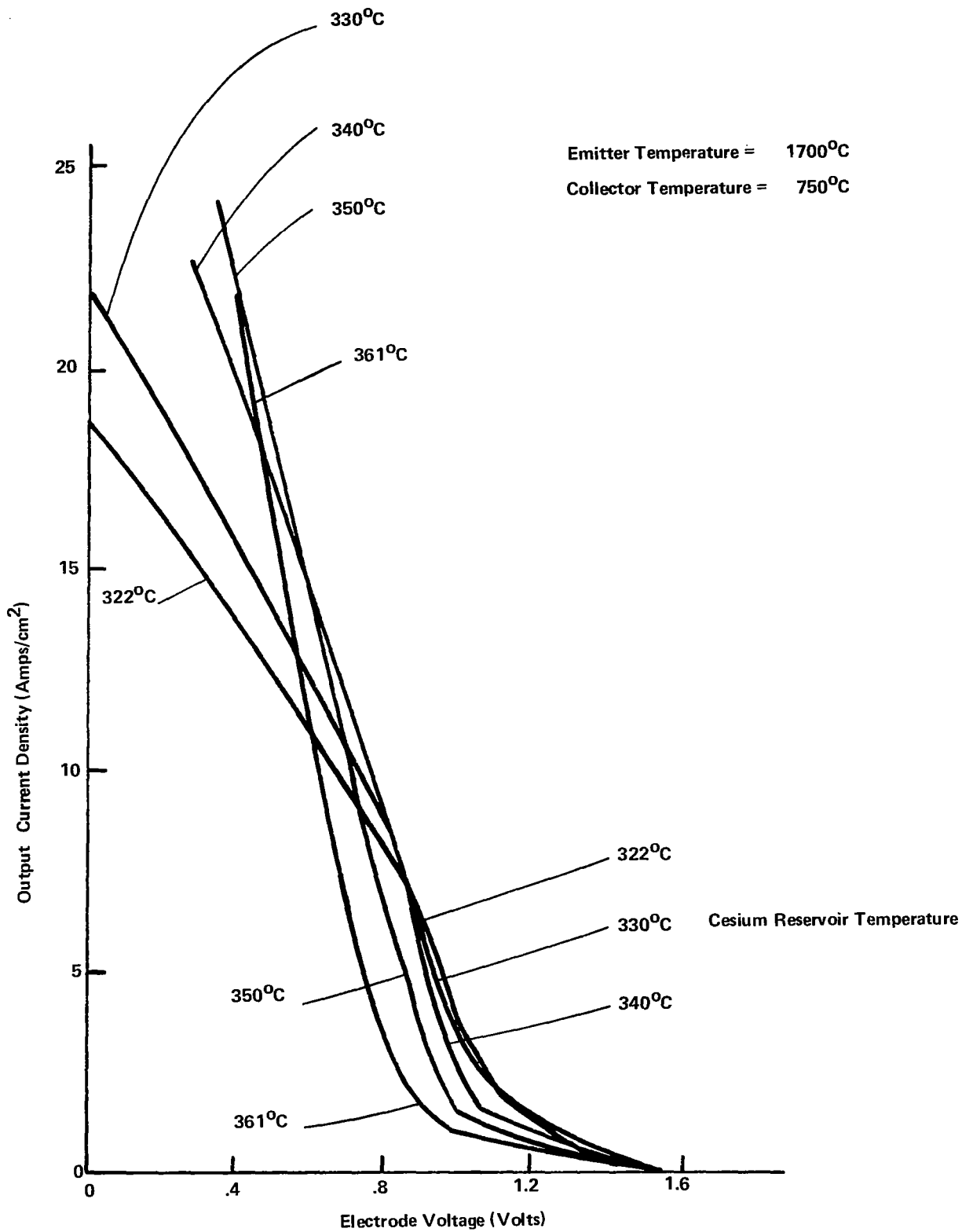
Figure 57. CONVERTER 364 VOLT-AMPERE CHARACTERISTICS --
INITIAL TESTING

86
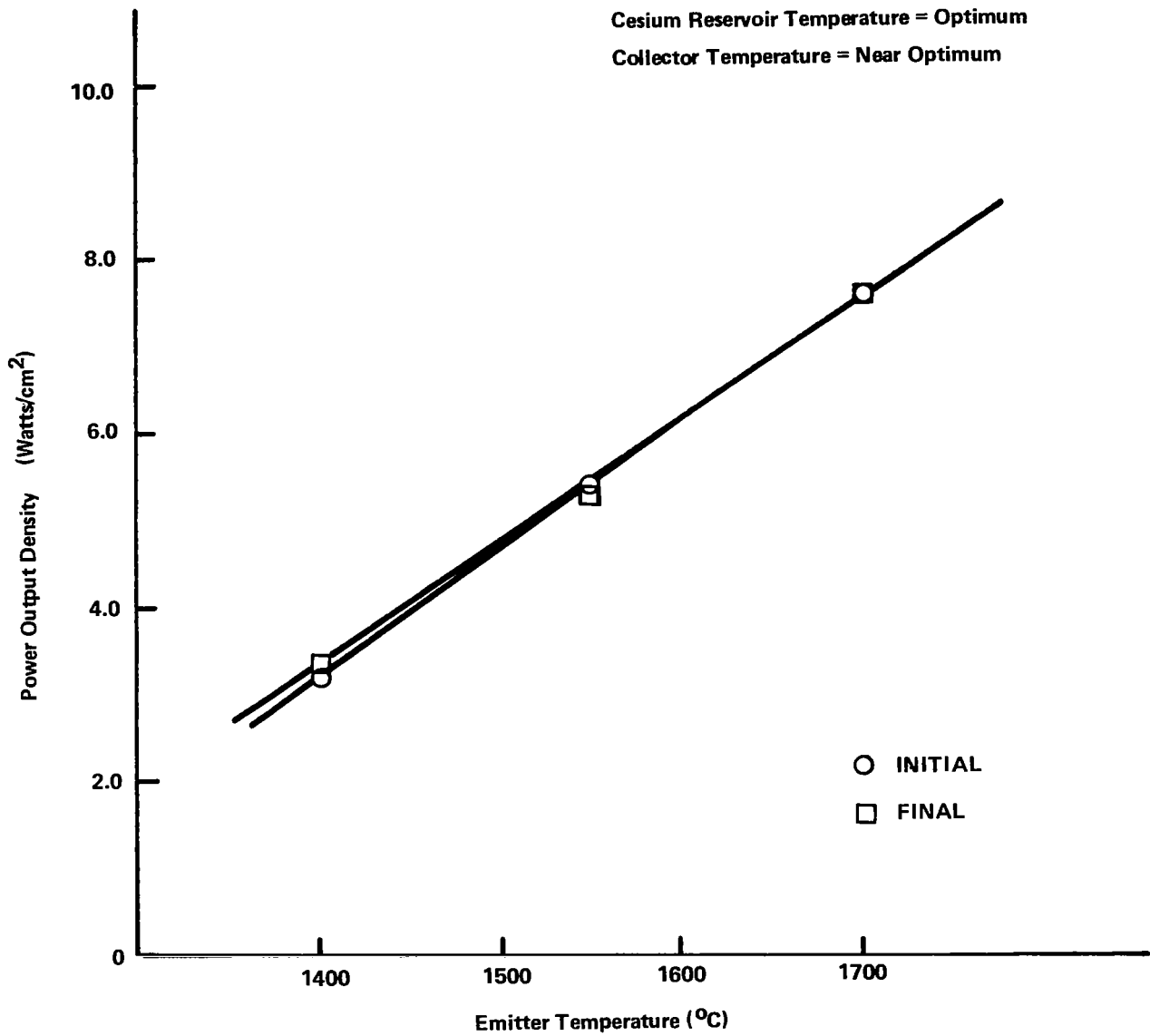
Figure 58.   CONVERTER 364 OUTPUT POWER DENSITY AT A CURRENT
DENSITY OF 10 Amps/cm^2
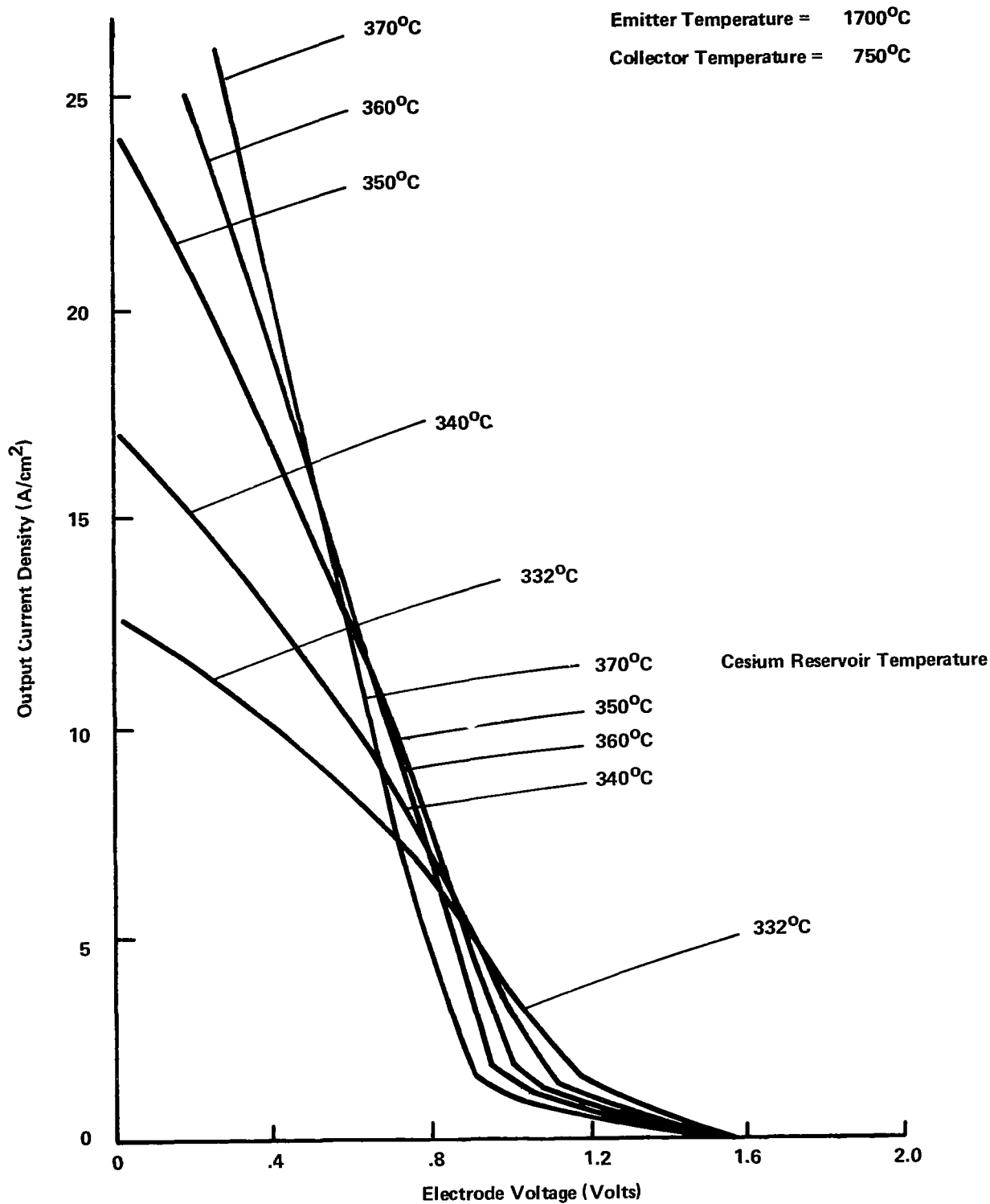
Figure 59. CONVERTER 364 VOLT-AMPERE CHARACTERISTICS -- FINAL
TESTING (4550 HOURS)

Further evidence of stability of this converter is shown by the electrode cesiated work function measurements. These measurements, made initially and at 1100, 3200, and 4550 hours are essentially identical, as shown in Figure 60 and Figure 61 (emitter and collector measurements, respectively).

3.   Post-test Examination

According to the scope of work under this program, the post-test examination of converter 364 was more comprehensive than that performed for converter 363 but not as inclusive as that conducted on converter 362.

a.   Emitter Examination

A comparison of the pre- and post-test dimensional measurements showed no change in the emitter diameter. Visual examination of the emitter (Figure 62) revealed a clean surface with a texture identical to that of the as-electroetched and as-deposited CVD-W. Scanning electron microscope examinations were performed on the emitter surface. Surface structures at 300 and 1000X magnifications are illustrated in Figure 63a and 63b, respectively. In comparing these structures with those of the as-electroetched condition (Figure 54a and b), significant rounding of the sharp edges of the crystal facets is evident. In spite of this rounding, the surface provided a steady and stable thermionic output of the emitter for 4550 hours of testing at 1700°C.

After the surface examinations were completed, a transverse section of the emitter was prepared for metallographic examination. While grain growth of the F-CVD-W was evident, the etched surface was preserved as shown in Figure 64. As shown in this figure, the depth of the etched facets was approximately 0.0025 cm (0.001 inch). The microstructure of the W was a clean single phase structure which is consistent with that observed for the starting material (Figure 7).

b.   Collector Examination

In order to examine the surface of the Nb collector, it was sectioned longitudinally (Figure 65). Visual examination of the collector
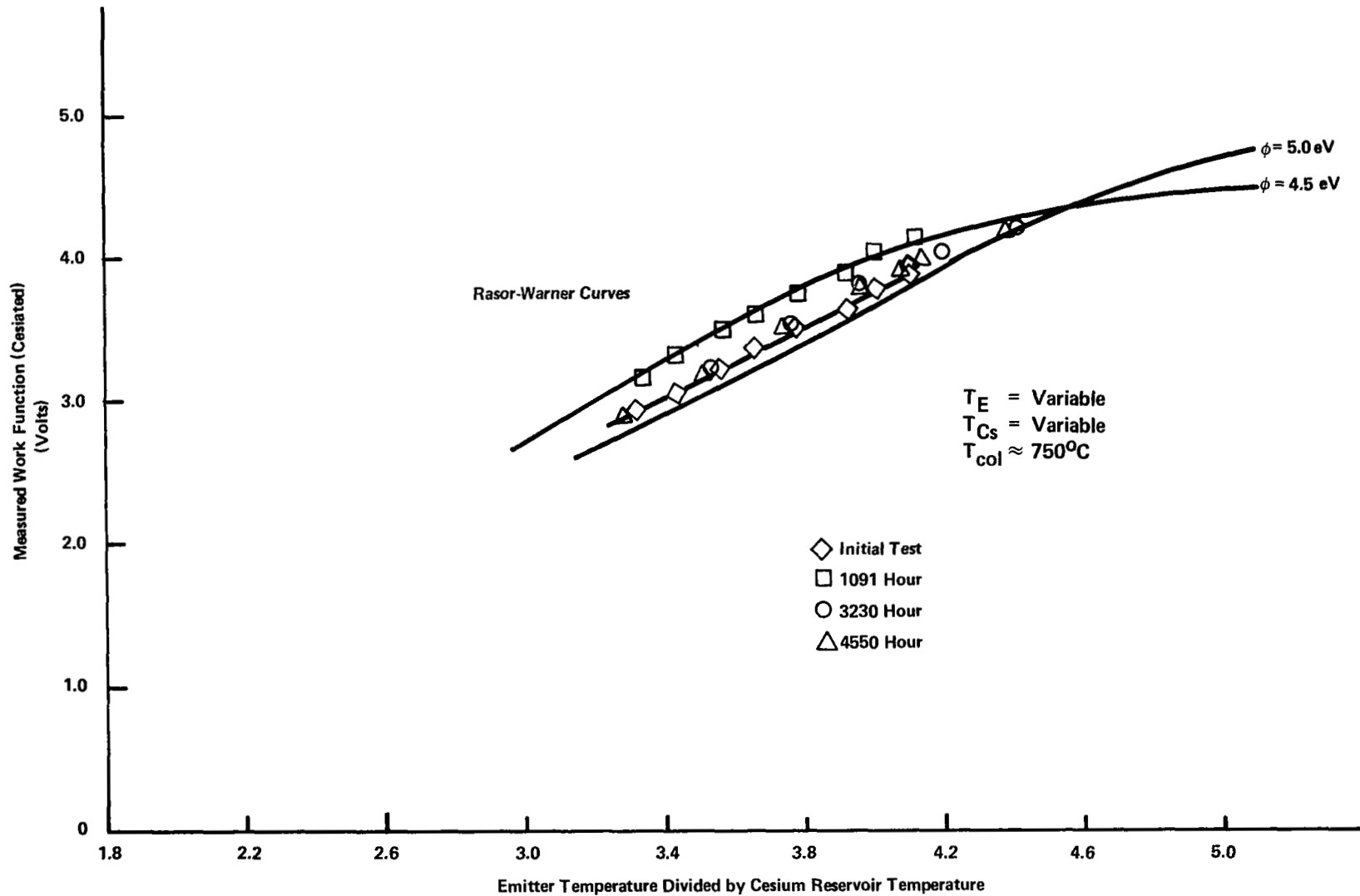
Figure 60.   CONVERTER 364 CESIATED EMITTER WORK FUNCTION MEASUREMENTS
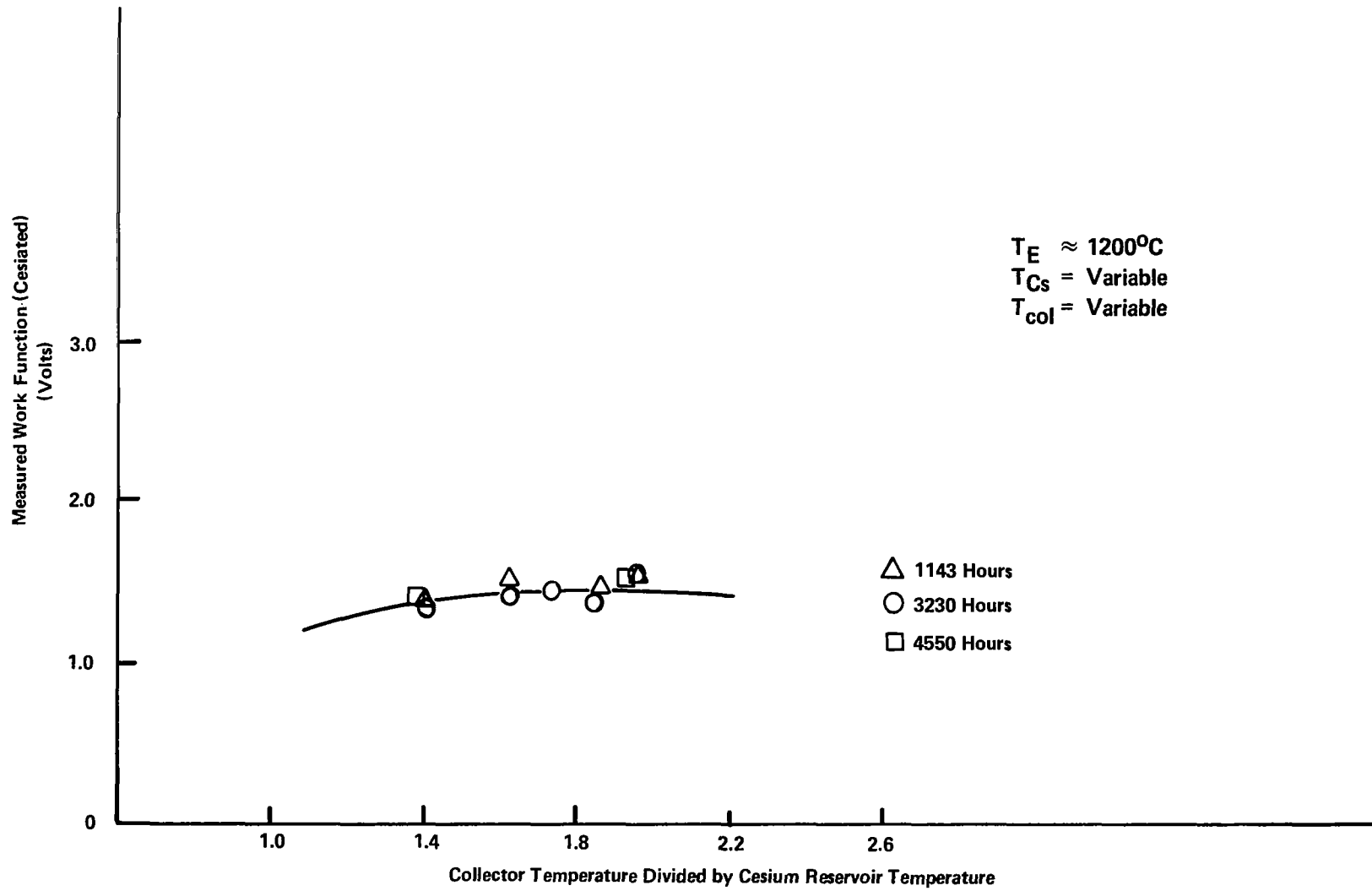
Figure 61. CONVERTER 364 CESIATED COLLECTOR WORK FUNCTION MEASUREMENTS
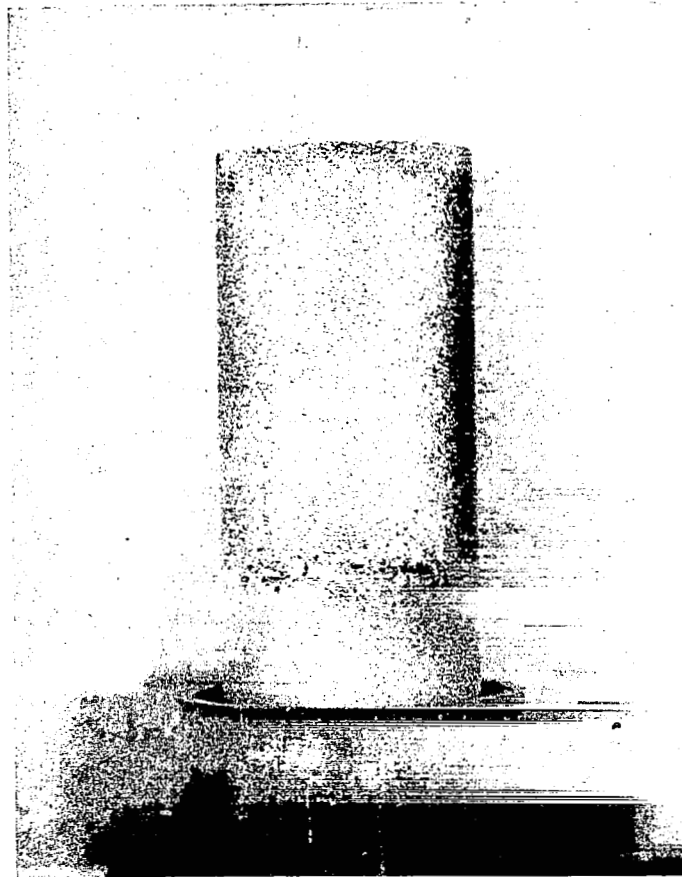
~2.5X

Figure 62. CONVERTER 364 EMITTER AFTER 4550
HOURS OF TEST AT 1700°C

(300X)

b. ——————————▶

a. ◀——————————

(1000X)

Figure 63. SCANNING ELECTRON MICROSCOPE VIEWS OF
364 EMITTER SURFACE AFTER 4550 HOURS OF
TEST AT 1700°C

Etched   100X

Figure 64.   MICROSTRUCTURE OF TRANSVERSE SECTION
             OF 364 EMITTER
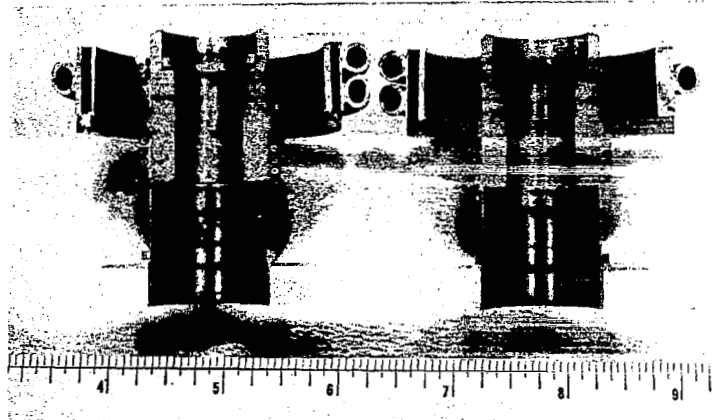
Figure 65.   PHOTOGRAPH OF LONGITUDINAL SECTION
             OF NIOBIUM COLLECTOR OF CONVERTER 364

94

surface showed no evidence of surface defects, deposits or contamination. A metallographic specimen was prepared of the transverse section of the collector. Examination of this specimen showed very large grains, a clean single phase microstructure and a clean collector surface with no evidence of any surface deposits (Figure 66).

c. Examination of Other Converter Components

A very small Cs leak occurred in the converter envelope during testing. This leak was identified by the presence of Cs on the walls of the stainless steel vacuum bell jar. The leak was found in the W-Re sleeve-to-emitter juncture. Evidently during the 18-hour electroetching treatment, the W-22 w/o Re emitter sleeve (0.020-inch thick) was also selectively etched. This probably weakened the material such that under normal operating conditions, steady state and thermal cycling, a small leak occurred.

COMPARISON OF RESULTS

Performance changes during life testing of converters 362 and 363, while not completely understood, are thought to be due to improper or inadequate outgassing prior to converter operation. The operation of each of these devices at the end of life is believed to be representative of the performance to be expected from (110) oriented, CVD-W. The performance of 364 remained essentially stable during its life, which is probably due to the use of improved outgassing techniques (Vac-Ion pumped outgassing system for component parts, as well as assembled converter and higher collector outgassing temperatures). The final performance of this device is shown plotted in Figure 67 at a current density of 10 Amps/cm^2 and compared with similar curves for converters 362 and 363. A striking similarity exists between these 3 converters in spite of the fact that the emitter for converter 364 was fabricated from normally (100) oriented, F-CVD-W and the converter had a larger interelectrode spacing (0.012 inch instead of 0.010 inch). This is due to the special etching which exposed the (110) facets on the surface of the 364 emitter.
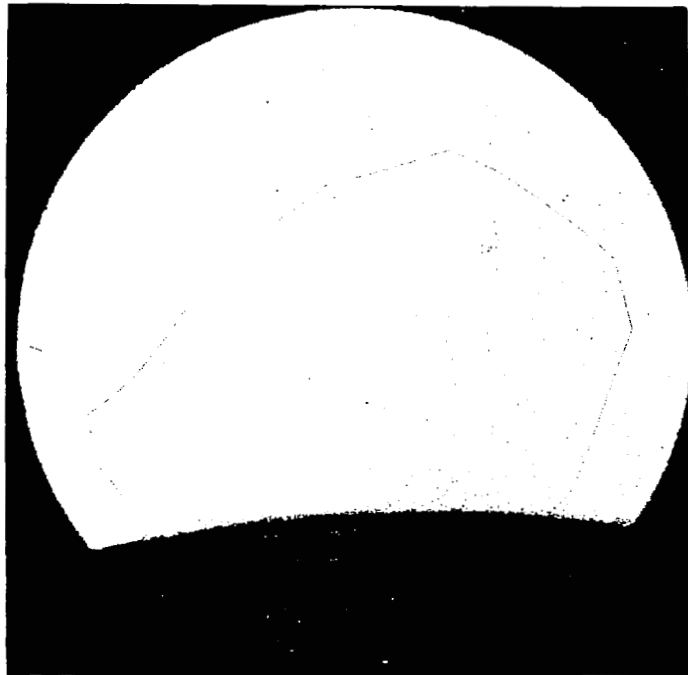
Etched   25X

Figure 66. MICROSTRUCTURE OF TRANSVERSE SECTION OF
NIOBIUM COLLECTOR OF CONVERTER 364
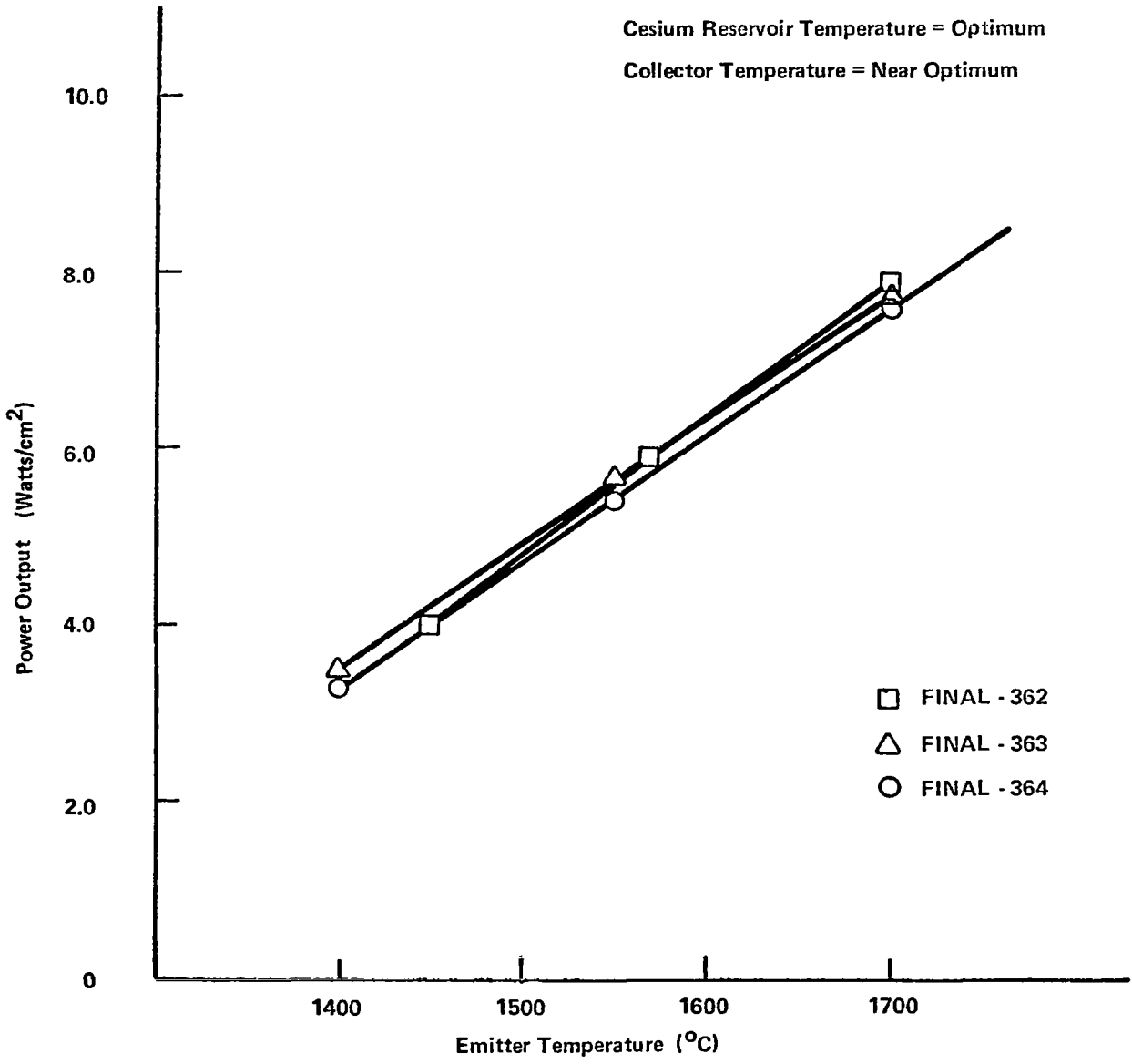
Figure 67. CONVERTER 362, 363 AND 364 PERFORMANCE
COMPARISON AT 10 AMPS/CM^2

97

Further evidence that (110)-type performance can be obtained starting with F-CVD-W emitter material is shown in Figure 68, where these three cylindrical converters are plotted along with similar (100) and (110) oriented planar research converters (Table 9). Included also are performance bands expected for these two types of orientation from a theoretical basis.[10] All three of the converters described in this report fall in the range of performance expected from (110) oriented emitters.
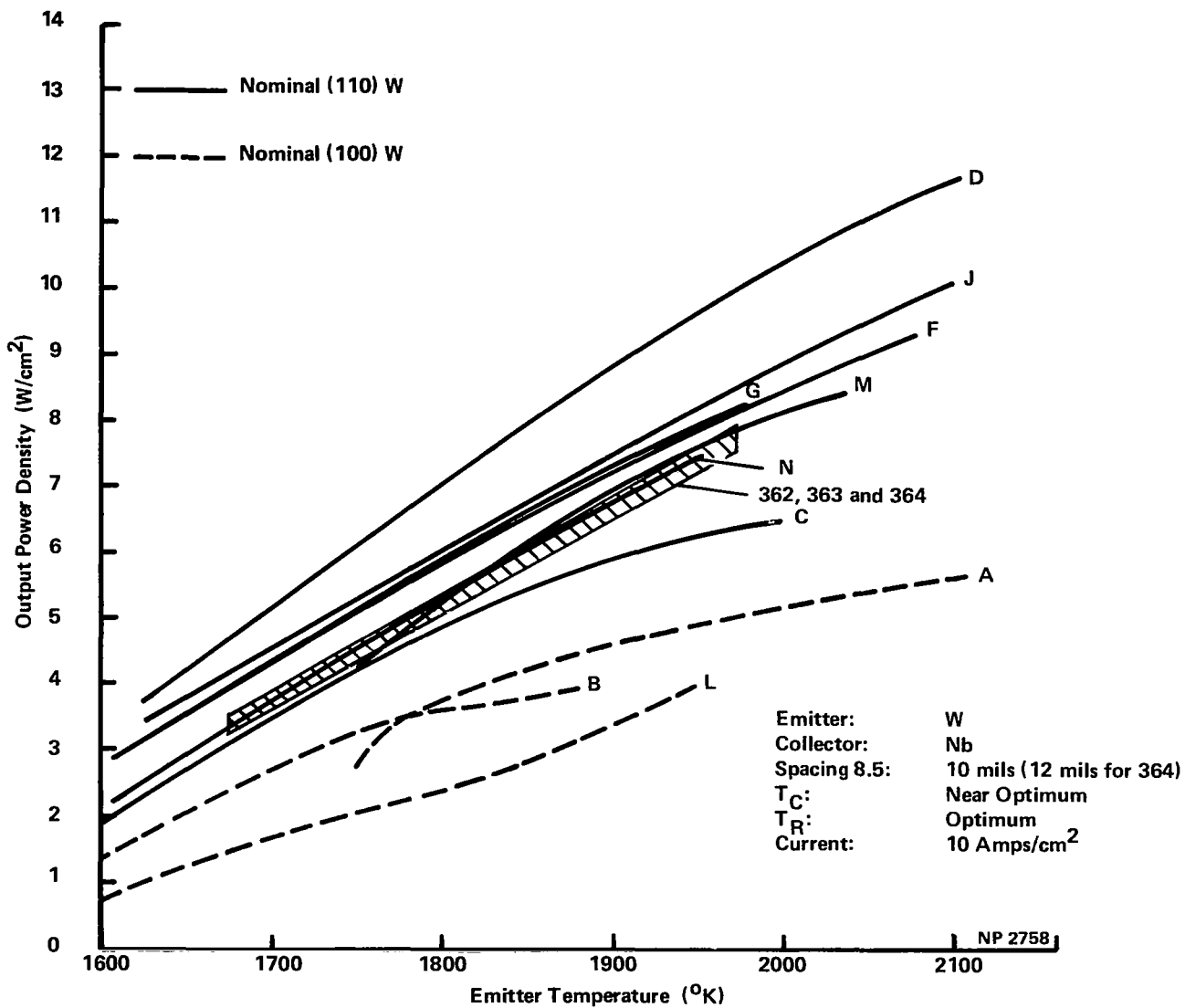
Figure 68. COMPARISON OF CONVERTER PERFORMANCE WITH
SELECTED RESEARCH DIODES (IDENTIFIED IN TABLE 9)

Table 9. ELECTRODE AND GEOMETRIC DATA FOR SELECTED RESEARCH DIODES

Symbol	Emitter	Preparation	Bare Work Function, Volts	Collector	Spacing Mils	Builder
D	F CVD W	Electropolished/ Electroetched	4.83	Nb	10	R&DC
F	Poly Powder Metallurgy W	Coldworked Resulting in Preferred (110) Orientation	4.58	Nb	10	R&DC
G	Cl CVD W	Electropolished	4.91	Nb	8.5	TECO
M	Cl CVD W	Electropolished	5.0	Nb	10	TECO
N	Cl CVD W	Electropolished	4.91	Nb	10	TECO
J	Cl CVD W	Preferred (110) Electropolished	4.95	Nb	10	R&DC
C	F CVD W	Electropolished/ Chemically Etched	4.77	Nb	8.5	TECO
A	F CVD W	Mechanical	--	Nb	8.5	TECO
B	F CVD W	Mechanical/ Electropolished	--	Nb	8.5	TECO
L	F CVD W	Mechanical	4.65	Nb	10	TECO

CONCLUSIONS

The preceeding section of this report described a development task which was conducted to evaluate high performance cylindrical thermionic converters having W emitters of preferred (110) crystal orientation. The course of this activity included a comprehensive program of test vehicle design and development, emitter characterization and selection, thermionic performance mapping and steady state testing, and post-test examination and analysis. The following are observations and conclusions resulting from this task.

The three devices built and tested under this program had strikingly comparable thermionic performance after 5000 hours of operation, as indicated by a plot of their output power versus emitter temperature at a current density of 10 Amps/cm^2 (Figure 67). Their emitters, however, were produced by two distinctly different methods. The first two devices, converters 362 and 363, employed W emitter surfaces of preferred (110) crystal orientation produced by the hydrogen reduction of WCl_6. The latter converter, 364, employed an emitter produced from the hydrogen reduction of WF_6, which was electroetched to expose the (110) crystal planes.

Perhaps equally important is that this work revealed a rather significant spread in emitter characterization (vacuum work function, x-ray diffraction and etched pits) was not reflected in thermionic performance. The maximum spread regarding the vacuum work function and x-ray diffraction is 0.2 eV and 0.1 fraction of the sample area having <110> lying with a tilt angle $\theta \leq 20°$. In the case of the etched pits converter 364 was deeply etched from 1 to 3 mils (approximately). Further, it is noteworthy that the closely-grouped band of thermionic performance produced by these three devices fell well within the band established by other reported converters having (110) emitter surfaces, both planar and cylindrical in geometry.

Converter 364 was an exceedingly stable performer, as indicated by both thermionic output and cesiated work function measurements taken over the 5000-hour period of operation. However, performance changes did occur during the life testing of converters 362 and 363. These changes, while not completely understood, are thought to be due to inadequate outgassing of these earlier devices. Nevertheless, the effects of the resulting contamination are believed to have reduced and stabilized to the point where there was no appreciable impact on the thermionic performances at the end of steady state testing.

Upon post-test examination of all converters, no dimensional changes or collector-electrode changes were revealed which could have influenced a corresponding change in thermionic performance. Some rounding of the etched crystal facets on emitter 364 was observed after test. This occurence, however, did not display any influence on the converters thermionic performance history. Carbide contamination was discovered on the emitters of both 362 and 363 after test. This discovery supports the contention that inadequate outgassing caused tne observed performance changes during the initial portions of their test history.

Finally, this converter test series, with its extensive instrumentation, provided the opportunity to evaluate and verify the Wilkins' diagnostic technique[1] for emitter temperature determination. Emitter temperatures of converter 363, as determined by this diagnostic tool; high temperature thermocouples; and optical pyrometry all cross checked well within a useful range ($\pm$ 50°C).

REFERENCES

(1)   Wilkins, D. R., and Gyftopoulos, E. P., "Theory of Thermionic
       Converter Extinguished-Mode Operation with Applications to Converter
       Diagnostics," Journal of Applied Physics, 38, No. 1, 12-18,
       January 1967.

(2)   Webster, H. F., "Advances of Electronics," 17, 146 (1962),
       Academic Press, New York.

(3)   Barrett, C. S., "Structure of Metals," Second Edition, McGraw-Hill
       Book Company, Inc., New York, NY (1952).

(4)   Yang, L. and Hudson, R. G., "Effect of Preferred Crystal Orientation
       and Surface Treatment on the Work Function of Vapor Deposited
       Tungsten," Thermionic Conversion Specialist Conference Record,
       p. 395, November 1966, Houston, Texas.

(5)   Yang, L., Hudson, R. G., Tagami, T., and Creagh, J. W. R.,
       "Preferred Crystal Orientation Evaluation and Vacuum Work Function
       Measurements on Chemically Vapor-Deposited Tungsten Emitters,"
       Thermionic Conversion Specialist Conference Record, p. 31, October
       1968, Framingham, Massachusetts.

(6)   Festa, J. V., and Danko, J. C., "Some Effects of Fluorine Content
       on the Properties of Chemically Vapor Deposited Tungsten," Proceedings
       of the Conference on Chemical Vapor Deposition of Refractory Metals,
       Alloys and Compounds, Gatlinburg, Tennessee, September 1967.

(7)   Thompson, J. R., Danko, J. C., Gregory, T. L., and Webster, H. F.,
       "Surface Characterization Studies on CVD Tungsten," IEEE Conference
       Record of 1968, Thermionic Conversion Specialist Conference,
       October 1968, Framingham, Massachusetts.

(8)   Danko, J. C., and Titus, G. W., "Surface Characterization of CVD
       Tungsten Emitters," IEEE Conference Record of 1969 Thermionic
       Conversion Specialist Conference, October 1969, Carmel, California.

(9)   Batzies, D., Demny, J. and Schmid, H. E., "Preparation and Investi-
       gation on Tungsten Surfaces with Preferred Orientations," Presented
       at Second International Conference on Thermionic Electrical Power
       Generation, May 27, 1968, Stresa, Italy.

(10)   McCandless, R. J., and Wilkins, D. R., "Theory of Thermionic
       Converter Surface Phenomena--Final Summary Report Under U. S. Navy
       Contract N00014-69-C-0247," GEST-9015, General Electric Company,
       May 1970.
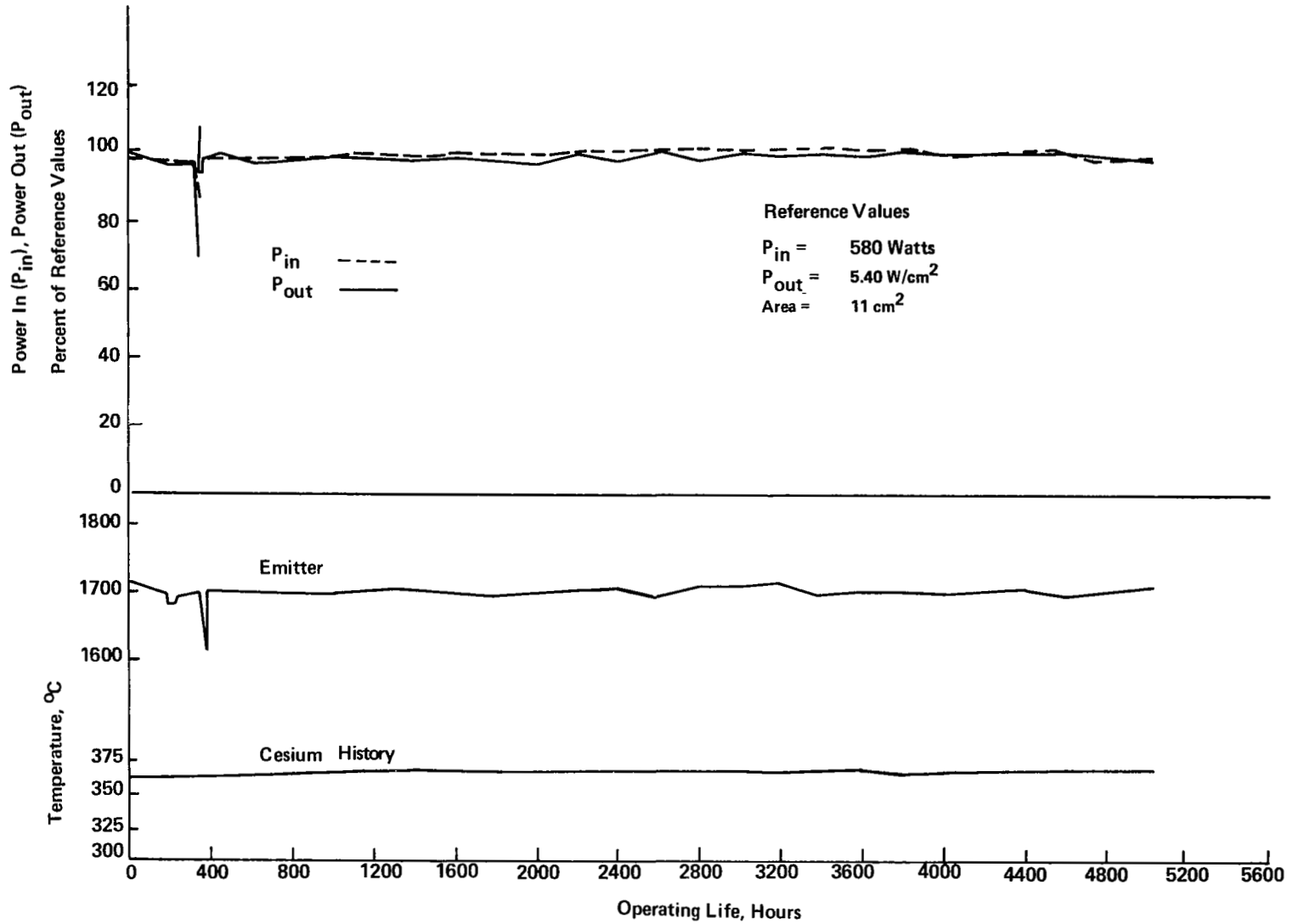
Figure A-1. CONVERTER 362 LIFE TEST PERFORMANCE HISTORY
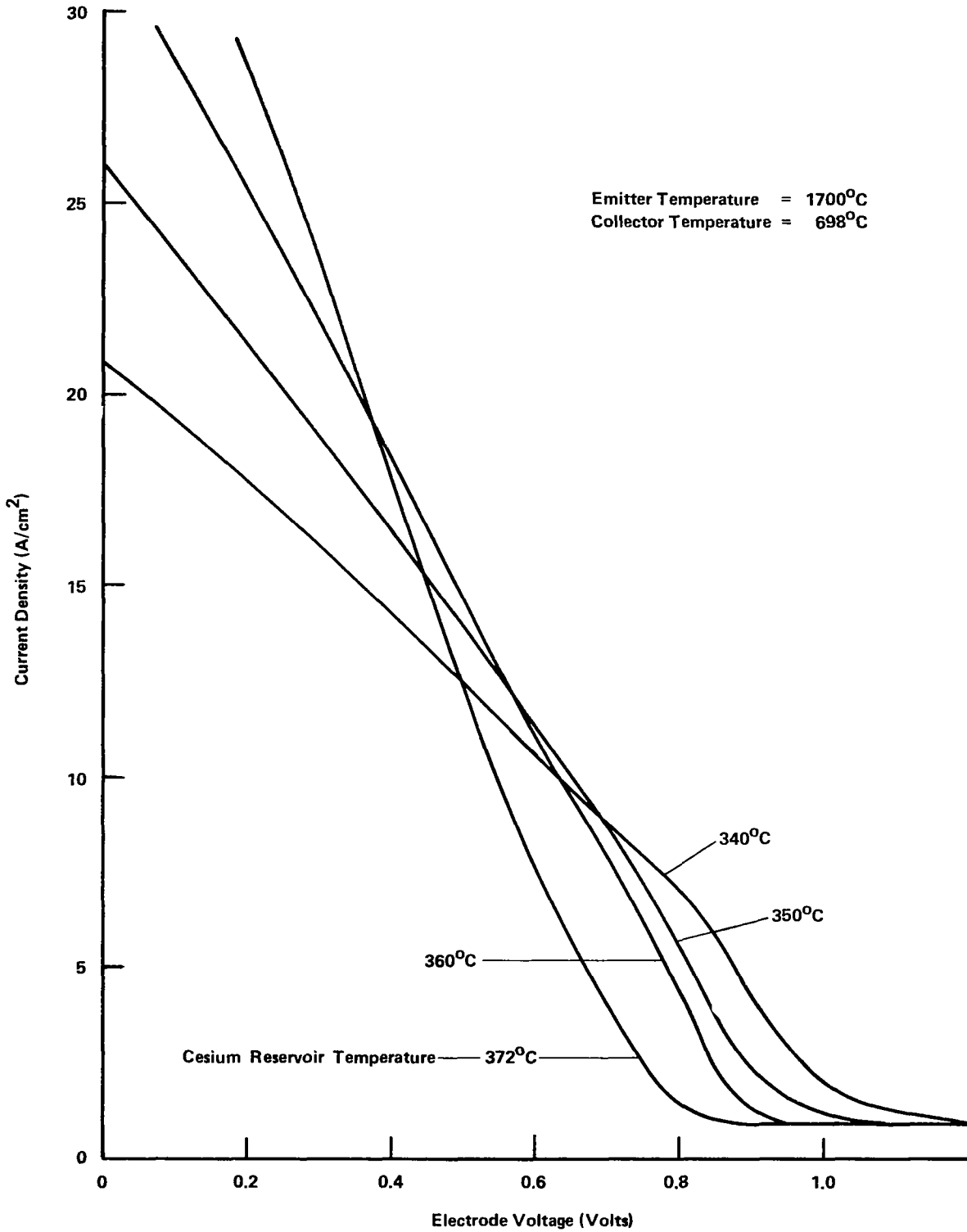
Figure A-2 CONVERTER 362 VOLT-AMPERE CHARACTERISTICS
(T_E = 1700°C, T_C = 698°C) -- INITIAL TEST
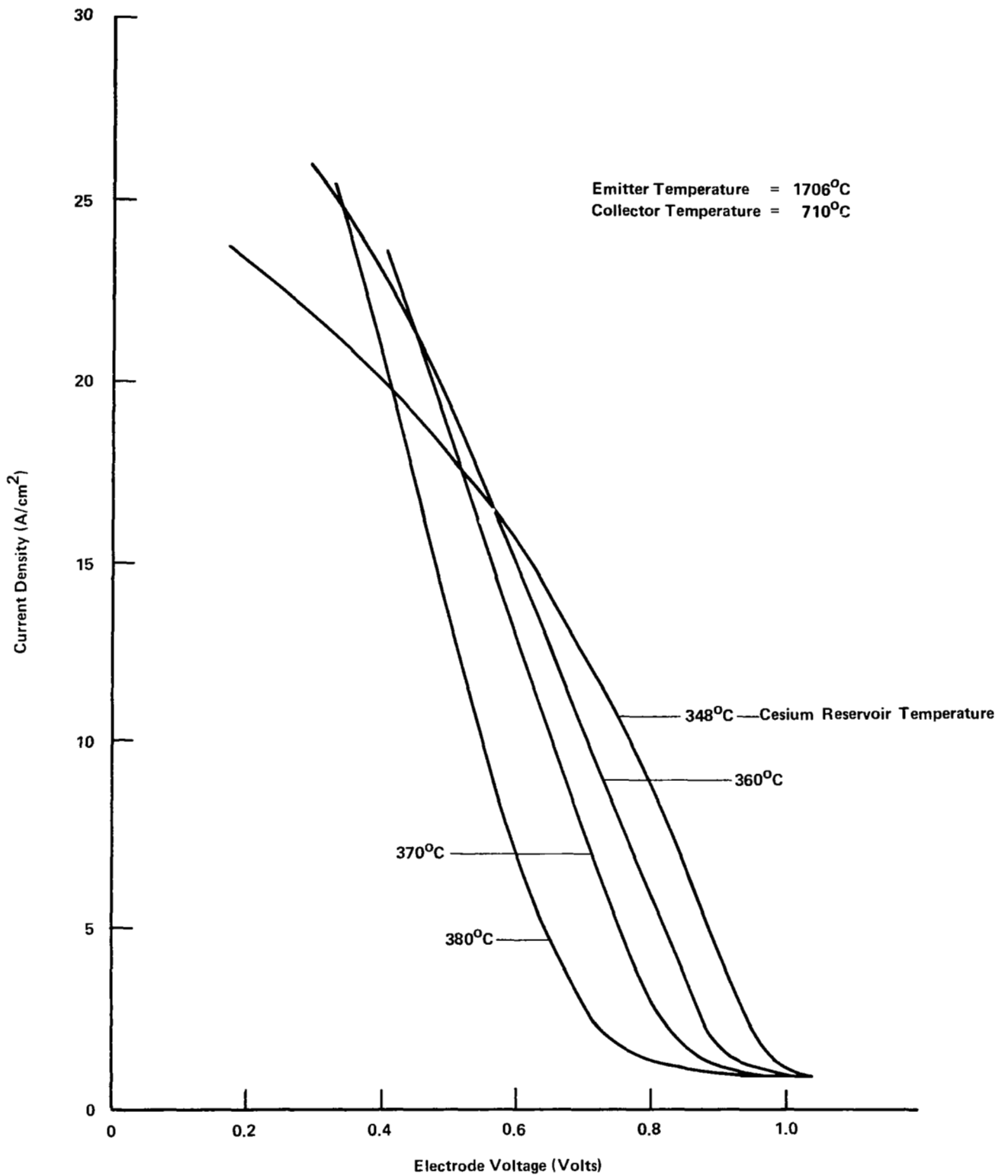
Figure A-3 CONVERTER 362 VOLT-AMPERE CHARACTERISTICS
(T_E = 1706°C, T_C = 710°C) -- INTERMEDIATE TEST (3068 HOURS)
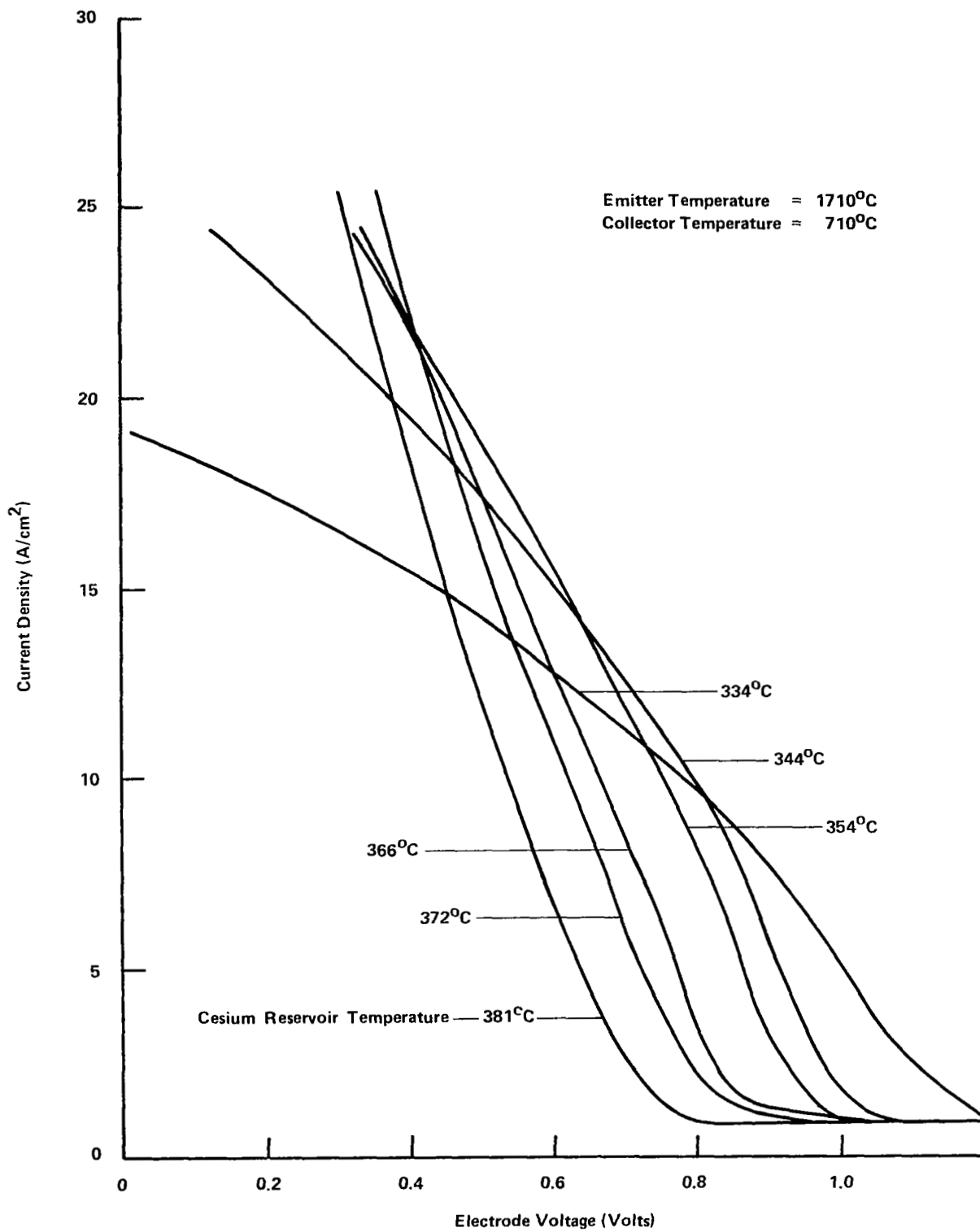
Figure A-4 CONVERTER 362 VOLT-AMPERE CHARACTERISTICS
(T_E = 1710°C, T_C = 710°C) -- FINAL TEST (5011 HOURS)
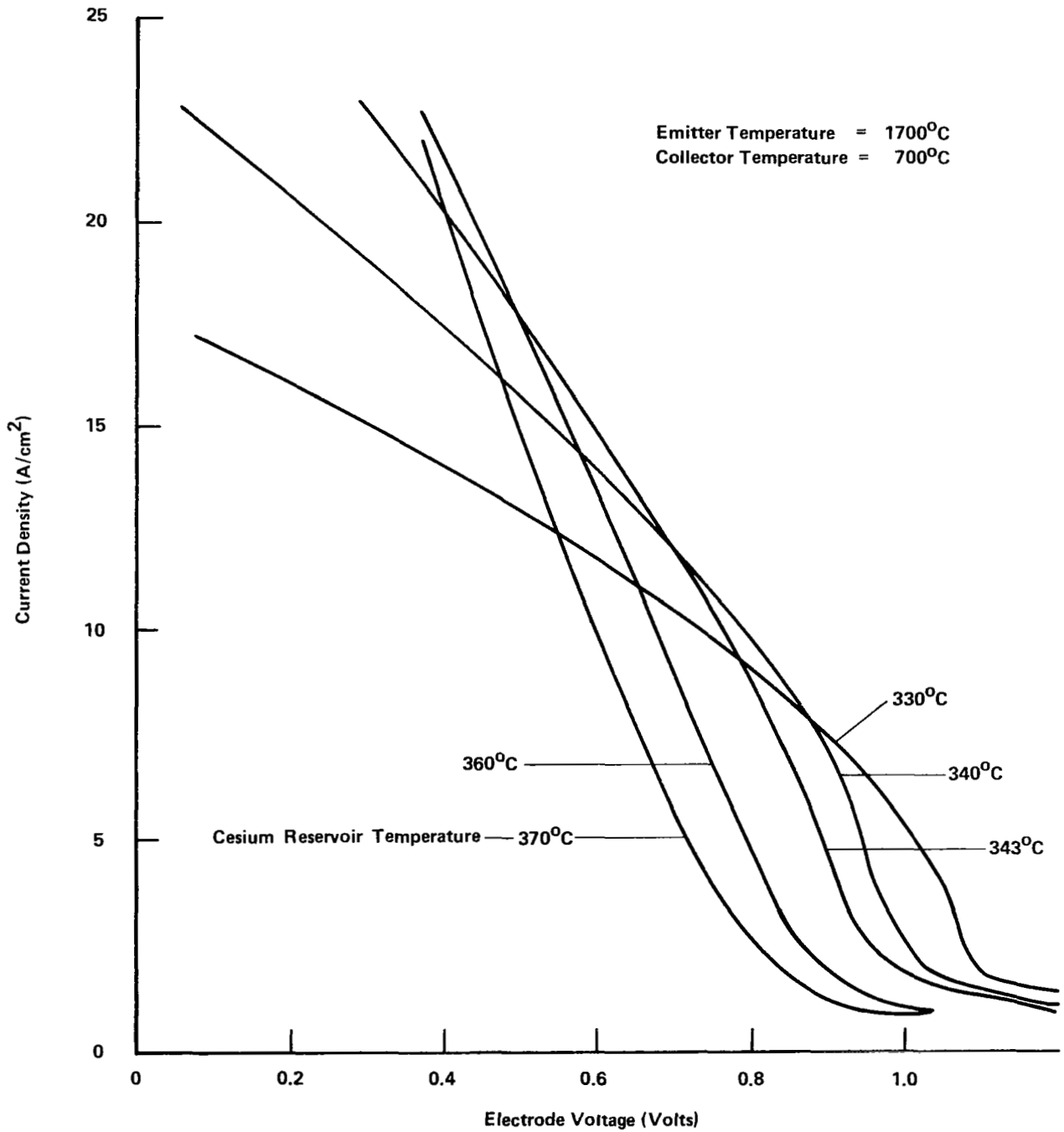
Figure A-5 CONVERTER 362 VOLT-AMPERE CHARACTERISTICS
(T_E = 1700°C, T_C = 700°C) -- FINAL TEST (5012 HOURS)
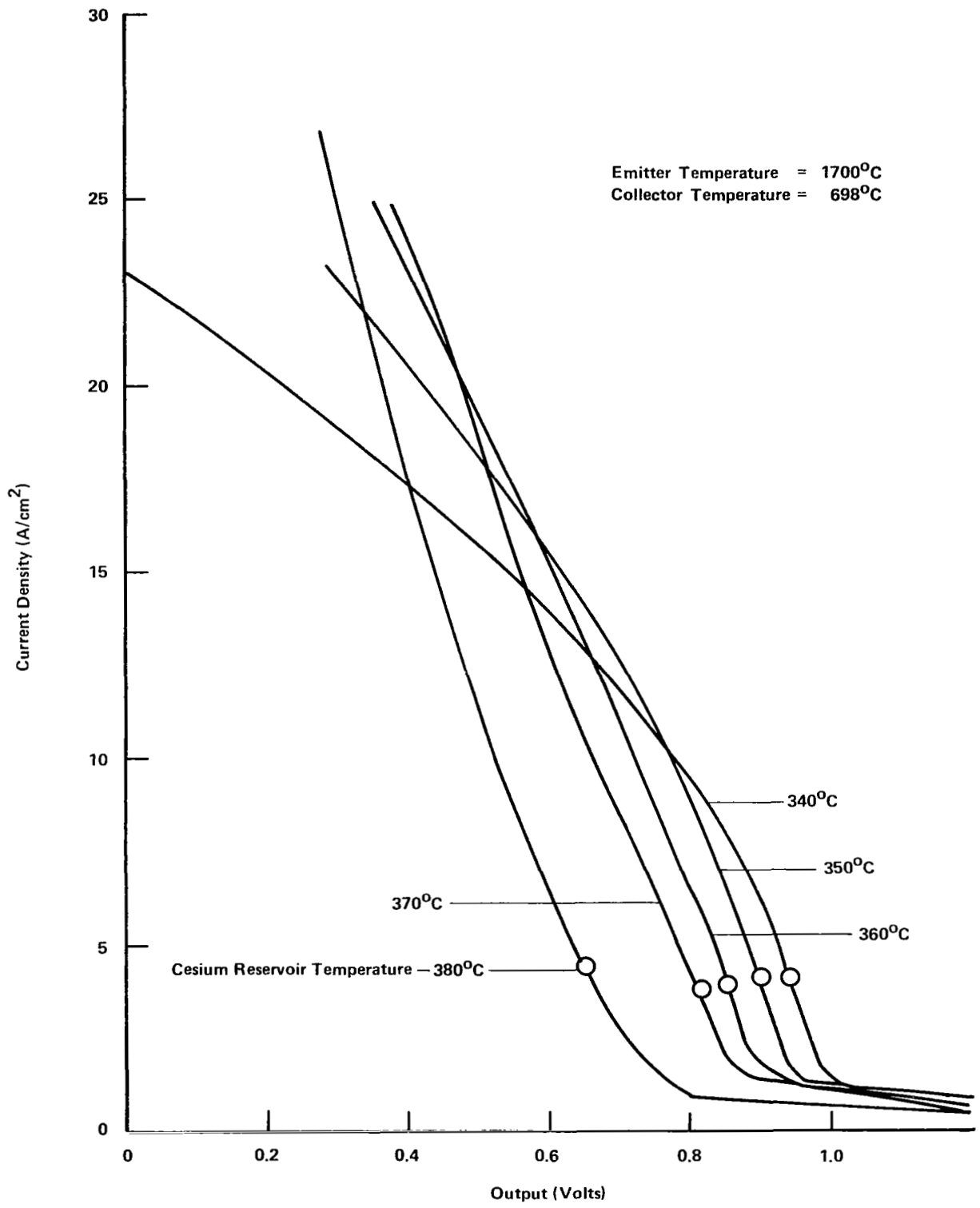
Figure A-6 CONVERTER 362 VOLT-AMPERE CHARACTERISTICS
(T_E = 1700°C, T_C = 698°C) -- FINAL TEST (5580 HOURS)

CONVERTER 363 INITIAL PERFORMANCE CHARACTERISTICS
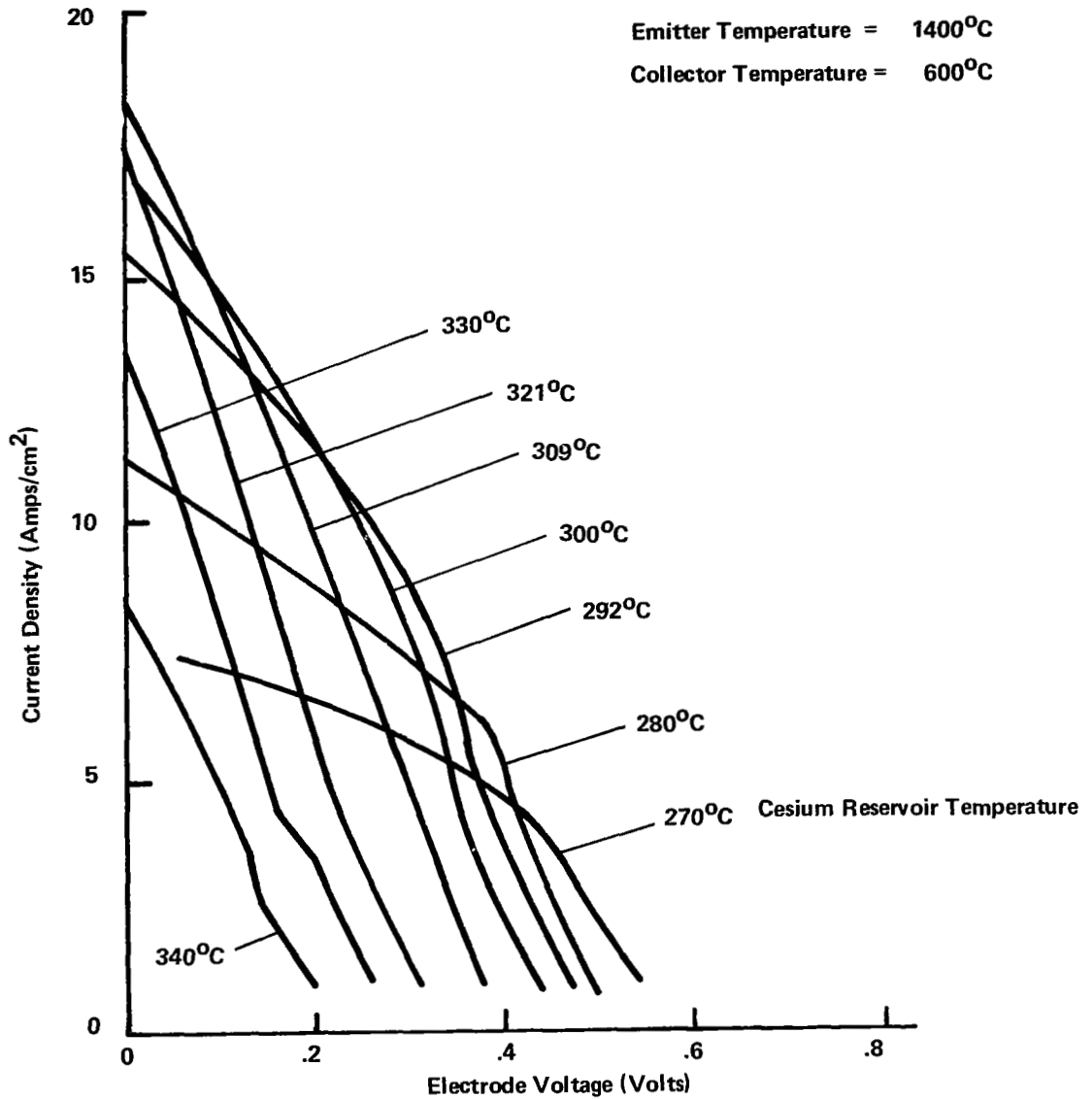
Figure B-1.1　CONVERTER 363 VOLT-AMPERE CHARACTERISTICS
$(T_E = 1400^\circ C, T_C = 600^\circ C)$ - - INITIAL TEST
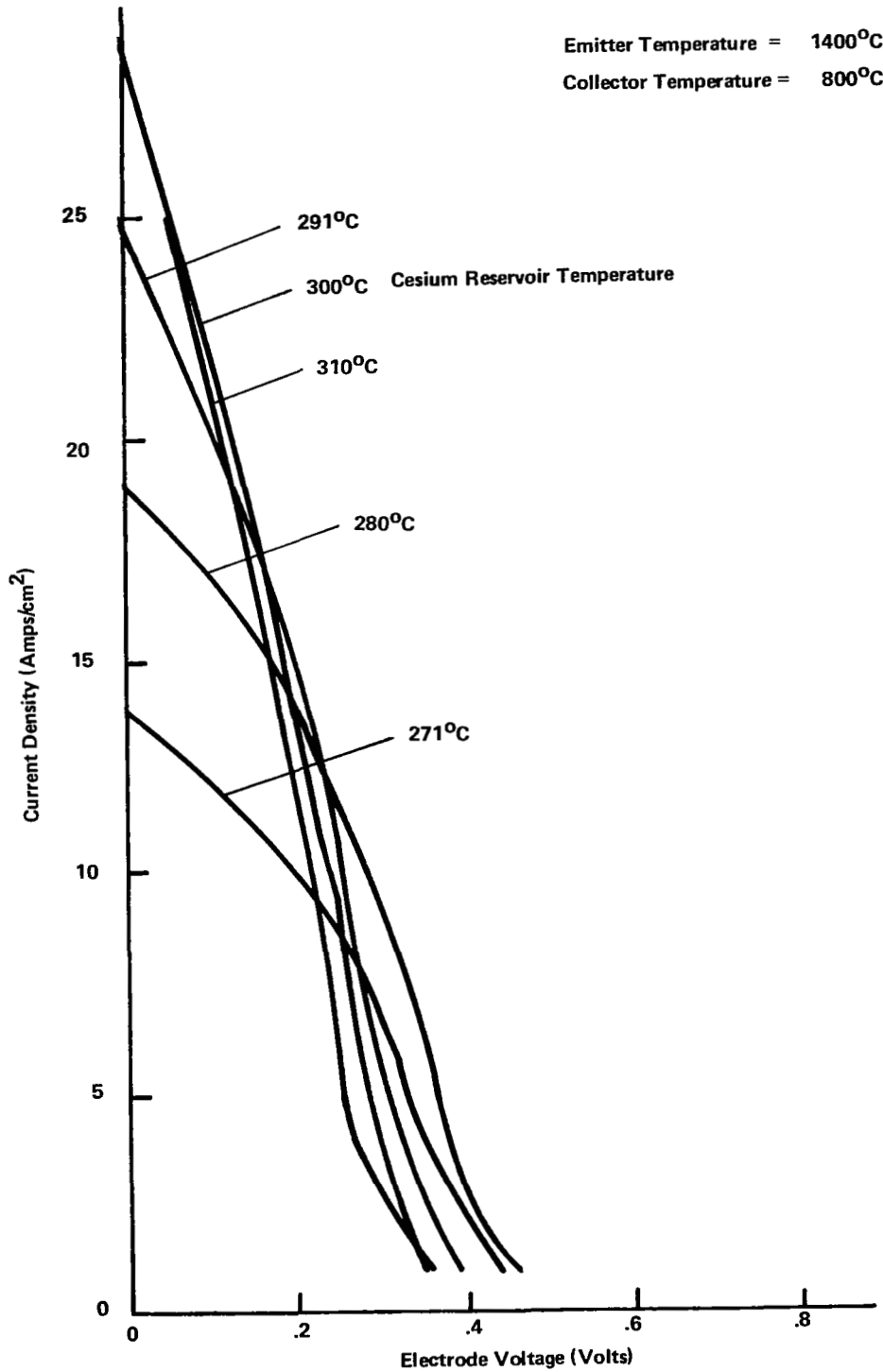
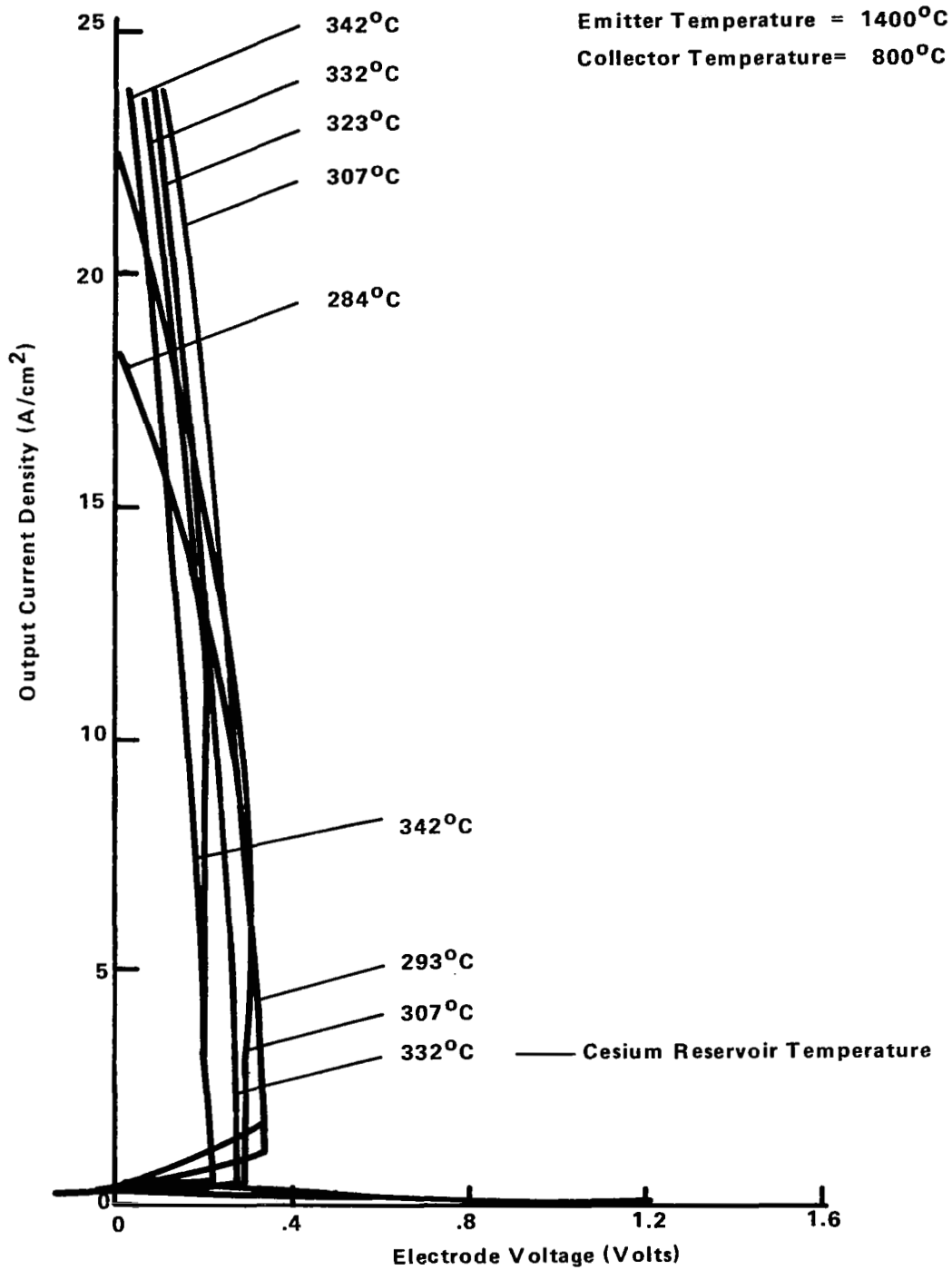Figure B-1.2   CONVERTER 363 VOLT-AMPERE CHARACTERISTICS
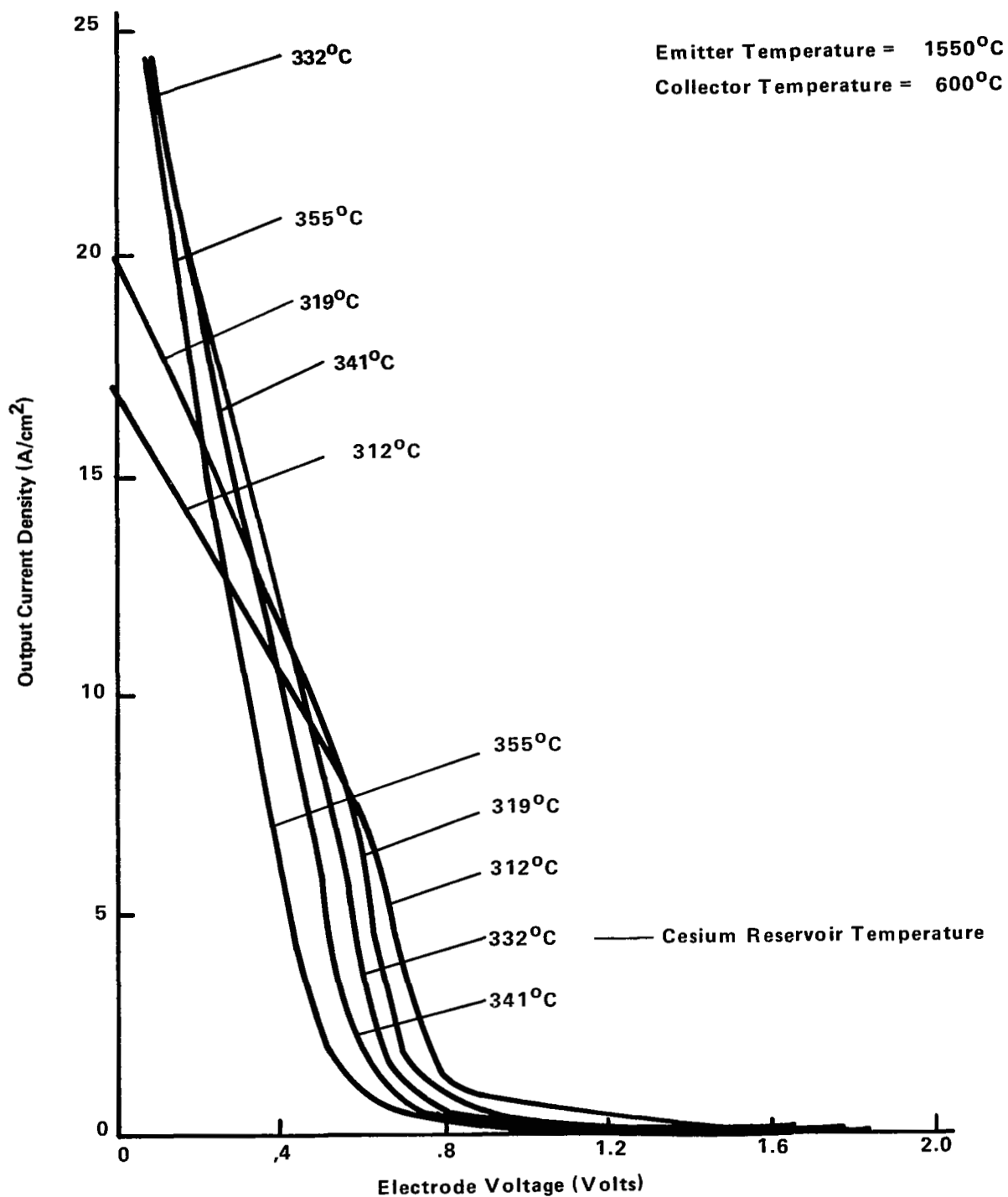$(T_E = 1400^\circ C, \ T_C = 800^\circ C)$ -- INITIAL TEST
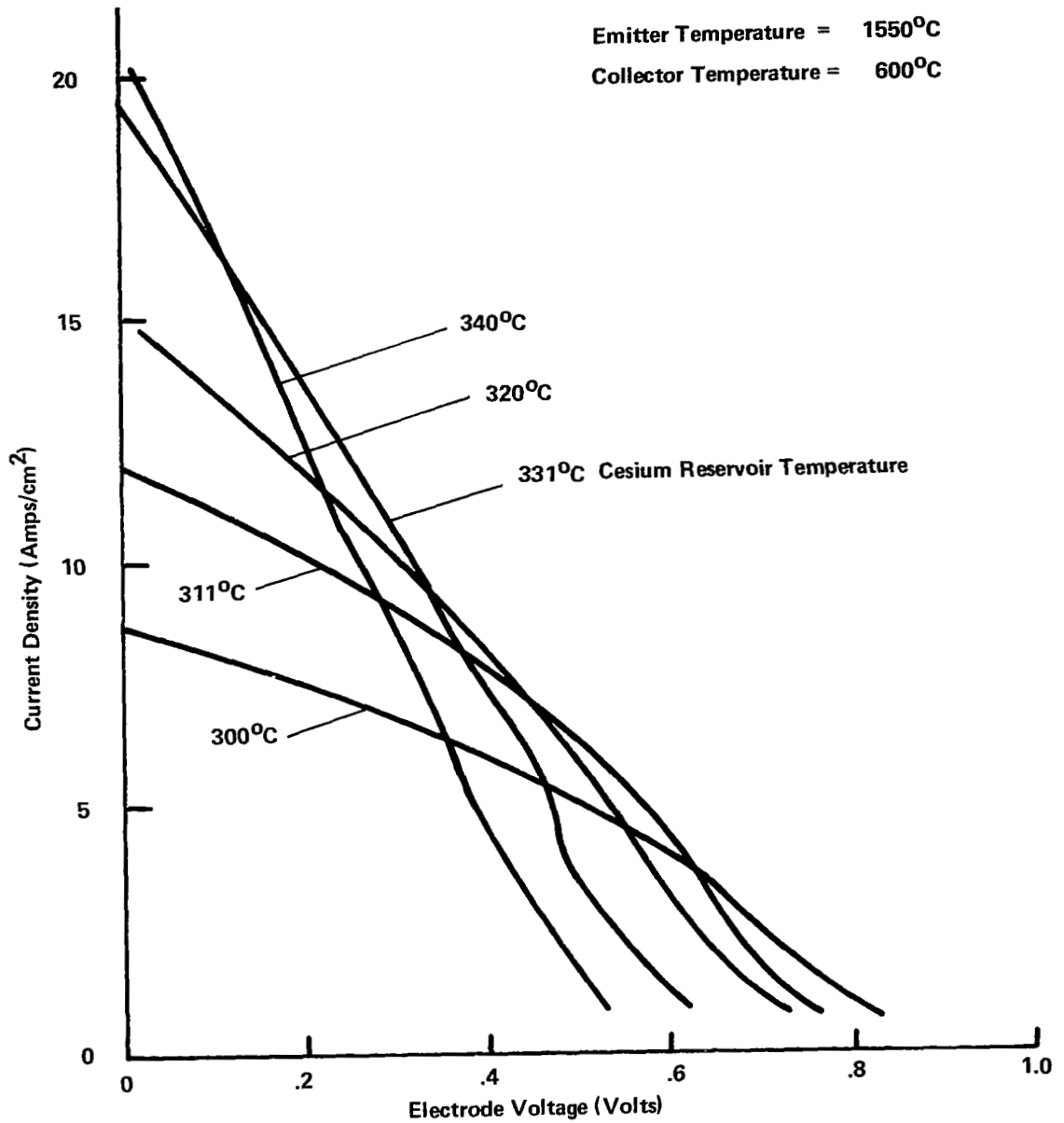
Figure B-1.3   CONVERTER 363 VOLT-AMPERE CHARACTERISTICS
(T_E = 1550°C, T_C = 600°C) -- INITIAL TEST
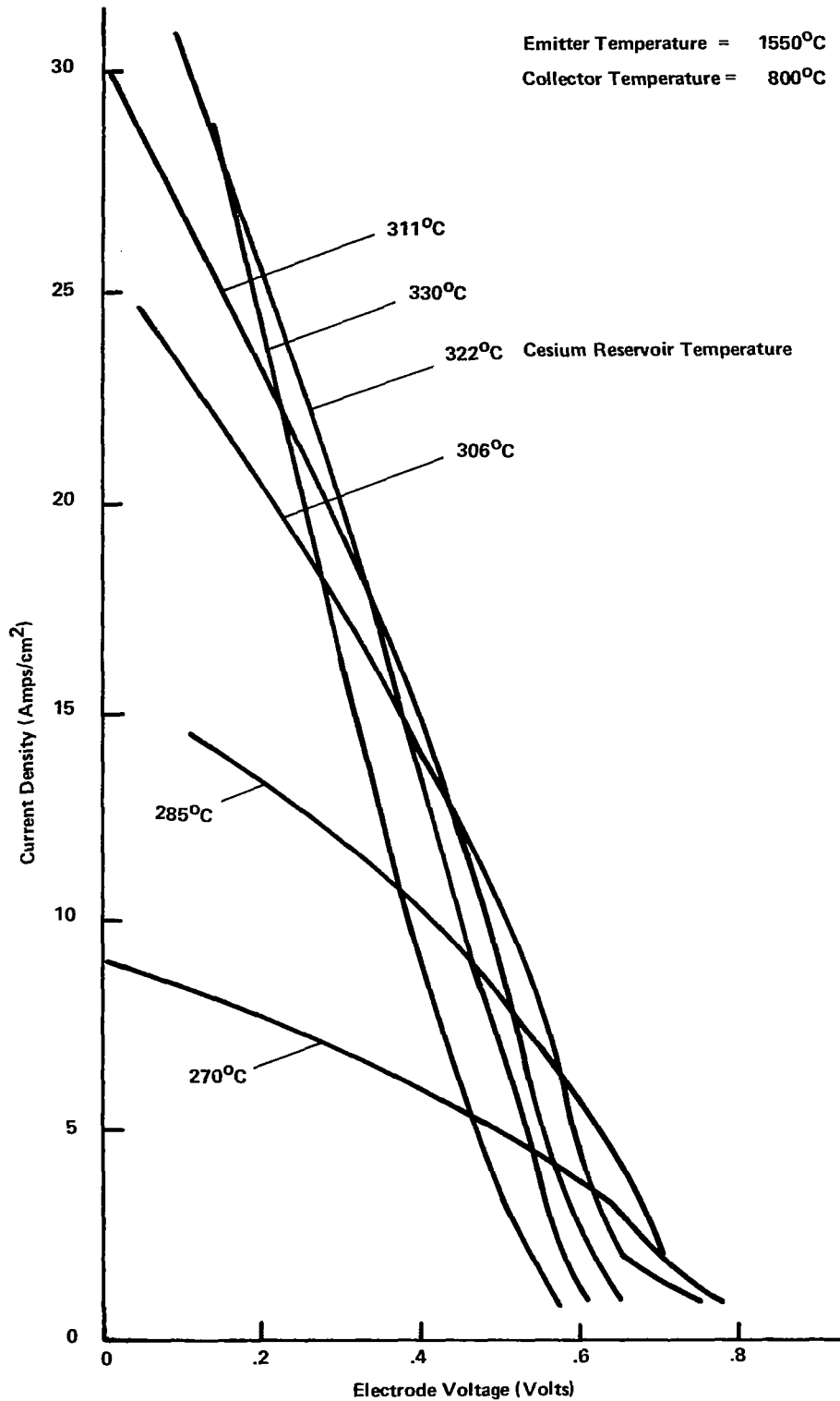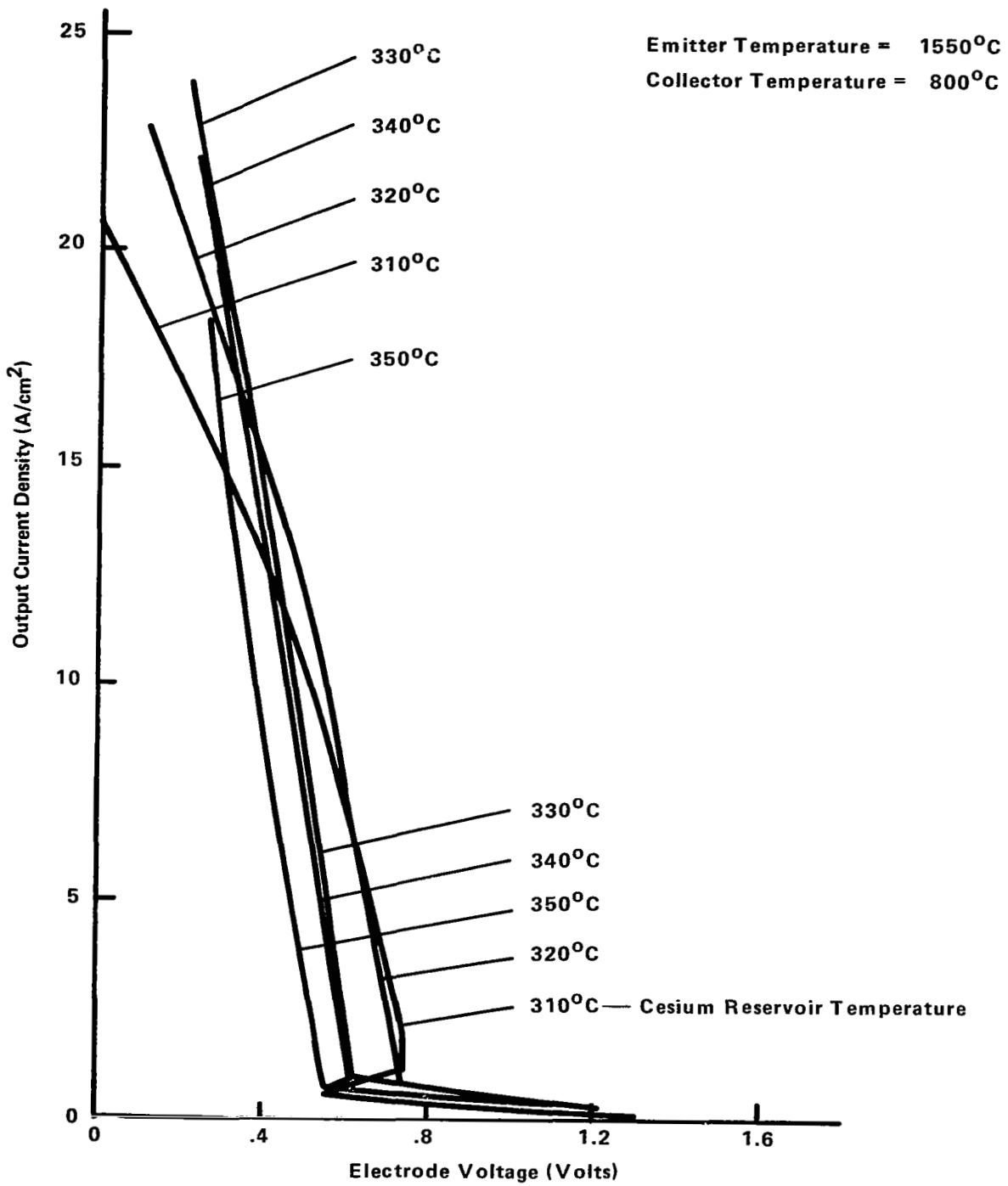
Figure B-1.4   CONVERTER 363 VOLT-AMPERE CHARACTERISTICS
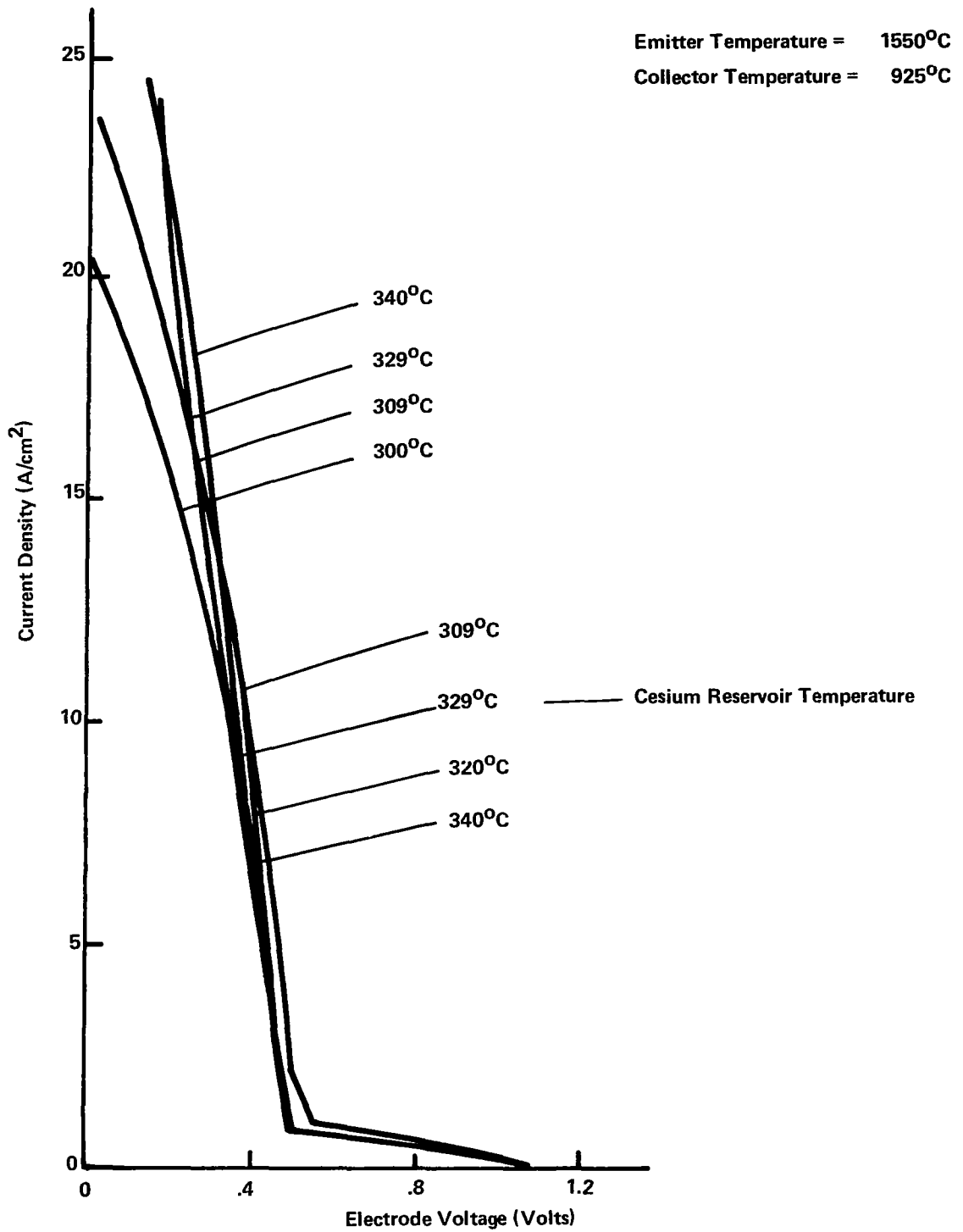$(T_E = 1550^{\circ}C, \ T_C = 800^{\circ}C)$ -- INITIAL TEST

113
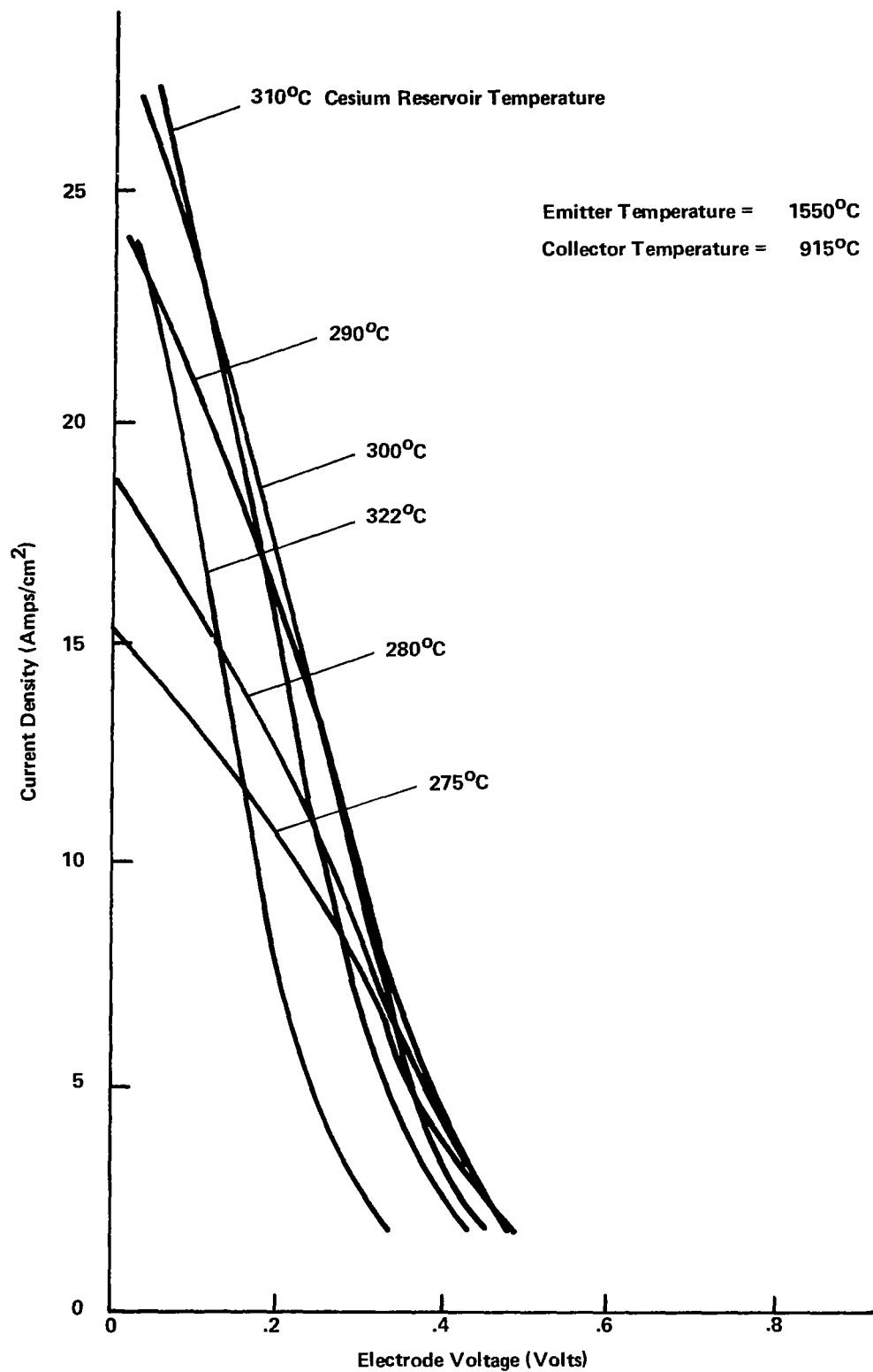
Figure B-1.5   CONVERTER 363 VOLT-AMPERE CHARACTERISTICS
(T_E = 1550°C, T_C = 915°C) -- INITIAL TEST

Emitter Temperature = 1700°C

Collector Temperature = 660°C

350°C

361°C Cesium Reservoir Temperature

340°C

330°C

320°C

310°C

300°C

Current Density (Amps/cm²)

Electrode Voltage (Volts)
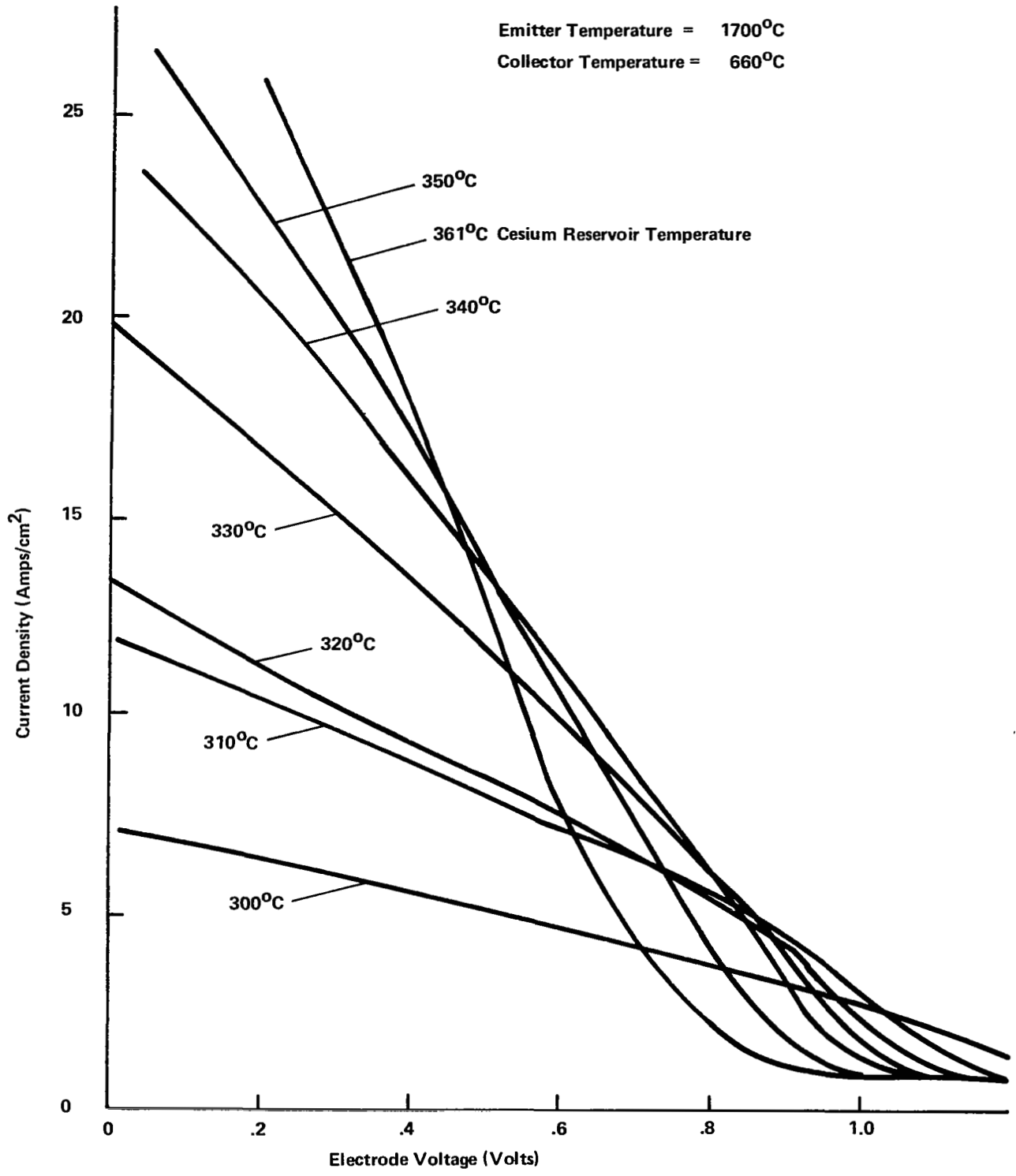
Figure B-1.6   CONVERTER 363 VOLT-AMPERE CHARACTERISTICS
(T_E = 1700°C, T_C = 660°C) -- INITIAL TEST
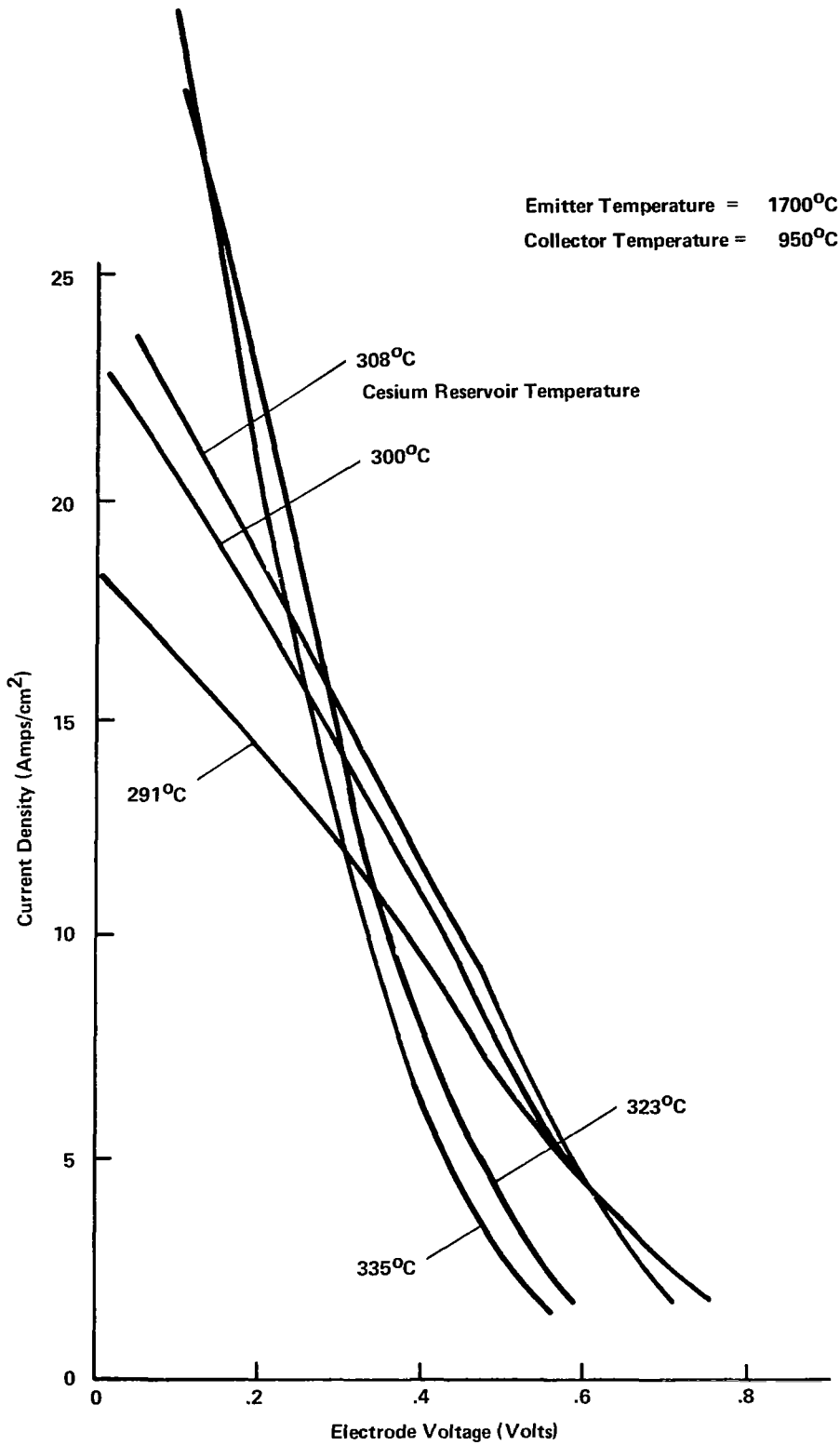
Figure B-1.7   CONVERTER 363 VOLT-AMPERE CHARACTERISTICS
(T$_E$ = 1700°C, T$_C$ = 950°C) -- INITIAL TEST

116

Reference Values

P_{in} = 736 Watts
P_{out} = 6.42 W/cm^2
Area = 11.0 cm^2

P_{in} -----
P_{out} ——
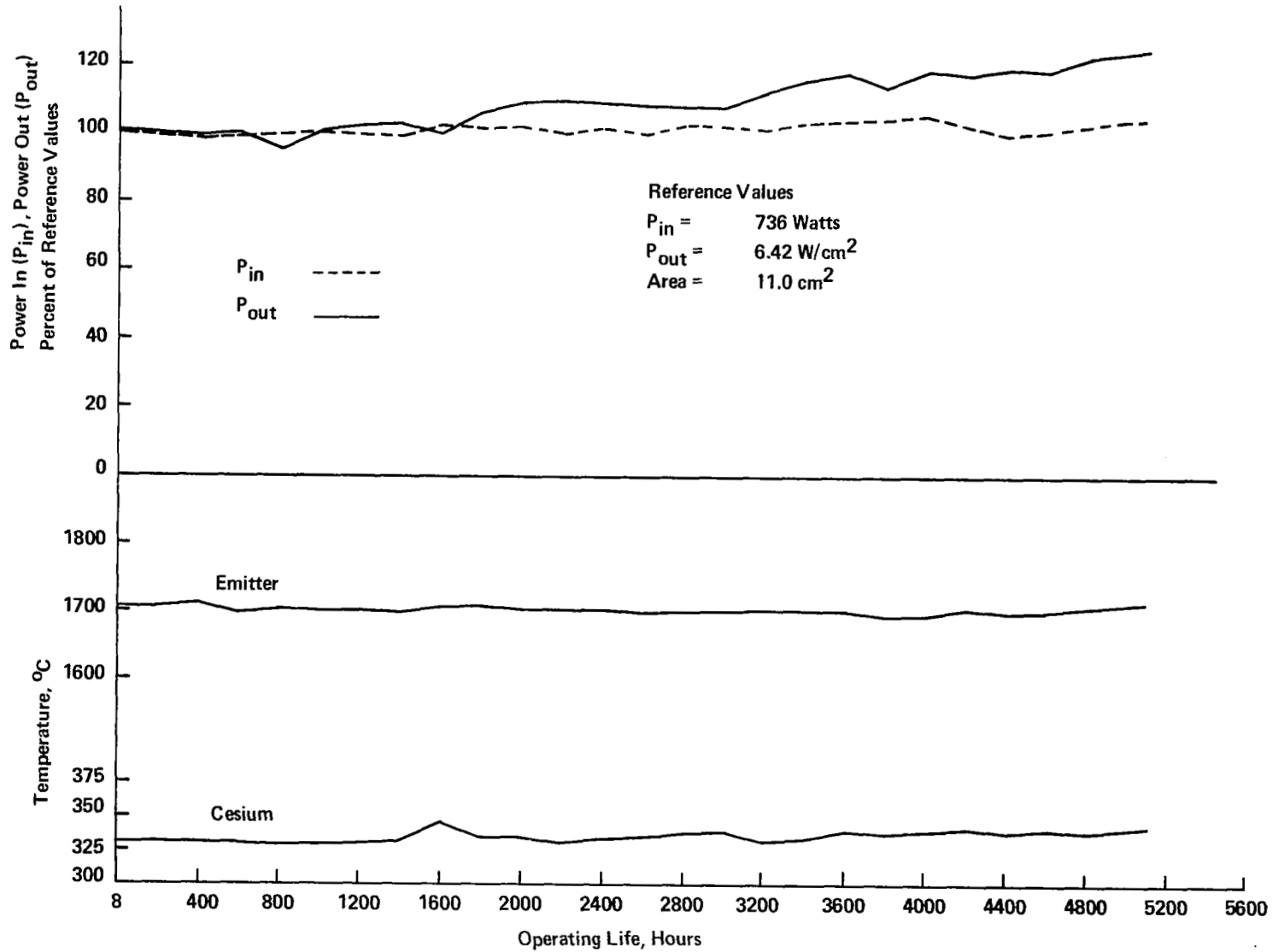
Figure B-2.   CONVERTER 363 LIFE TEST PERFORMANCE HISTORY

CONVERTER 363 FINAL PERFORMANCE CHARACTERISTICS
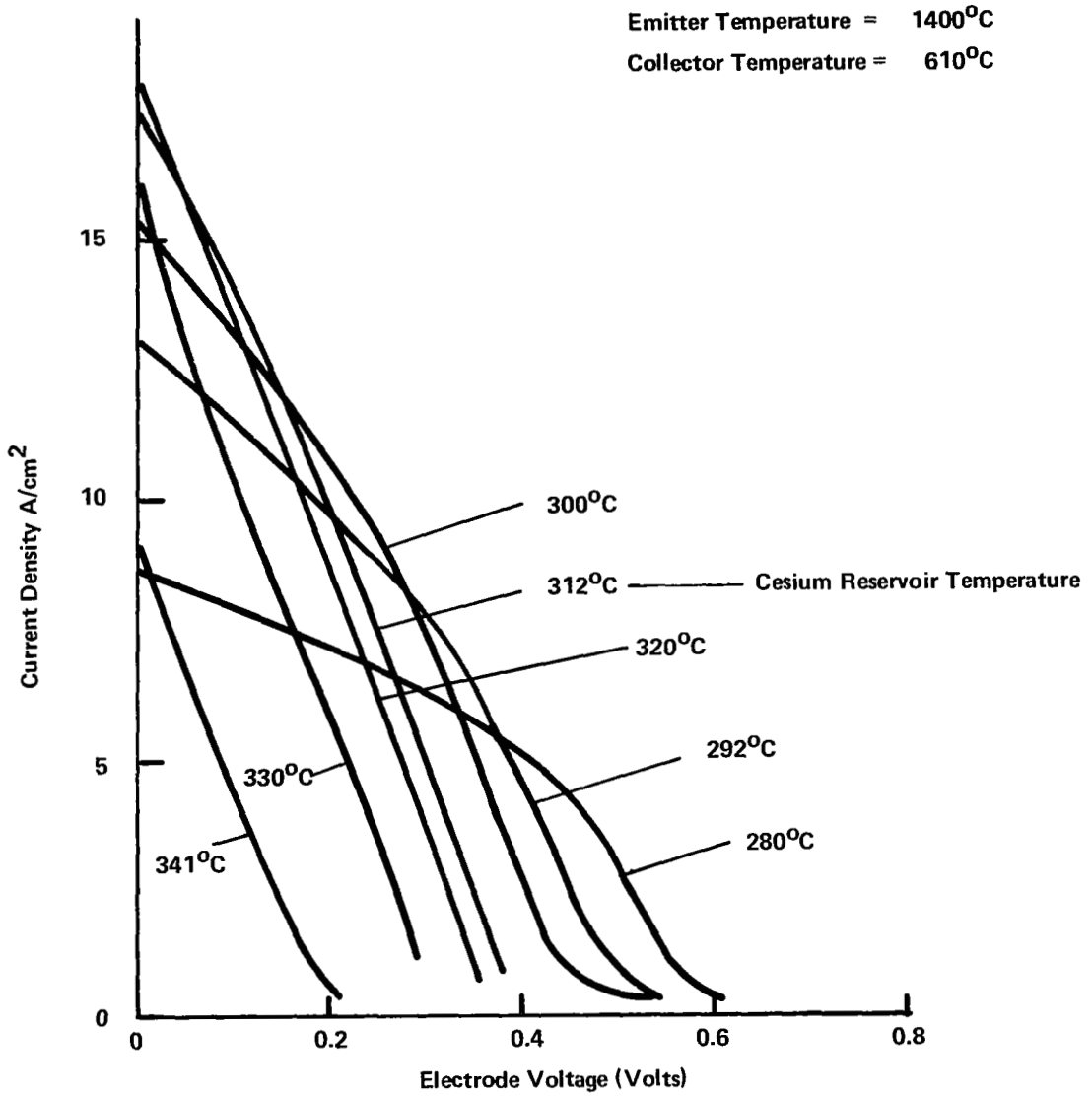
Figure B-3.1   CONVERTER 363 VOLT-AMPERE CHARACTERISTICS
(T_E = 1400°C, T_C = 610°C) -- FINAL TEST
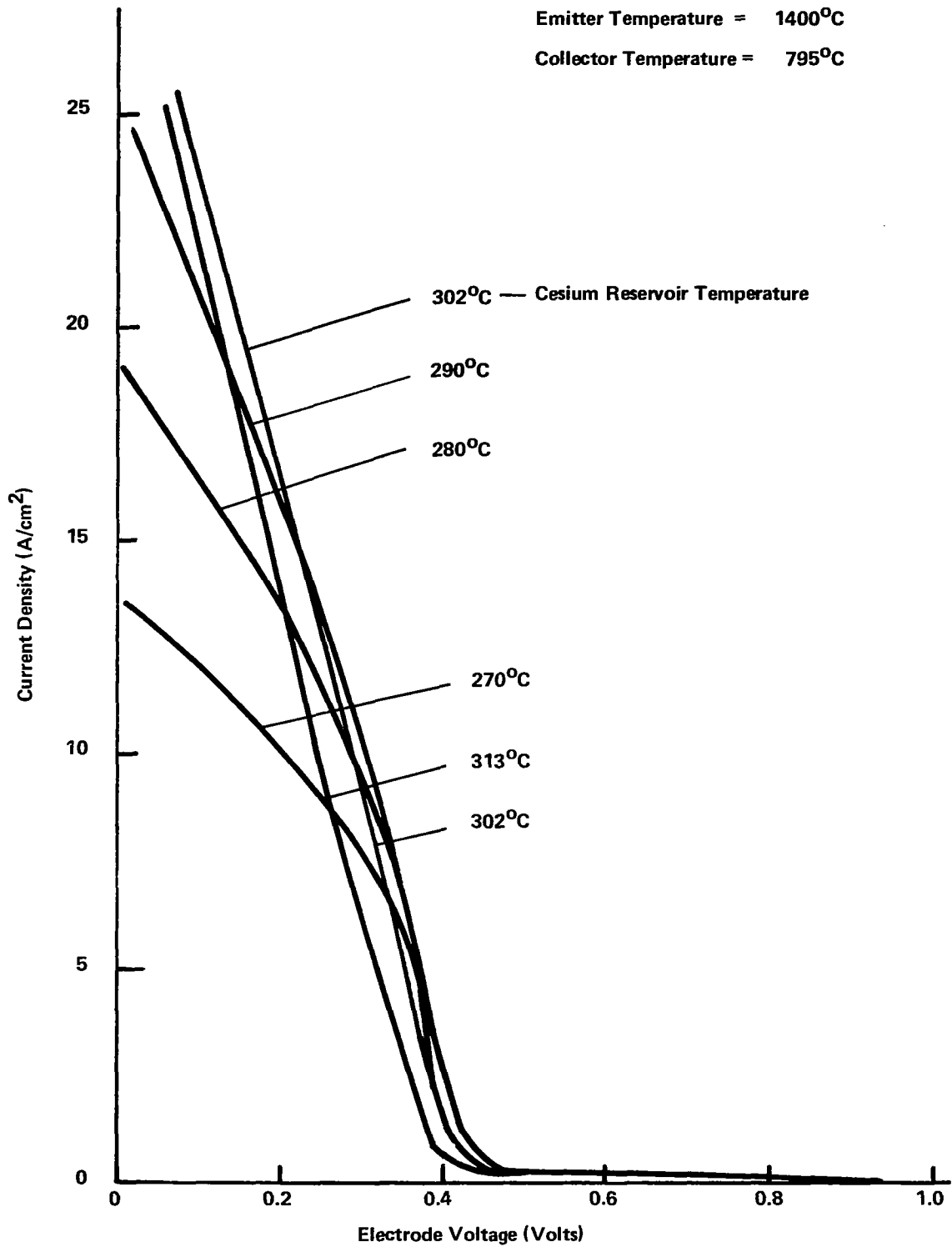
Figure B-3.2   CONVERTER 363 VOLT-AMPERE CHARACTERISTICS
(T_E = 1400°C, T_C = 795°C) -- FINAL TEST

119
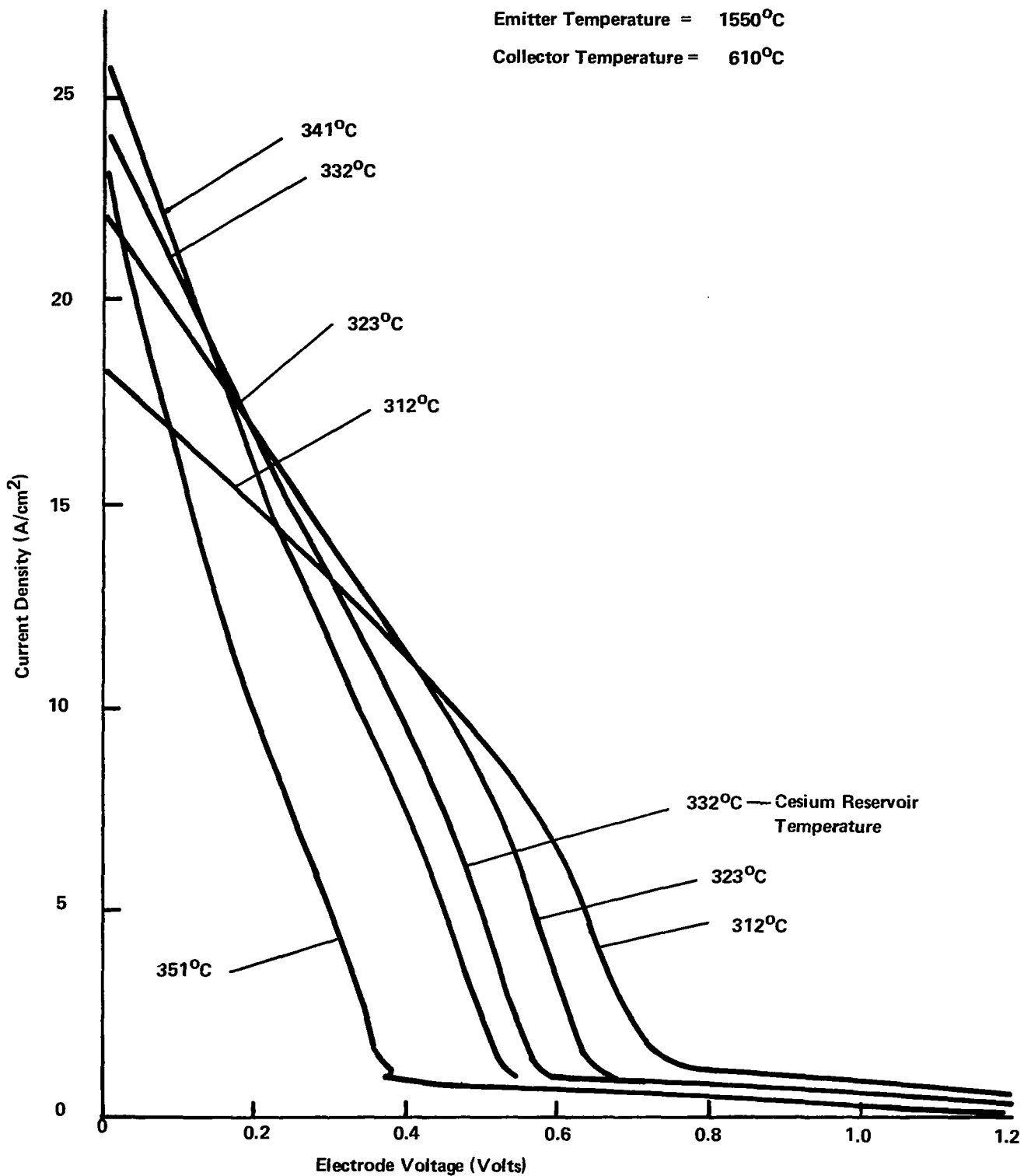
Figure B-3.3   CONVERTER 363 VOLT-AMPERE CHARACTERISTICS
($T_E = 1550°C$, $T_C = 610°C$) -- FINAL TEST

120
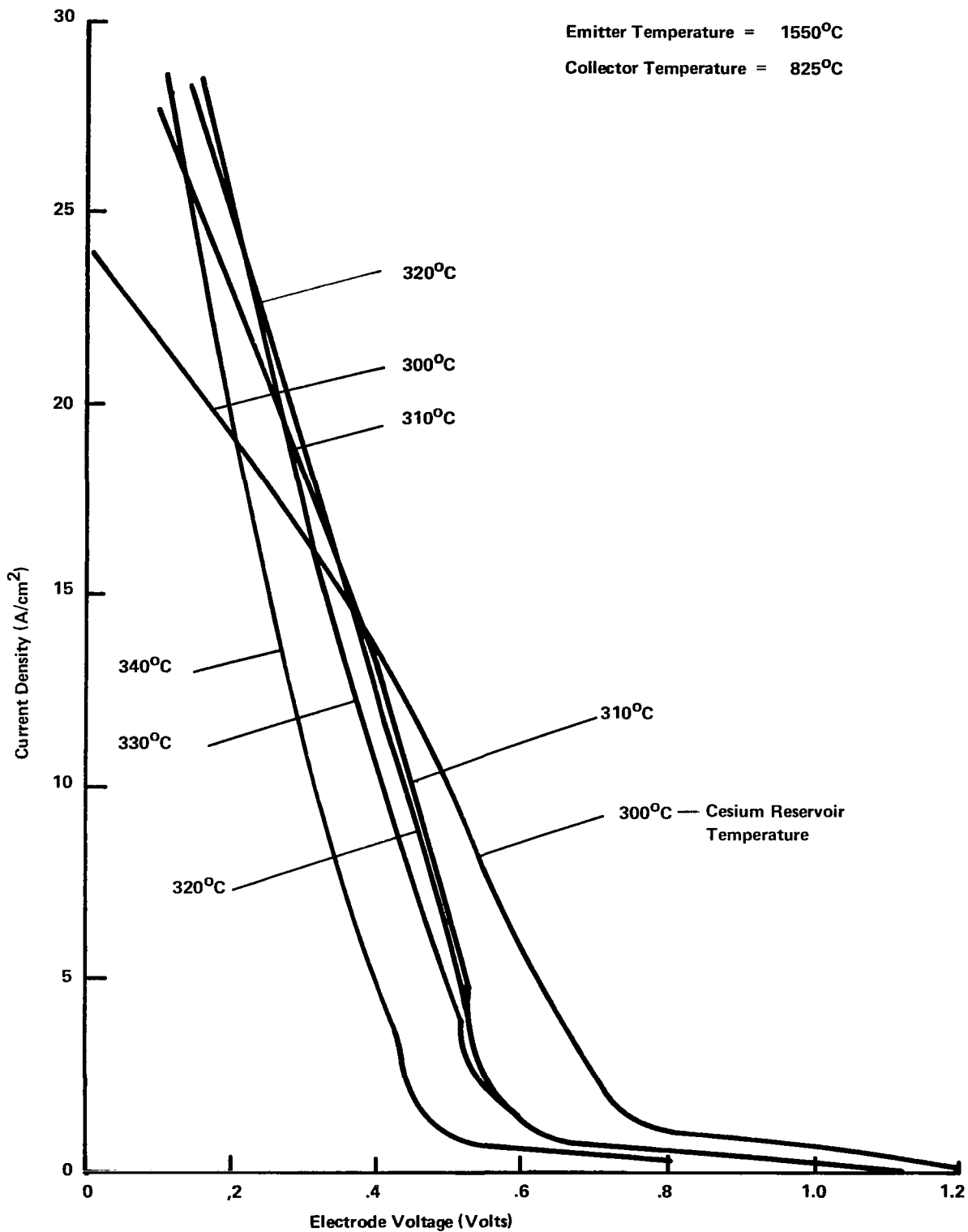
Figure B-3.4   CONVERTER 363 VOLT-AMPERE CHARACTERISTICS
($T_E = 1550^{\circ}C$, $T_C = 825^{\circ}C$) -- FINAL TEST

121
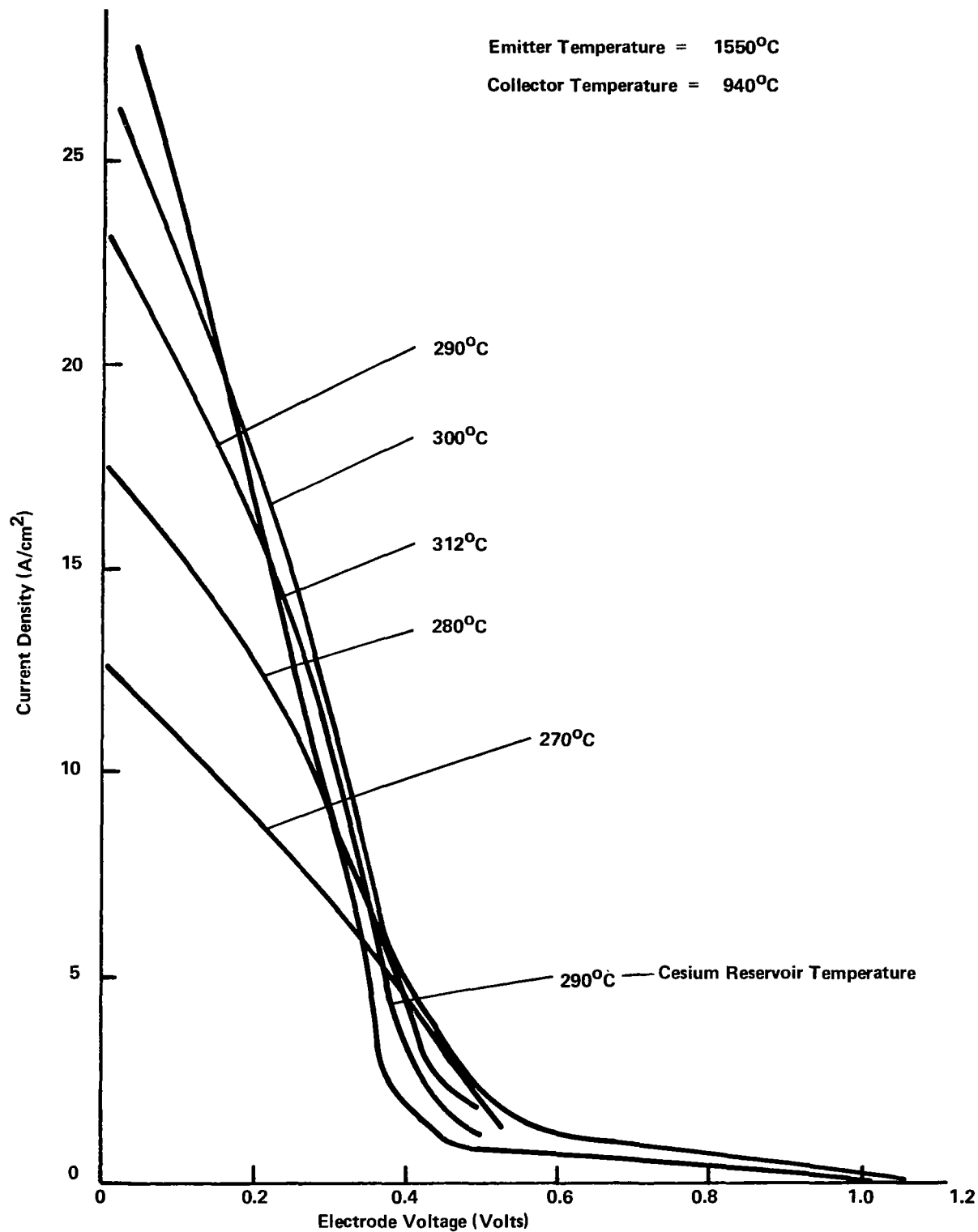
Figure B-3.5   CONVERTER 363 VOLT-AMPERE CHARACTERISTICS
(T_E = 1550°C, T_C = 940°C) -- FINAL TEST

122
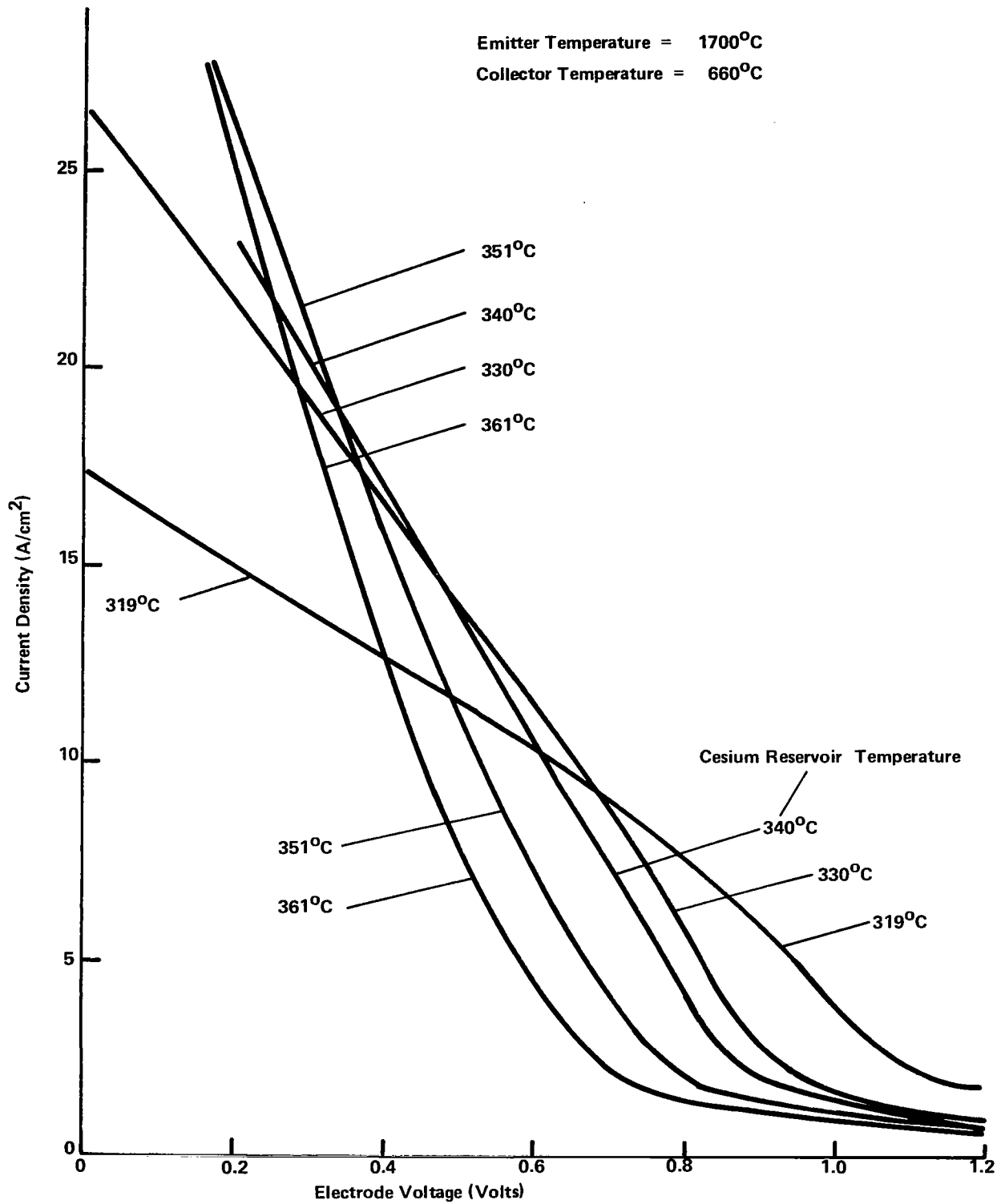
Figure B-3.6   CONVERTER 363 VOLT-AMPERE CHARACTERISTICS
($T_E = 1700^{\circ}C$, $T_C = 660^{\circ}C$) -- FINAL TEST
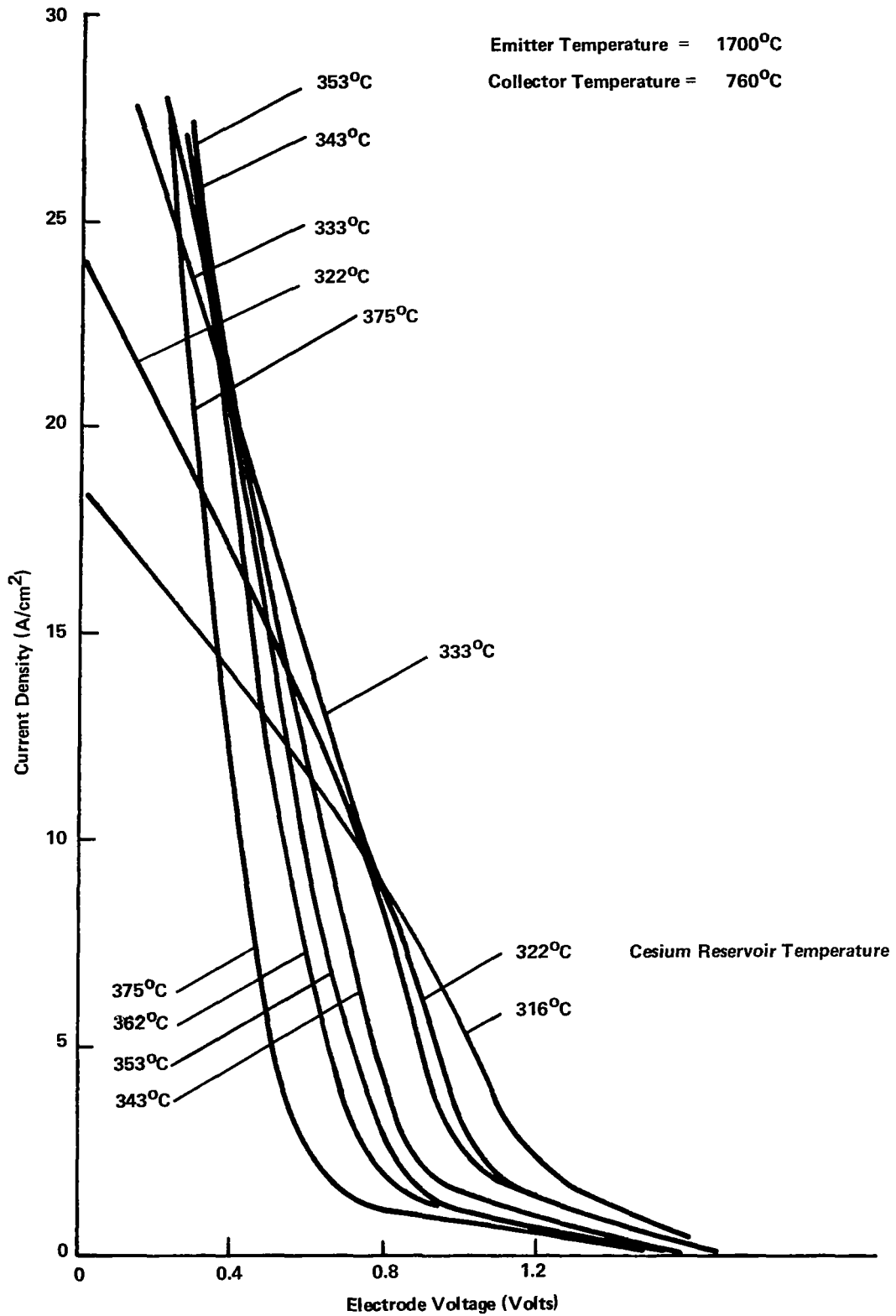
Figure B-3.7   CONVERTER 363 VOLT-AMPERE CHARACTERISTICS
(T_E = 1700°C, T_C = 760°C) -- FINAL TEST
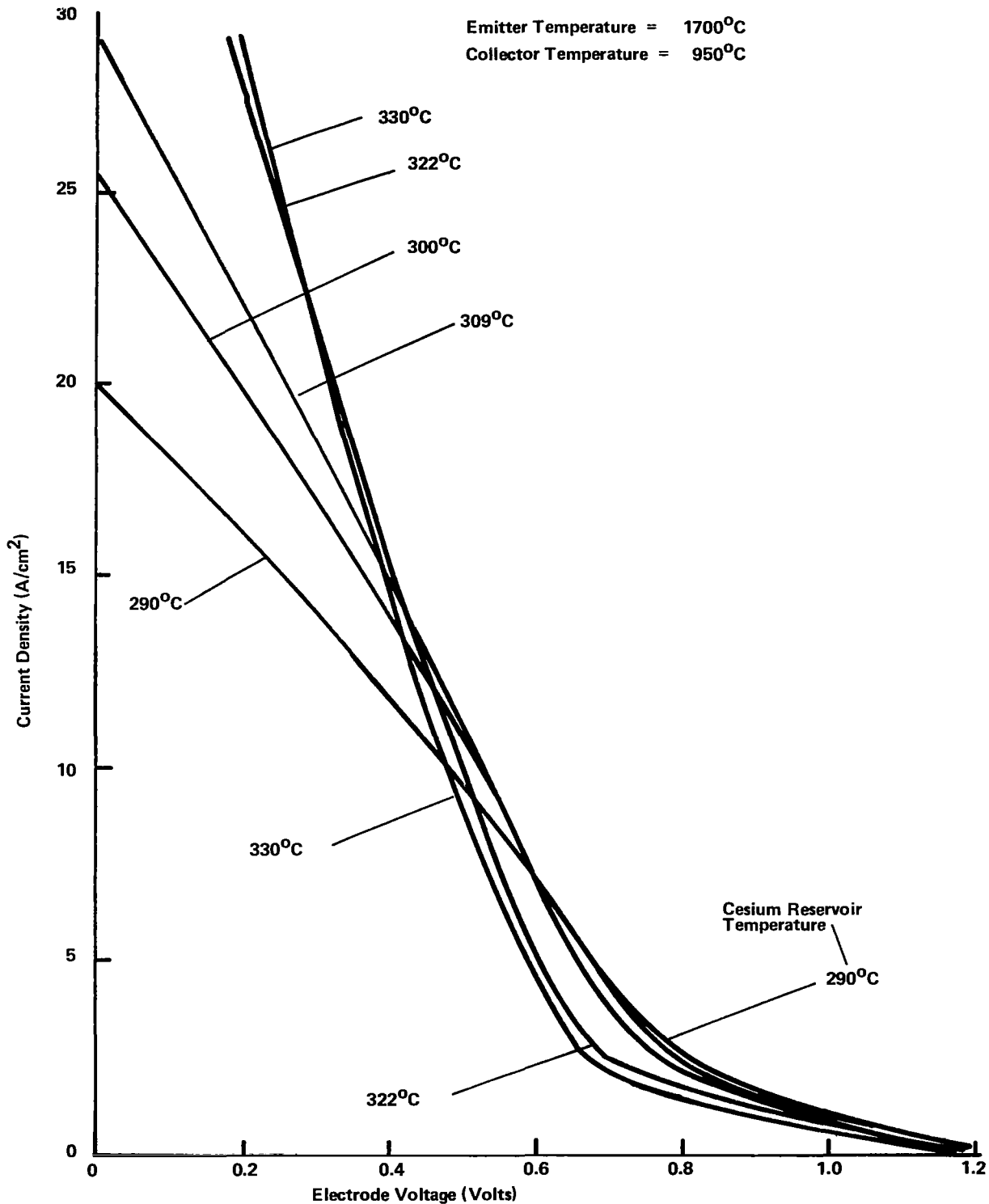
Figure B-3.8 CONVERTER 363 VOLT-AMPERE CHARACTERISTICS
(T_E = 1700°C, T_C = 950°C) -- FINAL TEST
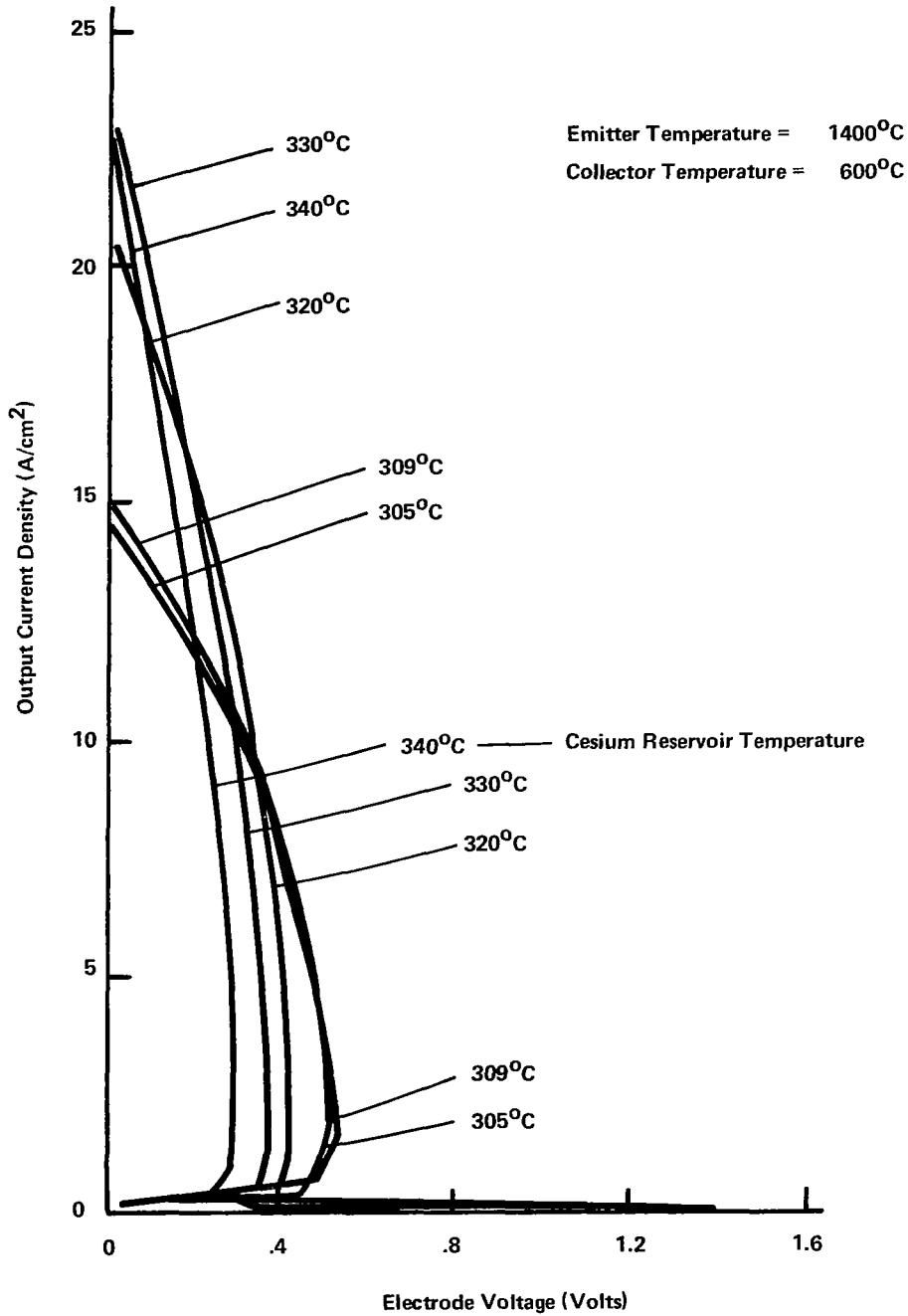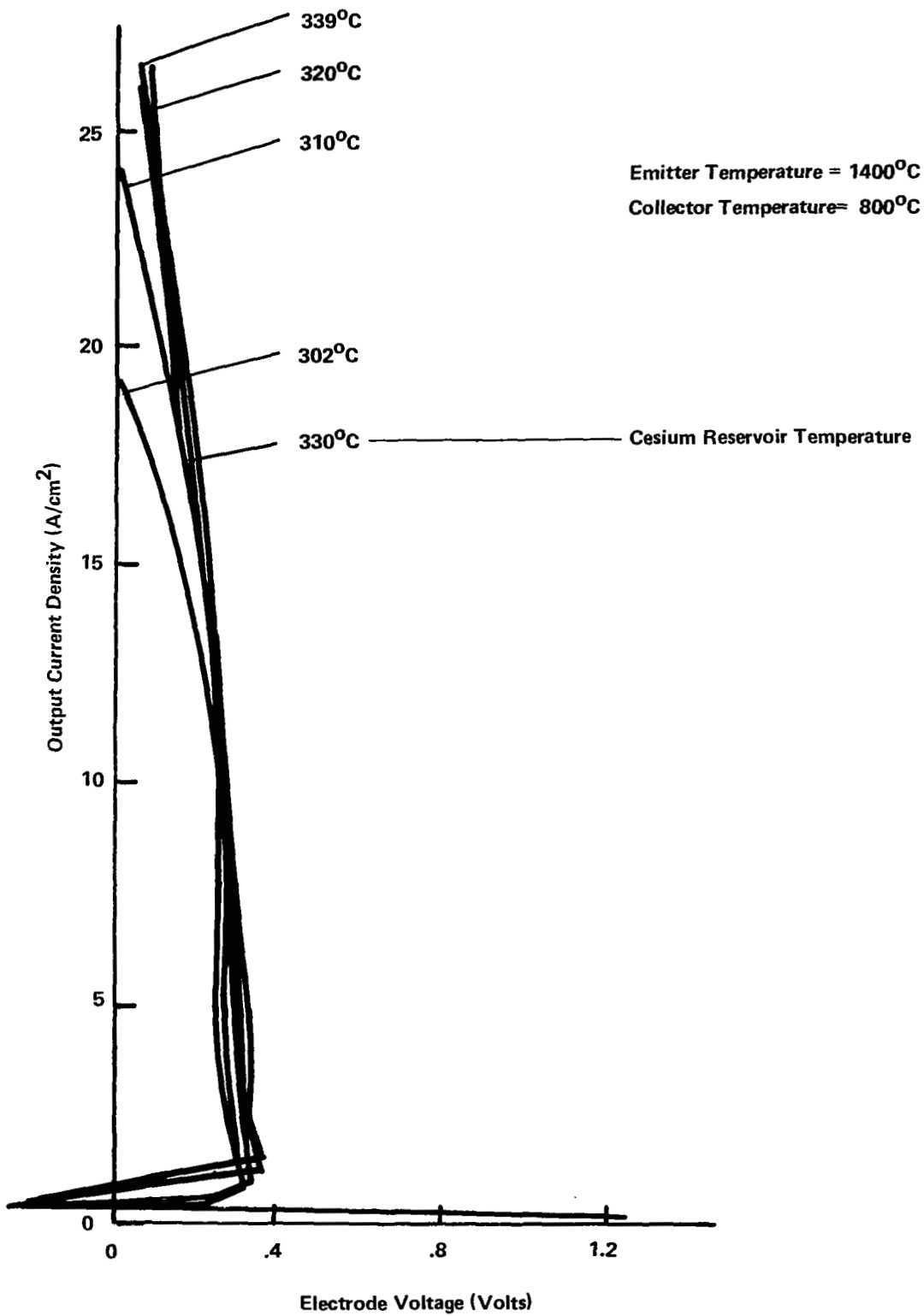
CONVERTER 364 INITIAL PERFORMANCE CHARACTERISTICS
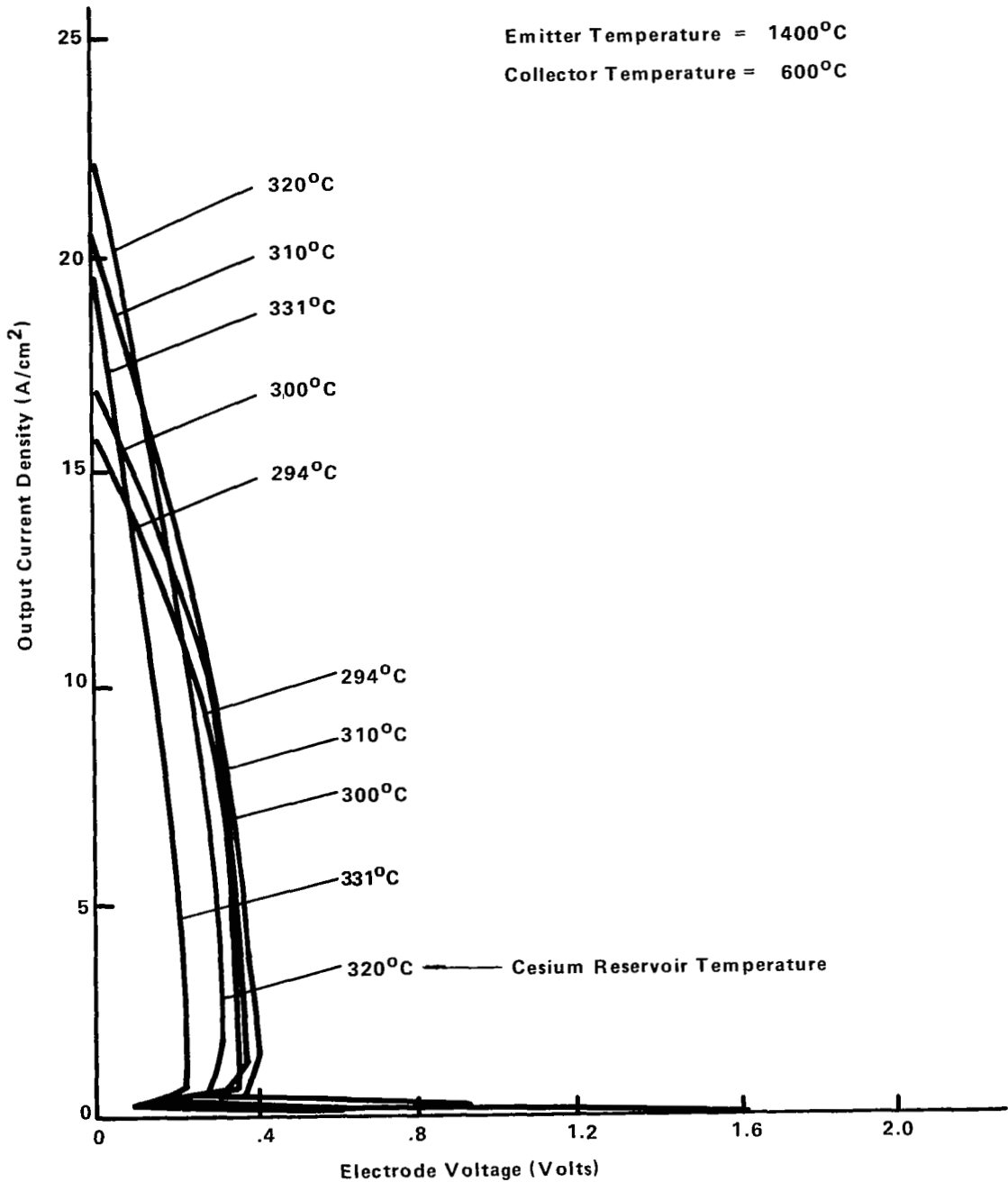
Figure C-1.1   CONVERTER 364 VOLT-AMPERE CHARACTERISTICS
$(T_E = 1400^{\circ}C,\ T_C = 600^{\circ}C)$ -- INITIAL TEST

Figure C-1.2   CONVERTER 364 VOLT-AMPERE CHARACTERISTICS
(T_E = 1400°C, T_C = 800°C) -- INITIAL TEST"

127

Figure C-1.3   CONVERTER 364 VOLT-AMPERE CHARACTERISTICS
(T_E=1550°C, T_C=600°C) -- INITIAL TEST

Figure C-1.4   CONVERTER 364 VOLT-AMPERE CHARACTERISTICS
(T_E = 1550°C, T_C = 800°C) -- INITIAL TEST

129

Figure C-1.5   CONVERTER 364 VOLT-AMPERE CHARACTERISTICS
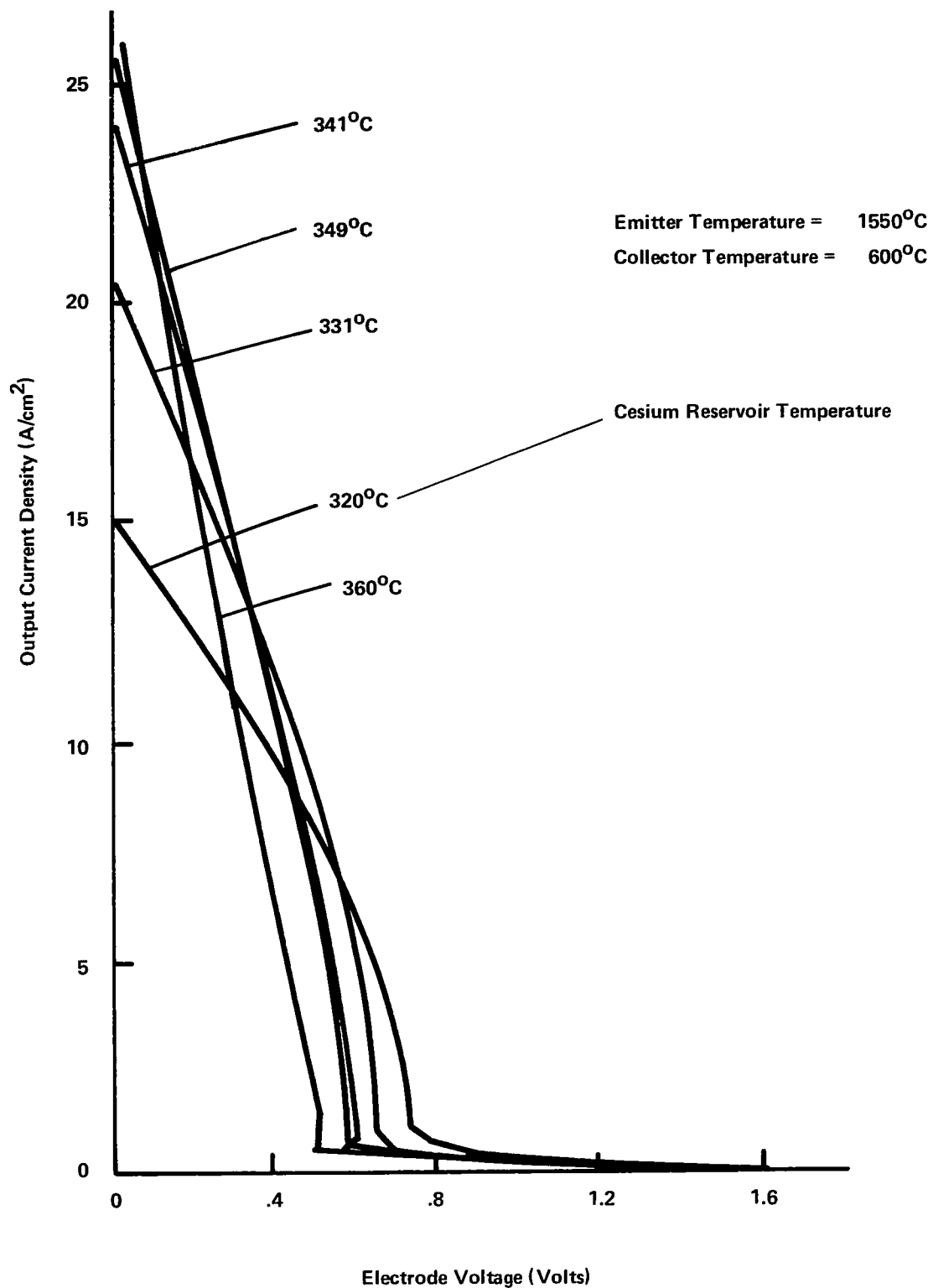(T_E = 1550°C, T_C = 925°C) -- INITIAL TEST
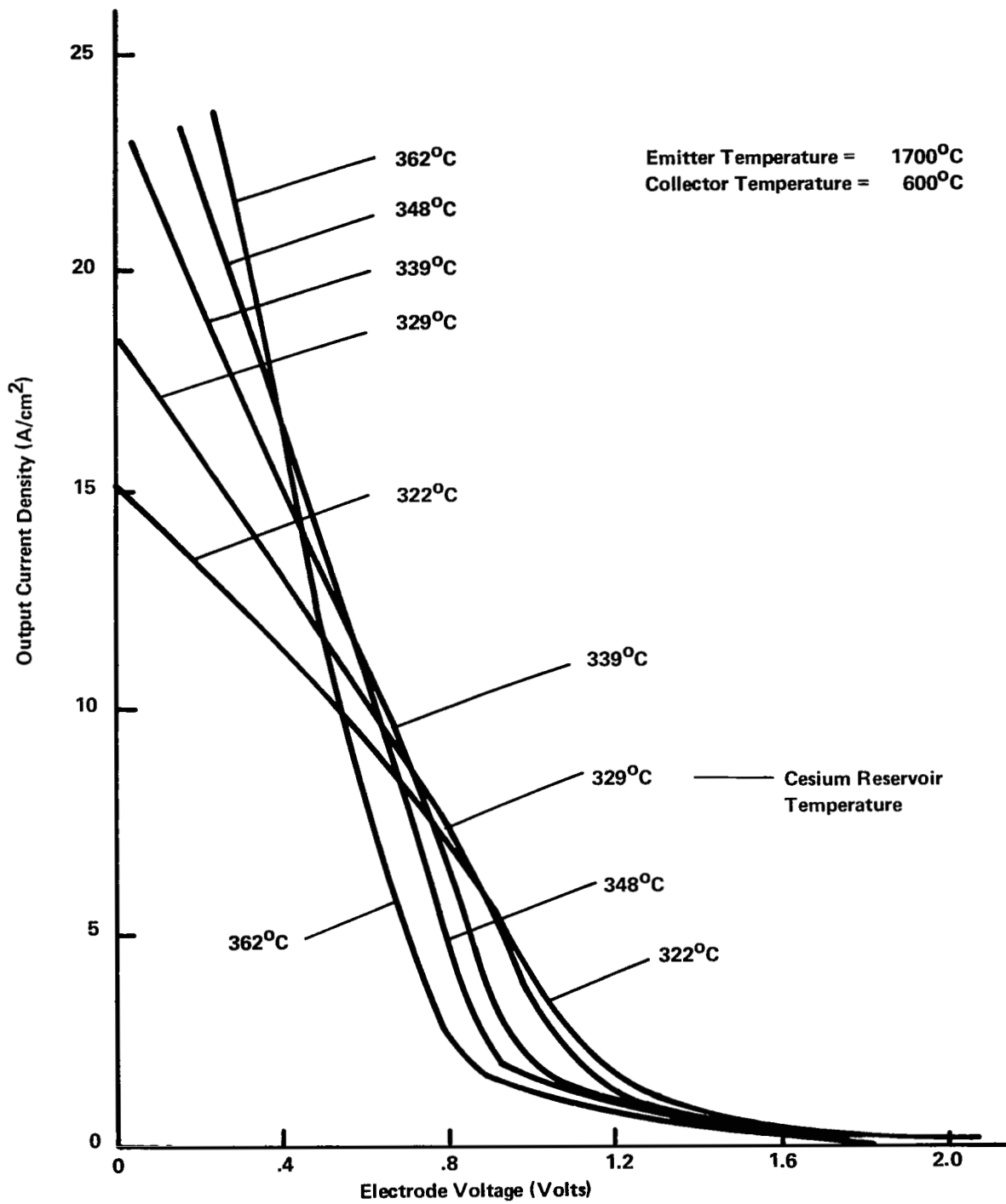
Figure C-1.6   CONVERTER 364 VOLT-AMPERE CHARACTERISTICS
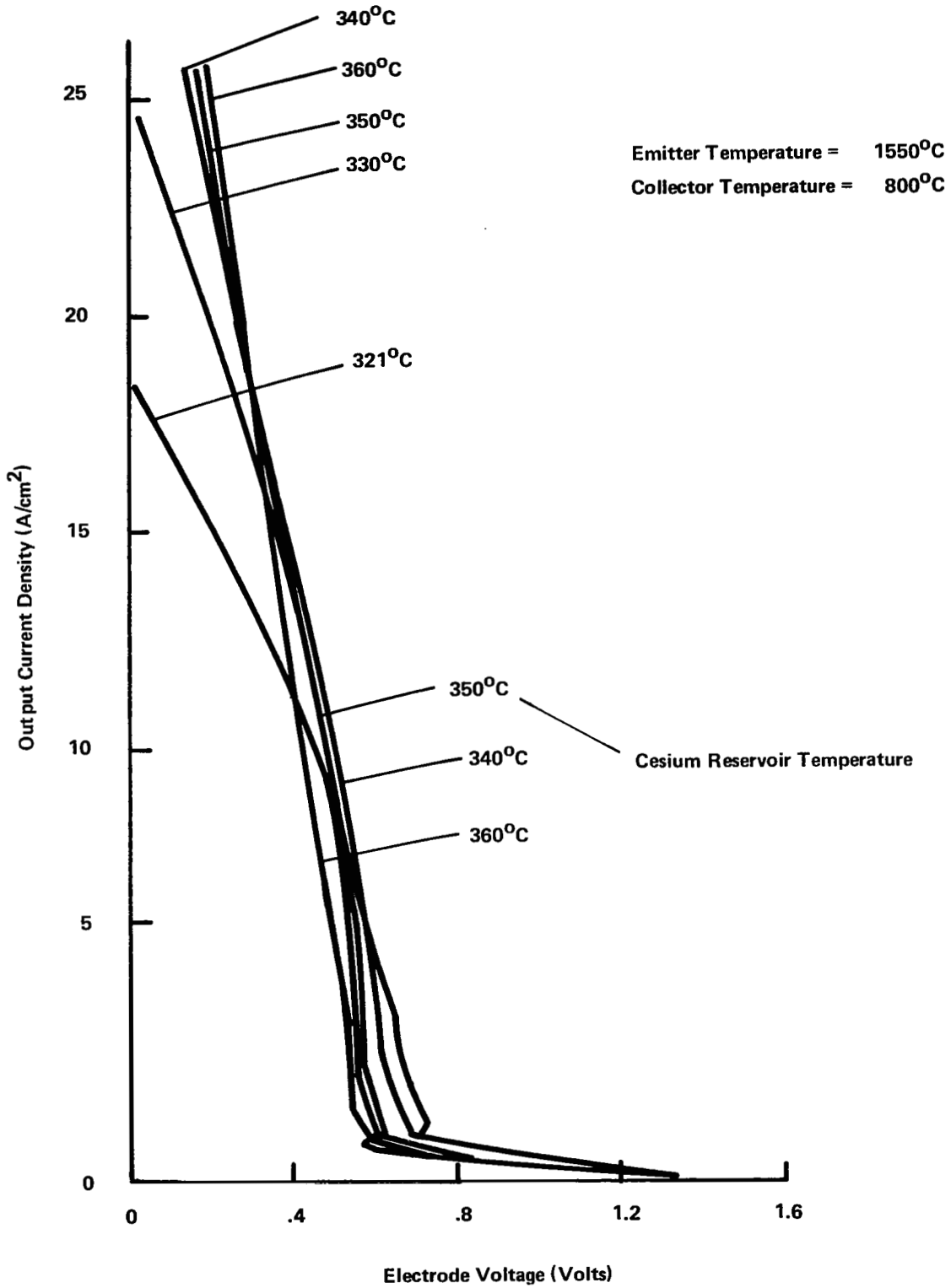($T_E = 1700^{\circ}C$, $T_C = 600^{\circ}C$) -- INITIAL TEST
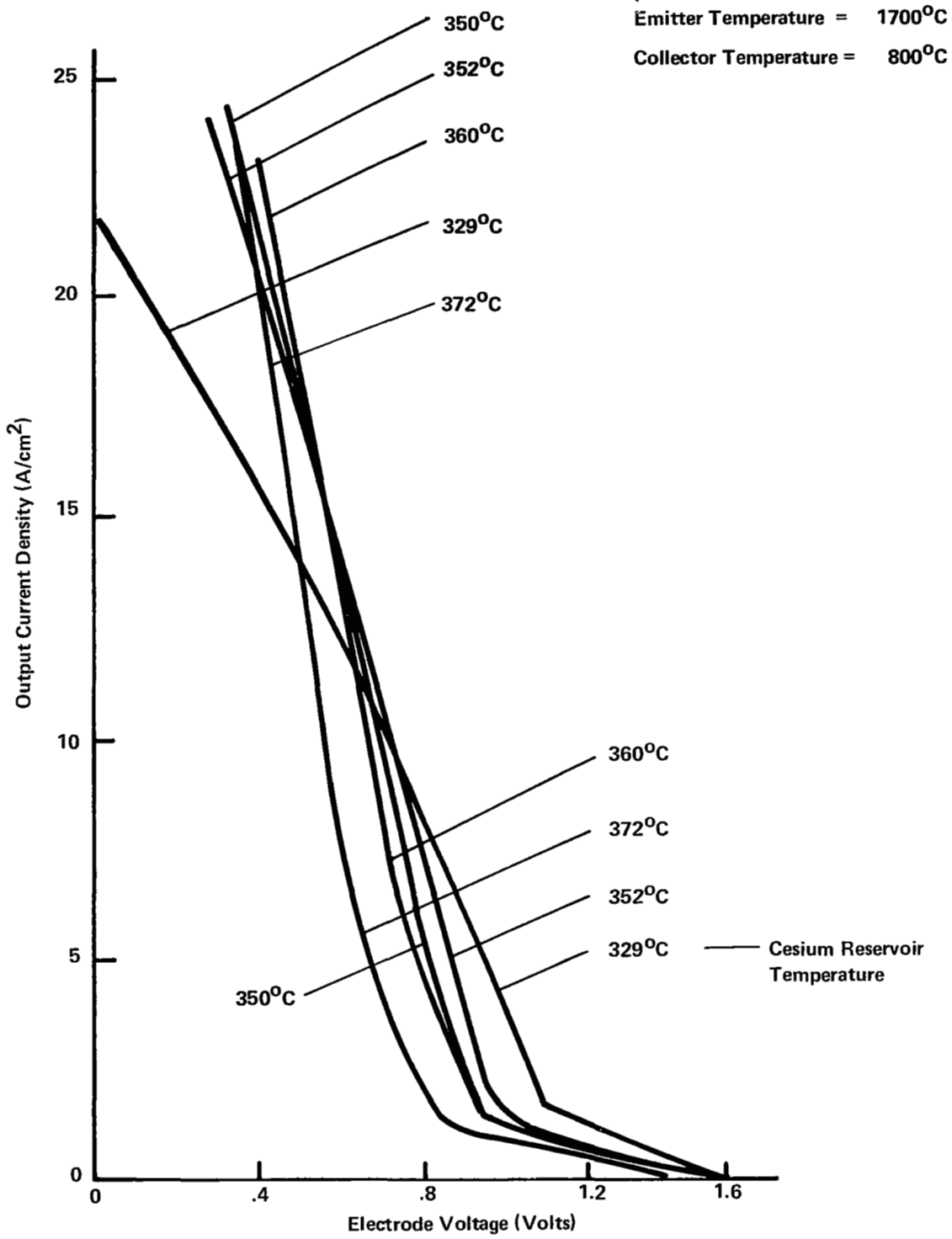
Figure C-1.7   CONVERTER 364 VOLT-AMPERE CHARACTERISTICS
$(T_E = 1700^\circ C, T_C = 800^\circ C)$ -- INITIAL TEST
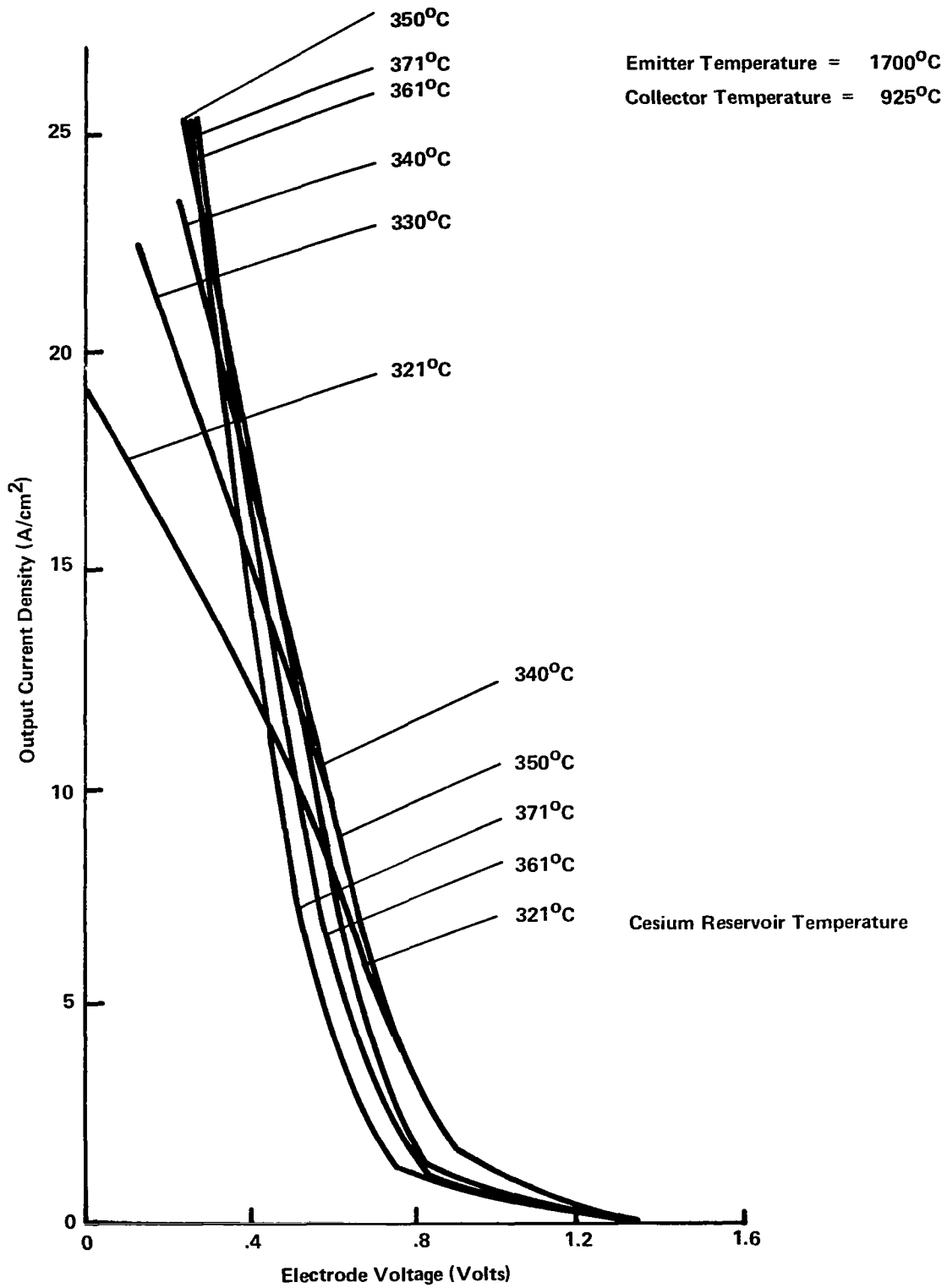
Figure C-1.8   CONVERTER 364 VOLT AMPERE CHARACTERISTICS
(T$_E$ = 1700°C, T$_C$ = 925°C) - INITIAL TEST

133
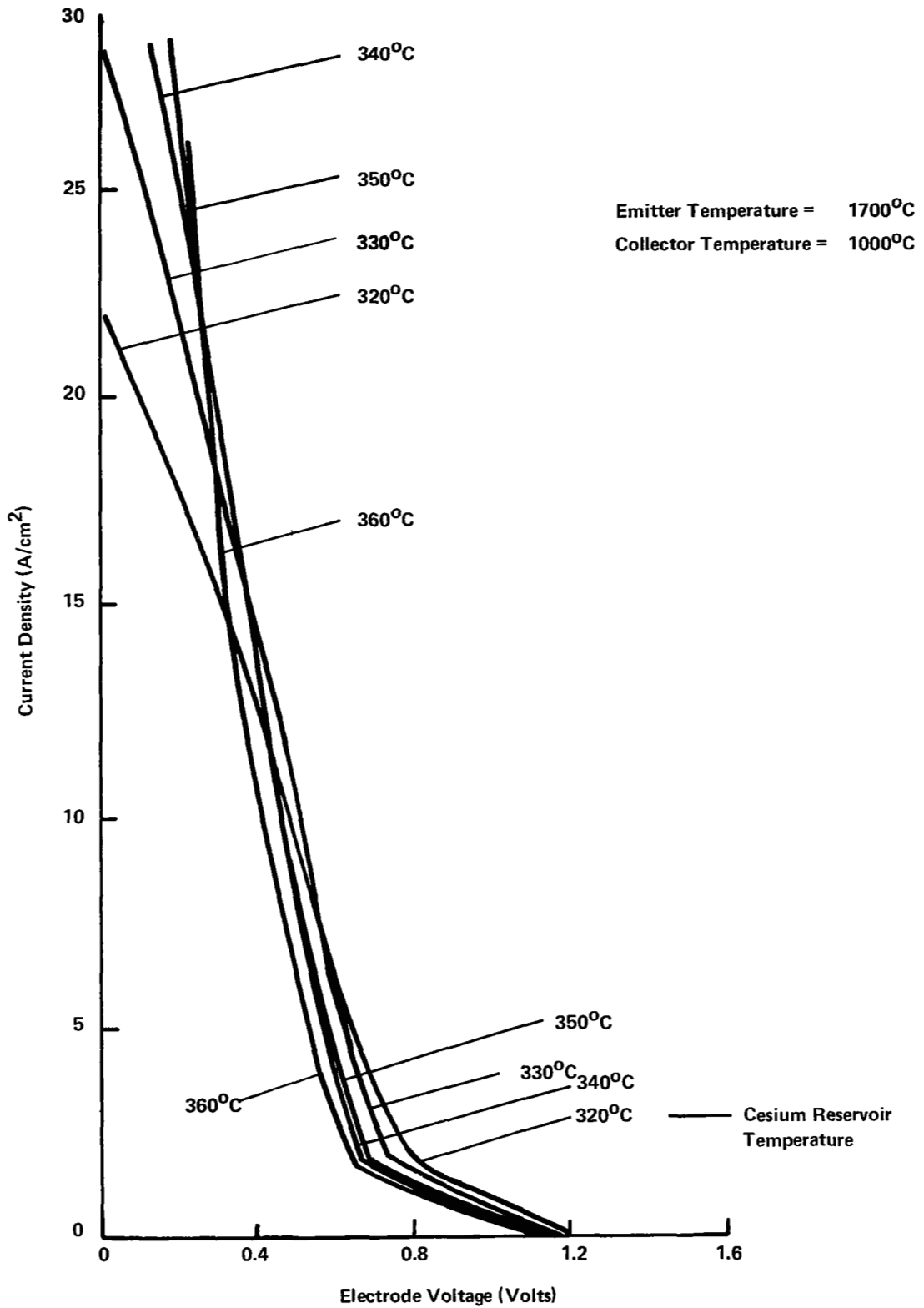
Figure C-1.9   CONVERTER 364 VOLT-AMPERE CHARACTERISTICS
$(T_E = 1700^{\circ}C, \ T_C = 1000^{\circ}C)$ -- INITIAL TEST

134

Figure C-2   CONVERTER 364 LIFE TEST PERFORMANCE HISTORY
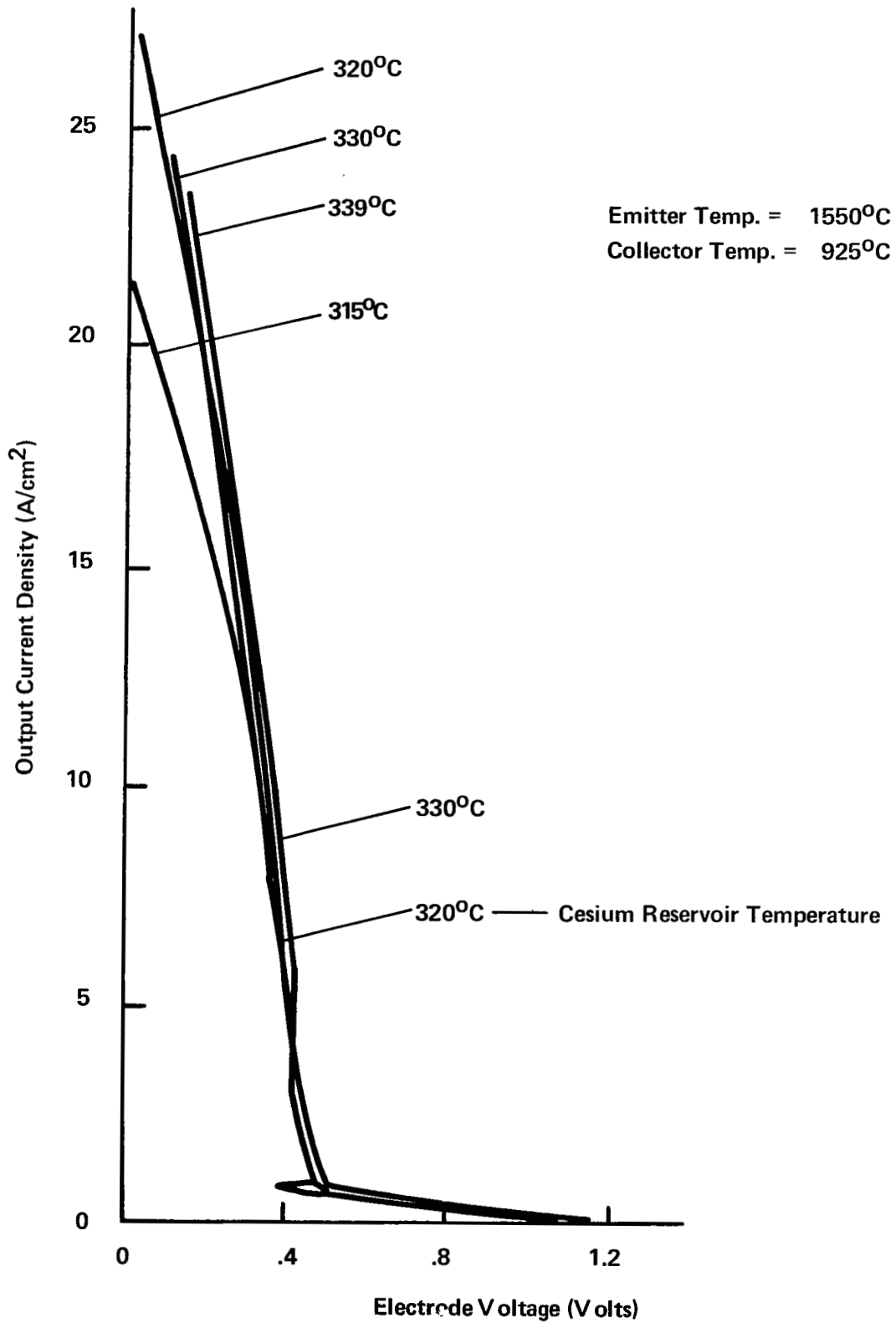
135

CONVERTER 364 FINAL PERFORMANCE CHARACTERISTICS

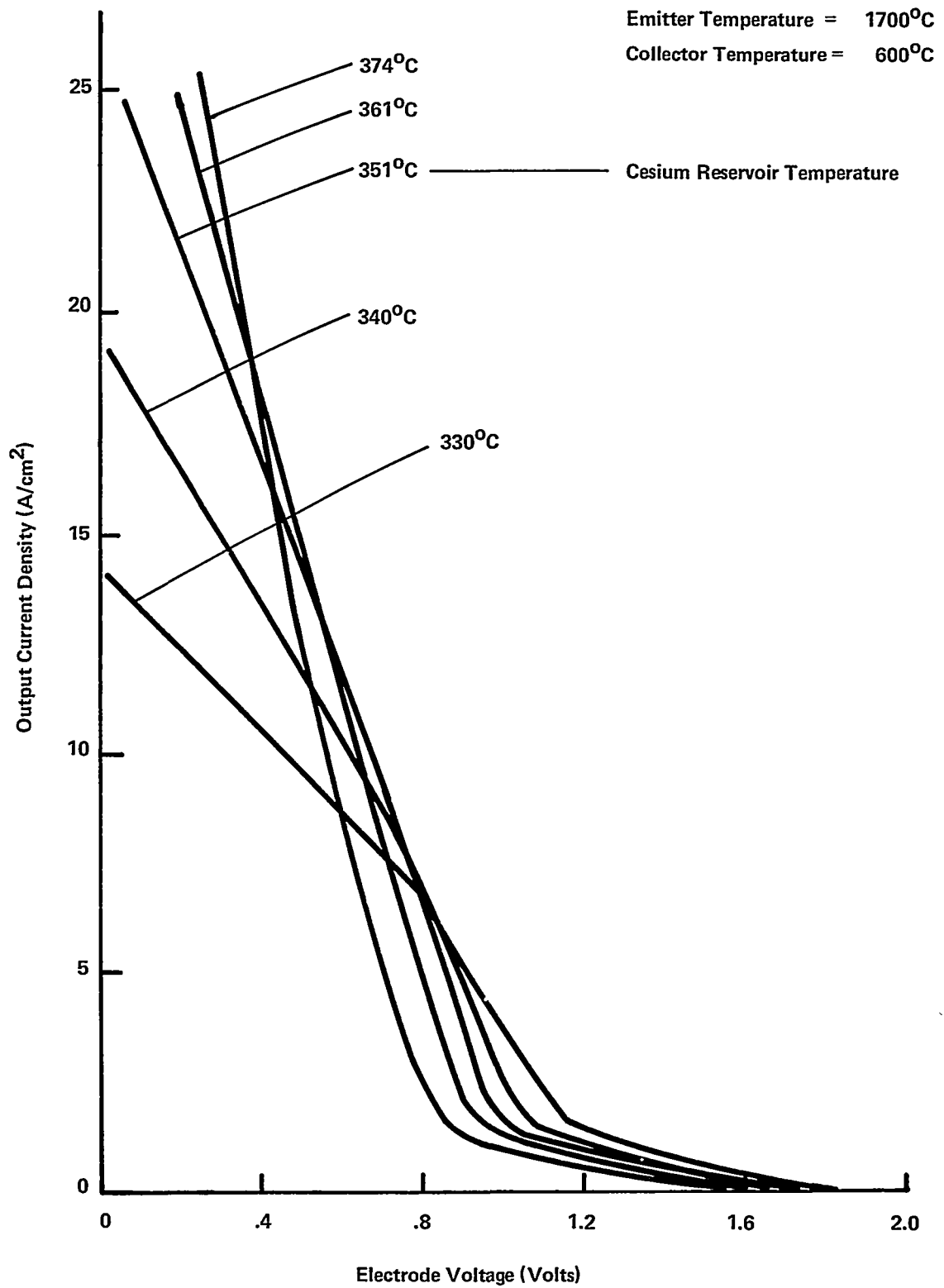Figure C-3.1 CONVERTER 364 VOLT AMPERE CHARACTERISTICS
$(T_E = 1400^\circ C, T_C = 600^\circ C)$ -- FINAL TEST

Figure C-3.2 CONVERTER 364 VOLT-AMPERE CHARACTERISTICS
$(T_E = 1400^oC, T_C = 800^oC)$ -- FINAL TEST
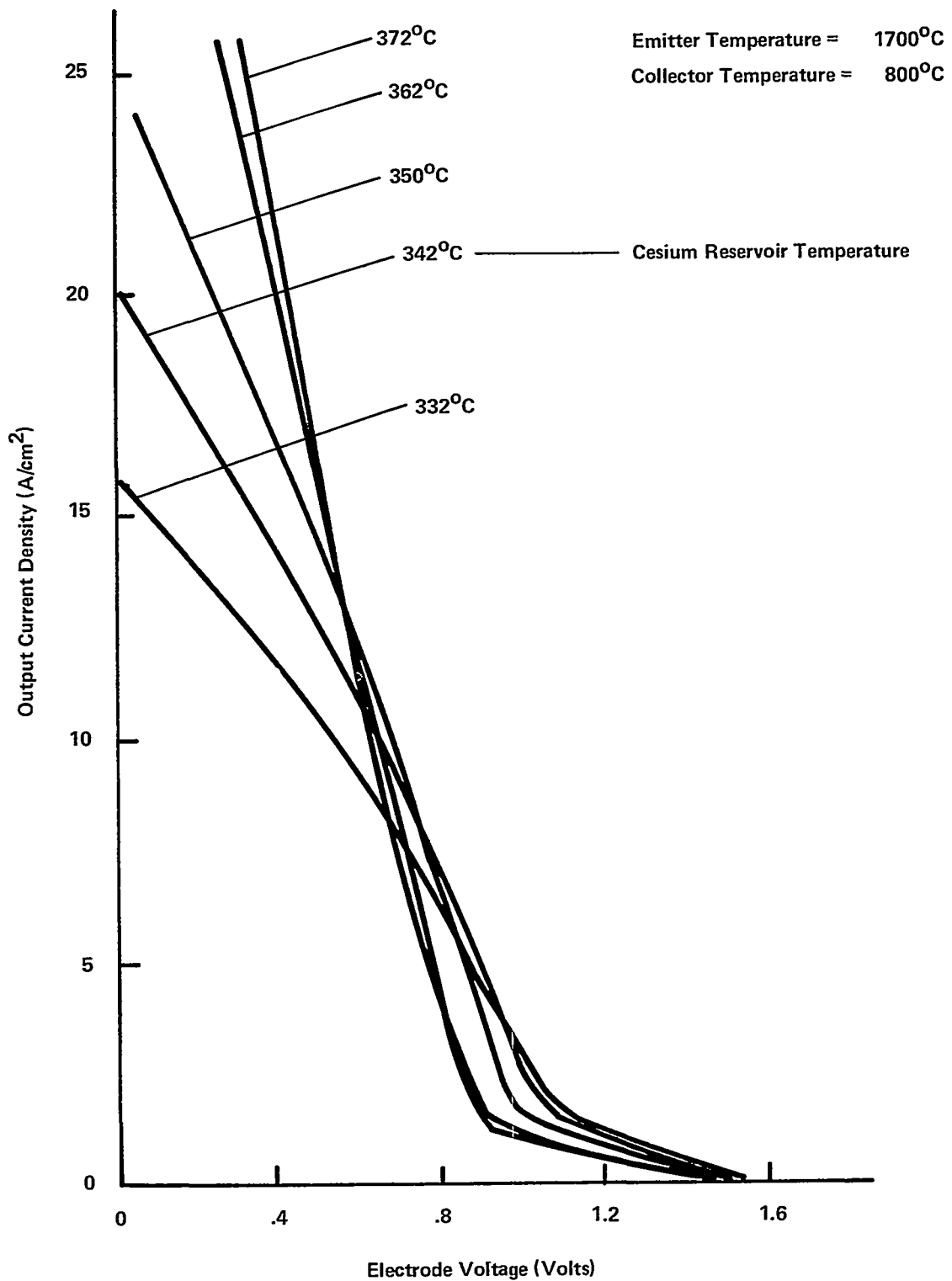
Figure C-3.3   CONVERTER 364 VOLT-AMPERE CHARACTERISTICS
(T_E = 1550°C, T_C = 600°C) -- FINAL TEST

138

Figure C-3.4   CONVERTER 364 VOLT-AMPERE CHARACTERISTICS
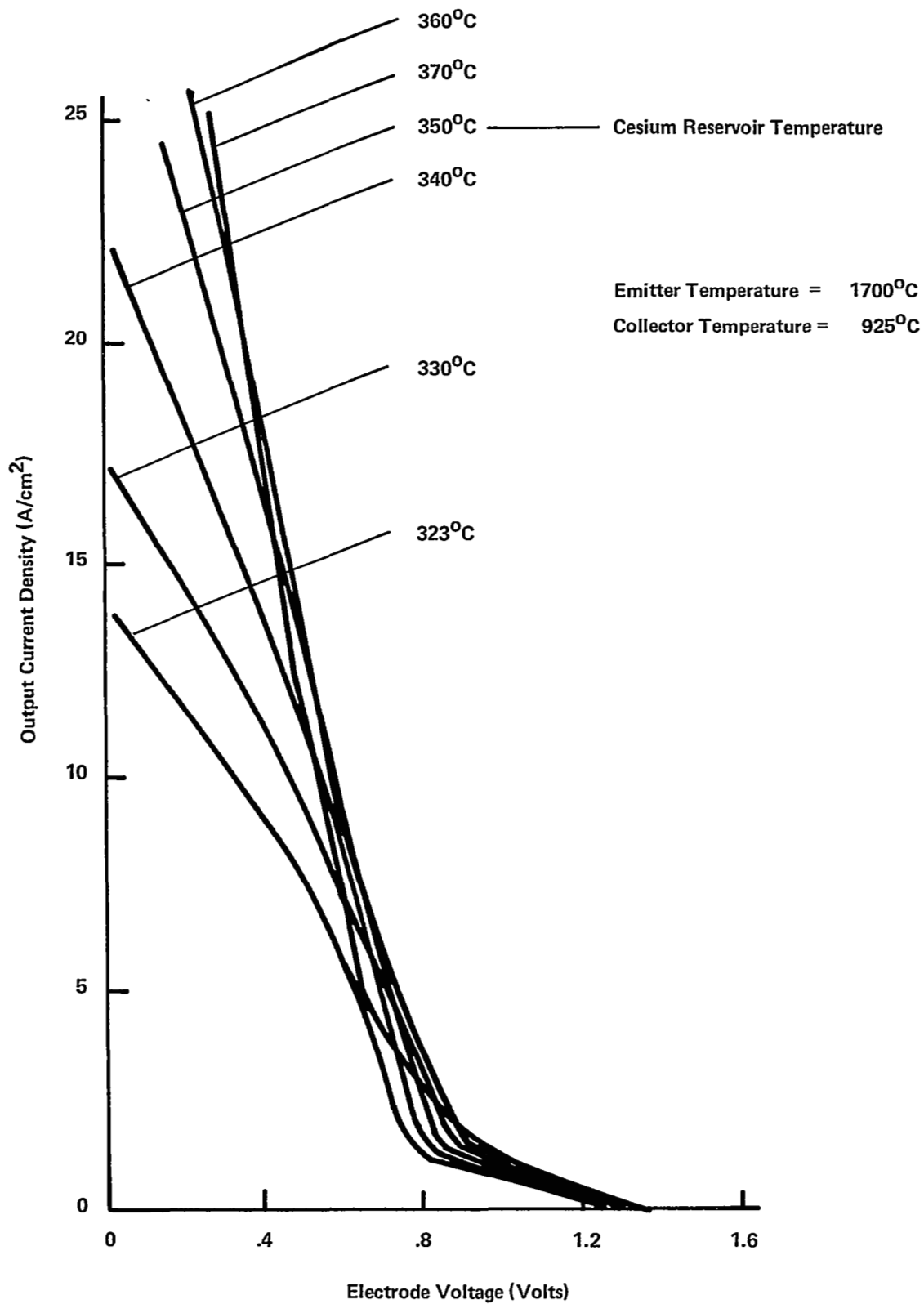$(T_E = 1550^{\circ}C,\ T_C = 800^{\circ}C)$ -- FINAL TEST

139

Figure C-3.5 CONVERTER 364 VOLT-AMPERE CHARACTERISTICS ($T_E = 1550^\circ C$, $T_C = 925^\circ C$) -- FINAL TEST

Figure C-3.6   CONVERTER 364 VOLT-AMPERE CHARACTERISTICS
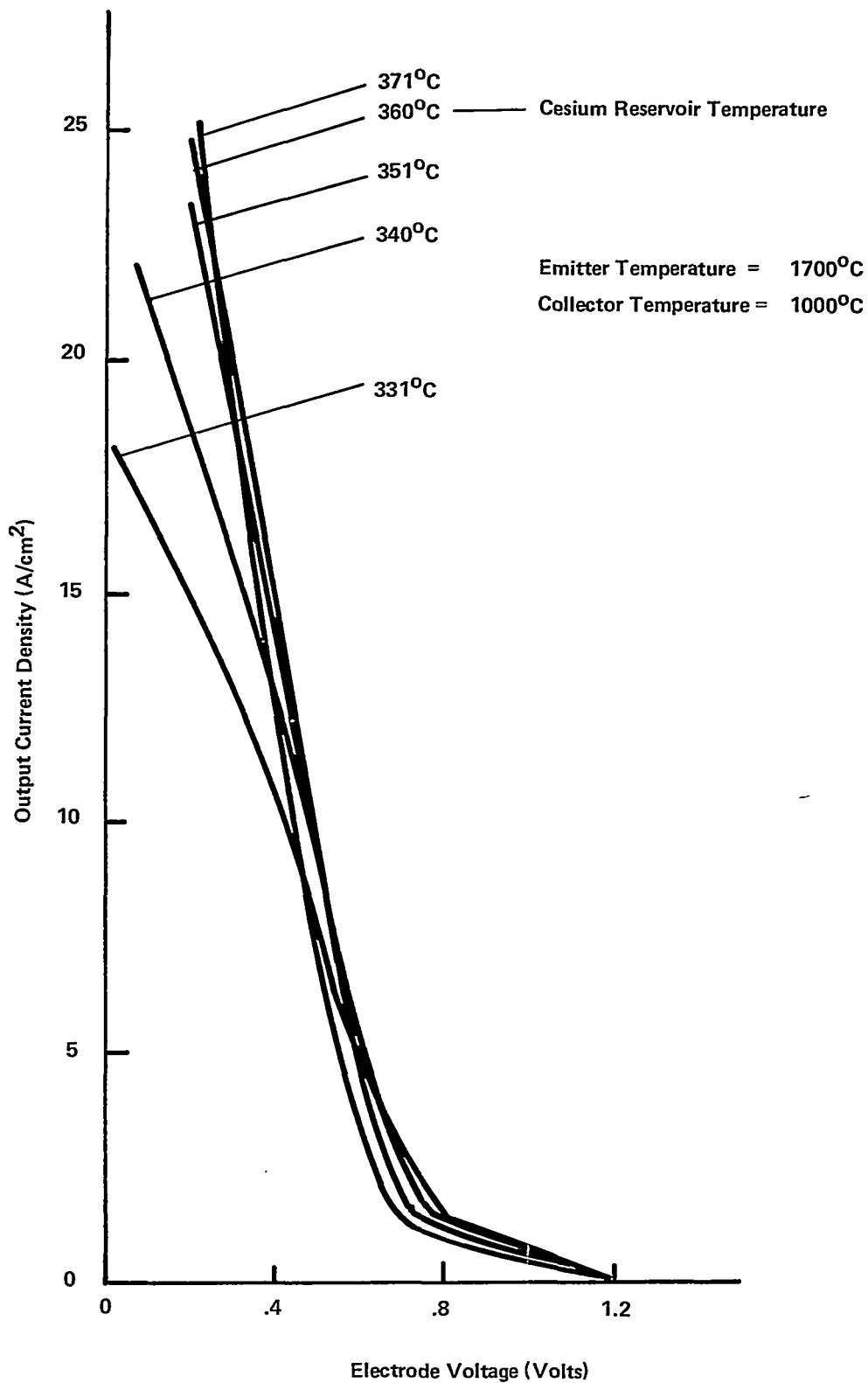(T_E = 1700°C, T_C = 600°C) -- FINAL TEST

141

Figure C-3.7　　CONVERTER 364 VOLT-AMPERE CHARACTERISTICS
$(T_E = 1700^\circ C, \ T_C = 800^\circ C)$ -- FINAL TEST

142

Figure C-3.8   CONVERTER 364 VOLT-AMPERE CHARACTERISTICS
(T_E = 1700°C, T_C = 925°C) - FINAL TEST

143

Figure C-3.9   CONVERTER 364 VOLT-AMPERE CHARACTERISTICS
(T$_E$ = 1700°C, T$_C$ = 1000°C) -- FINAL TEST

E-6375